Superhorizon evolution of curvature perturbation in multi-field inflation models

森　太朗

博士（理学）

総合研究大学院大学
高エネルギー加速器科学研究科
素粒子原子核専攻

平成３０（２０１８）年度

Superhorizon evolution of curvature perturbation in multi-field inflation models

Taro Mori

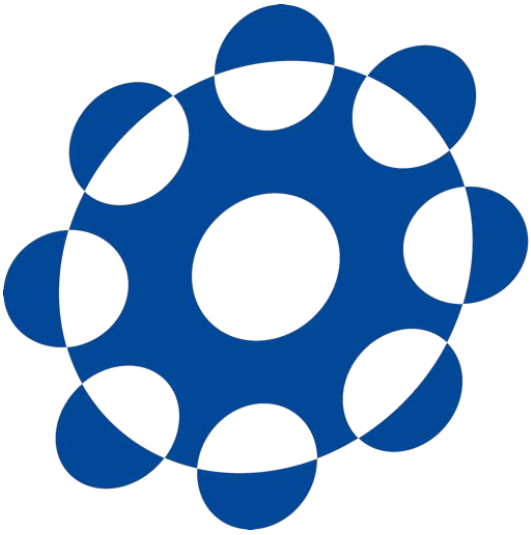

Doctor of Philosophy

Department of Particle and Nuclear Physics
School of High Energy Accelerator Science
The Graduate University for Advanced Studies,
SOKENDAI
December 10, 2018

Abstract

In this Ph.D thesis, I review a current status of multi-field inflation models and introduce theoretical predictions based on those models. Then, I discuss how to discriminate a true model from the others including our original models by using current and future cosmological observations. From a top-down viewpoint, it is natural to assume that multiple scalar fields can participate in primordial inflaton(s) because a lot of light scalar fields are predicted in theoretical models beyond the standard model in particle physics such as supergravity or superstring theory. However, an analysis of the multi-field inflation models is not as simple as that of single-field ones. In particular, computations of curvature perturbation in the multi-field models are quite different from those in the single-field ones due to the "multi-field effects." That is simply because the multi-scalar fields can have their own independent quantum fluctuations which should have been complexly mixed up each other during their evolutions in the cosmic history. In this thesis, I introduce so-called the δN formalism and the transport method to compute curvature perturbation and concretely analyze two multi-field models fully considering the multi-field effects. In Chapter 6, I introduce our own new inflation model based on superstring theory where the multi-field effects are important. Then, I discuss its theoretical predictions and how to verify this model by using new observational data in future.

Contents

Chapter 1

Introduction

In the standard Big Bang cosmology, it is well-known that a domination of energy in the Universe by radiation and/or matter can induce the cosmic expansion. However, there are serious problems which can not be solved by assuming that only radiation and/or matter contributed to the cosmic expansion. They are known as the Horizon Problem and the Flatness Problem. These two problems are attributed to the fact that *"The cosmic expansion caused by radiation or matter is decelerated"*. In fact, the above two problems can be solved by introducing an accelerated phase of the cosmic expansion in the earlier stage of the Universe. It is called inflation. The solution by assuming inflation was proposed by A. Starobinsky, K. Sato, A. Guth and D. Kazanas in the early 1980s [1, 2, 3, 4, 5]. In inflationary cosmology, a scalar field called inflaton field is introduced. When the energy density of the nearly-constant potential energy of this inflaton field dominated the energy of the Universe, the accelerated expansion was realized. As will be explained in details later, this accelerated expansion in the early Universe can solve the above two problems caused in the standard Big Bang cosmology.

So far, a lot of models which can realize inflation have been proposed with satisfying all of current observational constraints (for review, see e.g., Refs. [6, 7] and references therein). Thus, we have a strong motivation to discriminate a true model from the others by using future observations. It is informative to use observational data of temperature fluctuations and po-

larization of the Cosmic Microwave Background (CMB) radiation for this verification. Inflation generates density fluctuation (or curvature perturbation) on the spacetime. If curvatures are slightly different each other at points in the spacetime after inflation, these curvature perturbation affects the spatial distribution of the temperature fluctuations of CMB at a late time. Therefore, it is possible to verify a inflation model by comparing various theoretical quantities related with the temperature fluctuation and the polarization predicted in the model with the ones measured in the CMB observation. In this thesis, especially I focus the power spectrum calculated from two-point correlation function of the curvature perturbation and the so-called non-Gaussianity calculated from three-point correlation function. These are the most important quantities to test inflation models. Recently by using the CMB observations reported by the Planck satellite experiment, we can put severe bounds on these quantities. For the latest observational constraints on inflation, see Ref. [8].

Inflation models can be trivially classified into two classes: One is the single-field model where only a single inflaton contributes to inflation for simplicity. And the other is the multi-field model. From a top-down viewpoint, a construction of the multi-field model is much more natural. That is because it is known that in theories of new physics beyond the standard model such as superstring theory or supergravity, a lot of scalar fields appear (for the review of model-building based on these theories, see Ref. [9]). So far we have not verified these models only by using any terrestrial experiments such as collider experiments. However, if we can test the inflation models based on those models by using cosmological observations such as CMB in future, we should obtain unique insights into these theories. This is why the building of multi-field inflation models is an interesting and an exciting subject.

What is the difference between single-field and multi-field inflation models? In single-field cases, the superhorizon-scale mode of the curvature perturbation is almost constant during inflation [10]. Therefore, we just need to compute a perturbation when it exits the horizon during the inflation. On the other hand, in multi-field cases, we must have two modes of the

perturbation 1) adiabatic perturbation which is along to the inflaton trajectory and 2) isocurvature perturbation which is perpendicular to the inflaton trajectory [11]. Since isocurvature perturbation is transferred to adiabatic perturbation, it is time-evolving during inflation, and we need to trace its full time-evolution from the beginning to the end of inflation. This is a typical feature in the multi-field inflation model. In addition, almost all single-field inflation models predict a scale invariant power spectrum. Because of this invariance, there is a relation between a spectral tilt and non-Gaussianity of curvature perturbation. This is called the Maldacena's consistency relation [12]. In fact, in multi-field models, there are possibilities to break this relation. The current observational data are not so tight to test this relation. In future however, if we find a deviation from this relation, it should be a strong support of a multi-field inflation model.

In analyses of the multi-field models discussed in this thesis, we adapt the δN formalism [13, 14] and the transport method [15, 16, 17, 18]. Relying on these methods in calculations, we can compute curvature perturbation by just determining the classical dynamics of inflaton fields, and it is possible to trace time-evolutions of all observable quantities during inflation. Moreover, by using the transport method which is an extended version of the δN formalism, we can calculate curvature perturbation more efficiently by simply finding a gauge transformation between the constant-time slice and the uniform-density slice.

This thesis is organized as follows : In chapter 2, I briefly review the standard Big-Bang cosmology and what the problems of this theory are. In addition, I discuss how to solve these problems with introducing inflation. In chapter 3, I introduce a framework to compute curvature perturbation generated by inflation. chapter 4 is dedicated to an introduction of the δN formalism and the transport method. In chapter 5, I discuss a $R^2 + \chi^2$ model, namely the Starobinsky model with a mass term of another scalar field. A multi-field inflation model which is based on string inflation, named Multi-Moduli inflation, is discussed in chapter 6. Chapter 7 is devoted to the summary of this thesis.

Part I

Inflation and Primordial Curvature Perturbation

Chapter 2

Quick overview of inflation

This chapter is dedicated to the overview of inflationary cosmology. First, we will introduce the Friedmann cosmology and see serious problems of this theory, which are so-called the horizon problem and the flatness problem. After that, we introduce inflation and confirm how we can avoid these problems. Moreover, we show what conditions are required for successful inflation.

2.1 Friedmann cosmology

In this section we introduce so-called Friedmann cosmology, which describes the expanding universe based on general relativity. After that, we will point out problems of this theory.

2.1.1 Expanding universe

First we derive the Friedmann equation, which is a basic equation for describing expanding universe. The starting point is the Einstein equation,

$$R_{\mu\nu} - \frac{1}{2} g_{\mu\nu} R = 8\pi G T_{\mu\nu}. \tag{2.1.1}$$

From the requirement of cosmic principle which claims that the universe is almost homogeneous and isotropic, Friedmann-Lemaître-Robertson-Walker metric (FLRW metric for short) is derived as

$$ds^2 = -dt^2 + a^2(t)\left(\frac{dr^2}{1-Kr^2} + r^2(d\theta^2 + \sin^2\theta d\phi^2)\right). \tag{2.1.2}$$

Here K is a constant determined from the spacetime topology. Using this FLRW metric, we obtain following equations from diagonal components of the Einstein equation.

$$\begin{aligned} 00 \qquad & H^2 = \left(\frac{\dot{a}}{a}\right)^2 = \frac{8\pi G}{3}\rho - \frac{K}{a^2}, \\ ii \qquad & 3H^2 + 2\dot{H} = -8\pi G p. \end{aligned} \tag{2.1.3}$$

$H = \dot{a}/a$ defined here is representing the expansion rate of the universe and called Hubble parameter. In the natural units, Hubble parameter has the dimension of $[T^{-1}] = [L^{-1}]$. H^{-1} is interpreted as typical size of universe. For this reason H^{-1} is also called Hubble horizon or Hubble radius. On the other hand, ρ, p are the 00 component (energy density), ii component (pressure) of the energy momentum tensor. Once we determine how the scale factor $a(t)$ evolves based on these equations, we can describe the expansion of the universe. Here, we take $K = 0$ just for simplicity,

$$H^2 = \left(\frac{\dot{a}}{a}\right)^2 = \frac{8\pi G}{3}\rho. \tag{2.1.4}$$

In the case of $K \neq 0$, it is important to consider the Flatness Problem which will be explained in the next section.

Now we can check the relationship between the scale factor $a(t)$ and the energy density ρ in order to solve the Friedmann equation (2.1.3). Differentiating both sides of the equation (2.1.3) with respect to time,

$$2H\dot{H} = \frac{8\pi G}{3}\dot{\rho}, \tag{2.1.5}$$

By using this expression and (2.1.3), we get

$$\dot{\rho} + 3H(\rho + p) = 0. \tag{2.1.6}$$

On the other hand, ρ is related to p by the equation of state,

$$p = w\rho. \tag{2.1.7}$$

Here w is a constant associated with each energy contents of interest such as radiation or matter.

By substituting (2.1.7) into (2.1.6), we have

$$\dot{\rho} = -3H(1+w)\rho = \frac{-3\dot{a}}{a}(1+w)\rho. \tag{2.1.8}$$

However, this can be integrated immediately and after all we obtain

$$\rho \propto a^{-3(1+w)}. \tag{2.1.9}$$

This is the relation between the scale factor $a(t)$ and energy density ρ which we wanted and we can determine the time evolution of the scale factor $a(t)$ with this equation.

We can see some concrete examples. Here we consider matter-dominant universe. In this case we take $w = 0$ in (2.1.9). Therefore, using $\rho_m \propto a^{-3}$, we get

$$H^2 = \left(\frac{\dot{a}}{a}\right)^2 \propto \frac{8\pi G}{3}a^{-3}. \tag{2.1.10}$$

From this expression, time evolution of a is given by,

$$a(t) \propto t^{2/3}. \tag{2.1.11}$$

Next we consider the case where the energy density is dominated by radiation. In this case, since $w = 1/3$ and $\rho \propto a^{-4}$, solving the Friedmann equation, time evolution of a is given by

$$a(t) \propto t^{1/2}. \tag{2.1.12}$$

From (2.1.11) and (2.1.12), if the energy density of matter or radiation dominantly contributes to cosmic expansion, we find $\ddot{a} < 0$. This means expansion of universe is decelerated.

What about in the case of $w = -1$? In this case, in fact it corresponds to the case where vacuum energy ρ_v is dominant. However, it seems strange situation because their pressure is negative in this case. From the expression (2.1.9), the energy density does not depend on the scale factor a, and it becomes $\rho \propto$ Const. In such a case,

$$H^2 = \left(\frac{\dot{a}}{a}\right)^2 \propto \text{Const.} \tag{2.1.13}$$

Thus, after all, time evolution of a becomes

$$a(t) \propto e^{Ht} \tag{2.1.14}$$

In this situation, the universe expands exponentially and one can easily find that expansion is accelerated ($\ddot{a} > 0$).

Scale factor dependence of energy density ρ and time evolution of scale factor a are summarized for each cases (matter, radiation and vacuum energy) in Fig.2.1.1.

	w	ρ	$a(t)$
Matter	0	a^{-3}	$t^{2/3}$
Radiation	1/3	a^{-4}	$t^{1/2}$
Vacuum energy	-1	a^{0}	e^{Ht}

Figure 2.1.1: Relationship between ρ and a in each energy component and time evolution of a

In the epoch of Inflation which is the main theme of this thesis, we assume that the universe experienced accelerated expansion in the extremely

early epoch. In the following sections, We will discuss why such accelerated expansion is required and also how to realize the situation where vacuum energy becomes dominant, namely $w = -1$.

2.1.2 Problems of Friedmann cosmology

Horizon Problem

In the previous section we have learned the description of the expanding universe based on Friedmann cosmology. In this section, we will see Horizon Problem which is one of the serious problem of Friedmann cosmology.

First of all, let's consider observing a point far away from an observer by $l = \sqrt{x_0^2 + y_0^2 + z_0^2}$. This l is not a physical distance in Friedmann cosmology. Since FLRW metric is given by (2.1.2), the physical distance should be expressed as $L = al$. As we saw in the previous section, this a grows with time. Therefore, when we take large L, we must be careful to time dependence of a.

On the other hand, the Hubble horizon, which represents the typical size of the universe, is represented by H^{-1}. Here we compare the time evolution of a and H^{-1} in the case of radiation-dominant universe. H^{-1} has a dimension of length and a is dimensionless. However, in this comparison we can tune the dimension of a to that of length with multiplying a proper quantity. According to the previous section $a(t) \propto t^{1/2}$, H^{-1} is calculated as

$$H^{-1} = a/\dot{a} \propto t. \tag{2.1.15}$$

According to this result, we can see the problem of Friedmann cosmology as shown in Figure 1.2. When we trace back a and H^{-1} to the epoch of the CMB recombination, as shown in Figure 1.2, the scale factor a is larger than the Hubble horizon in the epoch of the CMB recombination. Because the Hubble horizon represents the typical size of causal contact in the universe, particles (such as photons) can not have a causal relationship over a scale that exceeds H^{-1}. Hubble horizon with scale of interest are in the relationship as

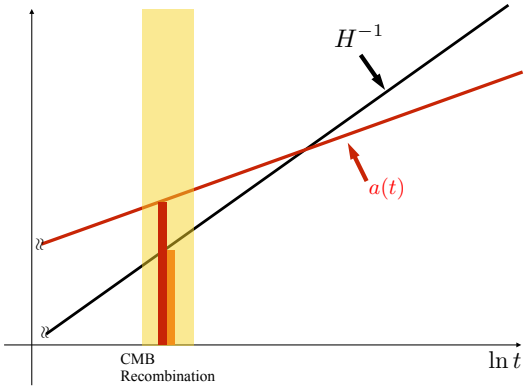

Figure 2.1.2: The scale factor and time evolution of the Hubble horizon. The Hubble horizon becomes smaller than the scale factor in the CMB recombination time. This means the observational scale of CMB becomes larger than the Hubble horizon at the time of the CMB recombination.

shown in Figure 2.2. It means that there were a lot of causally-disconnected regions in the early universe. This is completely contradict to homogeneity and isotropy of observed CMB temperature fluctuations. It is not acceptable to assume that lots of regions which do not have a causal contacts have the almost exactly same temperature by chance. This problem is called Horizon problem. The above discussion also holds in the case of $a \propto t^{2/3}$ which the matter dominated universe.

Horizon Problem can also be discussed in another coordinate system called comoving frame. Comoving frame is interpreted as "coordinates expanding with the universe". In comoving frame, we can reduce a dependence from quantities which have a dimension of length by dividing by the scale factor a.

First, FLRW metric in polar coordinates is given by,

$$ds^2 = -dt^2 + a^2(t)(dr^2 + r^2 d\theta^2 + r^2 \sin^2\theta d\phi^2) \tag{2.1.16}$$

Considering the geodesic of the photon, $ds = 0$, and focusing only on the radial component, the Particle horizon is defied as

$$x_{ph} \equiv \int_{t_i}^{t} \frac{dt'}{a(t')}. \tag{2.1.17}$$

This can be interpreted as the distance which photon can propagate during a certain time interval and represents the size of the region where photons can interact with each other (in the following discussion we take $t_i = 0$ just for simplicity). On the other hand, the quantity called comoving Hubble horizon is defined as $(aH)^{-1}$. If we calculate x_{ph} and $(aH)^{-1}$ in matter/radiation dominant universe, we straightforwardly obtain

$$\begin{aligned} \text{Matter} \qquad & x_{ph} \propto t^{1/3}, \qquad (aH)^{-1} \propto t^{1/3}, \\ \text{Radiation} \qquad & x_{ph} \propto t^{1/2}, \qquad (aH)^{-1} \propto t^{1/2}. \end{aligned} \tag{2.1.18}$$

From now on, we will treat the Particle horizon equivalent to comoving Hubble horizon. In addition, from (2.1.18), we find that $(aH)^{-1}$ is an increasing function of time in the dust or radiation -dominant universe.

On the other hand, since H is a constant in the case where the vacuum energy is dominant, then $(aH)^{-1} \propto a^{-1} \propto e^{-Ht}$ and $(aH)^{-1}$ is a decreasing function of time. In fact, Whether $(aH)^{-1}$ is an increasing or a decreasing function is one of the most important point in later discussions.

Since we can drop a from $L = al$ in the comoving frame, simply take this as the scale of CMB observation as $l = \text{Const}$ and illustrate it with $(aH)^{-1}$. It is as shown in Figure 2.3. Here again we realize the same problem as before. That is, currently observed Particle horizon is smaller than the CMB observational scale where there is a region where photons can not interact causally. Again this contradicts the homogeneity and isotropy of CMB temperature fluctuation.

As mentioned above, looking at the time evolution of the scale factor a, the Hubble horizon and the Particle horizon, if we assume that only matter and radiation dominantly contributed to the expansion of the universe, the present CMB homogeneity. The problem that we can not explain the directionality is the Horizon problem.

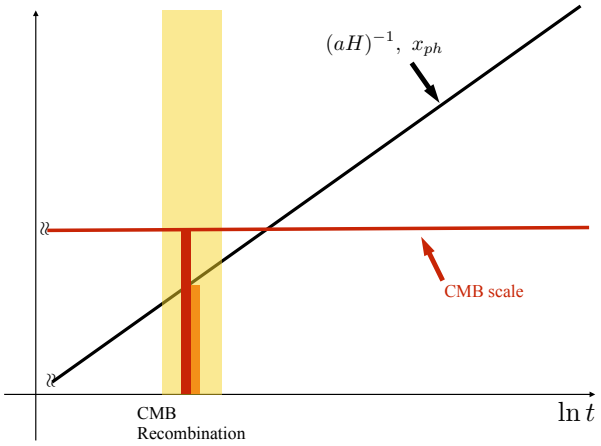

Figure 2.1.3: Comparison between comoving Hubble $(aH)^{-1}$ and CMB observation scale. $(aH)^{-1}$ becomes smaller than CMB's observation scale.

Flatness Problem

Next we will address so-called Flatness Problem. Calculating the Ricci scalar R from the FLRW metric, we get

$$R = \frac{K}{a^2} \tag{2.1.19}$$

We find found that this corresponds to the second term of the right-hand side of (2.1.3). We call this term curvature term. Whether or not this curvature term contributes to cosmic expansion is strictly constrained by observation and it is known that this contribution is very small. Therefore, it this curvature term is very small in the present universe.

On the other hand, we can rewrite the Friedmann equation (2.1.3) as follows.

$$1 = \frac{8\pi G\rho}{3H^2} - \frac{K}{(aH)^2}. \tag{2.1.20}$$

As mentioned in the previous section, the comoving Hubble radius $(aH)^{-1}$ is an increasing function in the decelerated and expanding universe. That means the curvature term $K/(aH)^2$ was extremely small in the early epoch

of the universe even though it is very small in the current universe.

By tracing the time evolution of the scale factor to the beginning of the universe, its size can be estimated. For example, at the time of Big Bang Nucleosynthesis or at the time of Grand Unified Theory (GUT) where it is considered that three gauge interactions are unified, the magnitude of the curvature term is

$$\left(\frac{K}{(aH)^2}\right)_{BBN} < \mathcal{O}(10^{-16}), \qquad \left(\frac{K}{(aH)^2}\right)_{GUT} < \mathcal{O}(10^{-55}). \tag{2.1.21}$$

From this result, in order to explain the flatness of the present universe, we have to assume that the universe began with a fine-tuned state such that the curvature is extremely small. The above fine-tuning problem concerning the curvature of the universe is called the Flatness Problem.
The cause of the Horizon Problem and the Flatness Problem are same. In the decelerated universe contributed by matter or radiation comoving Hubble $(aH)^{-1}$ is a monotonically increasing function with respect to time and the fact that $(aH)^{-1}$ gets very small when we going back to that early epoch of the universe.

In the Horizon problem, Particle Horizon x_{ph} is represented by comoving Hubble and when we go back to the time of recombination of the universe this x_{ph} becomes smaller than the CMB scale. Therefore, there are lots of regions where photons can not interact causally in this period and there is no reason why different regions have the almost same temperature in such a phase.

In other words, if we assume that only matter or radiation contributed to the expansion of the universe, we can not explain observational fact that CMB temperature fluctuation is extremely small.

Similarly in the Flatness Problem, $(aH)^{-1}$ becomes small at the beginning of the universe. Thus the curvature term $K/(aH)^2$ becomes very small. As a result, to explain the flatness of the current universe, the universe must have

begun with extremely small curvature. This is a kind of fine tuning problem.

In fact, it is known that these two problems can be solved by introducing an idea that "In the early universe there was a phase when the comoving Hubble $(aH)^{-1}$ became a decreasing function with respect to time (*i.e.* there was a time when the universe experienced accelerated expansion)". At the beginning of the next section we will review this point and introduce inflation to cause such acceleration.

2.2 Inflation

This section explains how accelerated expansion of the universe solves the problems of Friedmann cosmology described in the previous section. After that, We will learn how to realize such an accelerated phase.

2.2.1 A first look at inflation

As mentioned at the end of the previous section, in order to solve the problems of Friedmann cosmology, there should be a phase in which comoving Hubble $(aH)^{-1}$ decreases with time at the early epoch of universe. The condition that $(aH)^{-1}$ becomes a decreasing function is

$$\frac{d}{dt}\left(\frac{1}{aH}\right) = -\frac{1}{a}\left(\frac{\dot{H}}{H^2} - 1\right) < 0 \quad \Rightarrow \epsilon \equiv -\frac{\dot{H}}{H^2} = -\frac{d\ln H}{dN} < 1. \tag{2.2.1}$$

The ϵ defined here is called the slow-roll parameter. When the condition (2.2.1) is satisfied, $(aH)^{-1}$ becomes a decreasing function. Especially when ϵ gets a sufficiently small $\epsilon \ll 1$, it turns to be $\dot{H} \sim 0$ then we solve this for $a(t)$,

$$a(t) \propto e^{Ht} \tag{2.2.2}$$

The limit of $\epsilon \to 0$ is called de Sitter limit. Considering such a limit, we can obtain a solution in which the universe expands exponentially.

Then let's see how the problems of Friedmann cosmology are solved by adding the phase when $(aH)^{-1}$ is decreasing function.

As shown in the figure (2.2.1), when we add the phase $(aH)^{-1}$ is decreasing, comoving Hubble (or Particle Horizon) becomes larger as going back to the past.

Even if Particle Horizon becomes small at the early epoch, then it becomes sufficiently large at the time of the added accelerated expansion, inflation. And as a result, homogeneity and isotropy of CMB can be explained .

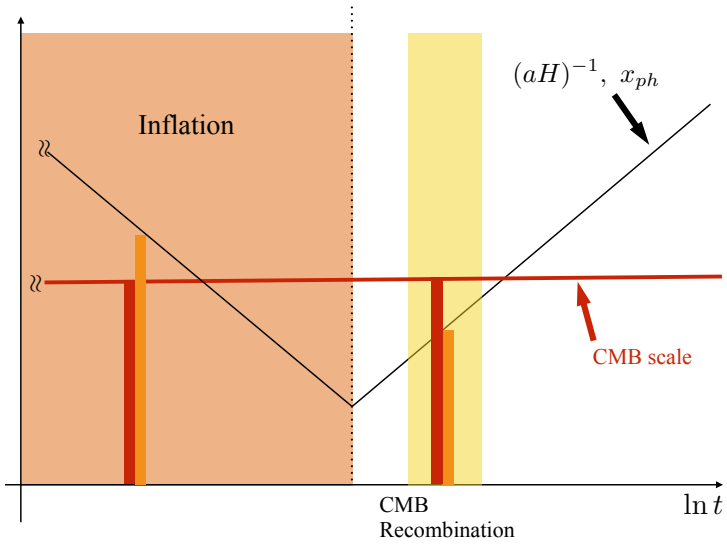

Figure 2.2.1: Comparison between time variation of comoving Hubble and observation scale of CMB when Inflation is introduced. While Inflation is occurring, $(aH)^{-1}$ decreases and it turns out that it can become bigger than the CMB scale when going back to the past. This can explain the uniform isotropy of the universe.

Let us estimate how long inflation should continue to solve the Horizon Problem. We set the scale factors at the beginning and end of inflation as

a_i, a_f and define

$$N \equiv \ln\left(\frac{a_f}{a_i}\right) = \int_i^f \frac{da}{a} = \int \frac{\dot{a}}{a} dt = \int H dt \tag{2.2.3}$$

N is called e -folding and is an important quantity that frequently appears in discussions of inflation. In addition, for the sake of explanation here, we introduce new parameters.

$$\Omega_0 \equiv \frac{8\pi G}{3H_0}\rho_0 \tag{2.2.4}$$

Here, H_0 and ρ_0 represent the current universe Hubble and energy density, respectively.

In order to explain homogeneous and isotropic universe, we need the following condition we are interested in the scale which is more interesting than the comoving Hubble $(a_i H_i)^{-1} a_0 H_0)^{-1} = H_0^{-1}$.

$$H_0^{-1} < (a_i H_i)^{-1} \tag{2.2.5}$$

This means the size of comoving Hubble at the epoch of inflation should be larger than that of the current universe (for simplicity here we set the current universe scale factor to $a_0 = 1$). In such a situation, every region of the universe have causal contact. As we will see in the later section, since H is almost constant during Inflation,

$$\frac{a_f}{a_i} > \frac{a_f H_f}{H_0}. \tag{2.2.6}$$

Here we just assume that radiation became dominant immediately after inflation, but when radiation is dominant, scale factor grows as $a \propto t^{1/2}$ and $H \propto a^{-2}$. Thus, we define boundary conditions to be consistent with the current value H_0,

$$H = \frac{H_0^2\sqrt{\Omega_0}}{a^2} \tag{2.2.7}$$

This gives $H_f = H_0^2\sqrt{\Omega_0}/a_f^2$ and (2.2.6) can be rewritten as

$$\frac{a_f}{a_i} > \frac{\sqrt{\Omega_0}}{a_f} \sim 10^{27} H_0^{-1} \frac{\rho_{\rm inf}}{10^{15}{\rm GeV}} \sim 10^{26}. \tag{2.2.8}$$

Therefore, if the scale factor at the end inflation is larger than initial size by 10^{26}, then required e -folding N is

$$N = \ln\left(\frac{a_f}{a_i}\right) = \ln 10^{26} \sim 60. \tag{2.2.9}$$

If we have an expansion of $N > 60$ or more, we can solve the Horizon Problem. In this thesis, if we need N to calculate some physical quantities, we basically take $N = 50 - -60$.

In the above discussion, we focused on the relationship between comoving Hubble $(aH)^{-1}$ and the CMB scale, but we can also confirm the relationship between the scale factor a and the Hubble horizon H^{-1}. If the universe is under accelerated expansion, H^{-1} is almost a constant. On the other hand, a is $a \propto e^{Ht}$. Therefore it gets smaller as going back to the past. This is shown in Figure 2.2.2. Also in this case, a becomes smaller than H^{-1} during accelerated expansion. In the meantime, the photons have a causal relationship, and so it is possible to explain the homogeneity and isotropy of the CMB.

What about the Flatness Problem? When we go back to the universe to the early epoch with decelerated expansion, $(aH)^{-1}$ becomes smaller and smaller, and along with this, the curvature term $K/(aH)^2$ becomes extremely small. However, if the accelerated expansion phase is added, $(aH)^{-1}$ increases at that phase. As we checked in previous discussion, in order to explain the homogeneity and isotropy of CMB, we need the expansion $a_f/a_i \sim e^{60} \sim 10^{26}$. This implies the enough expansion by inflation can significantly relax the fine-tuning problem. If there was inflation, we do not need to assume fine-tuned flatness of the universe in the beginning. In this way the Flatness Problem is also solved.

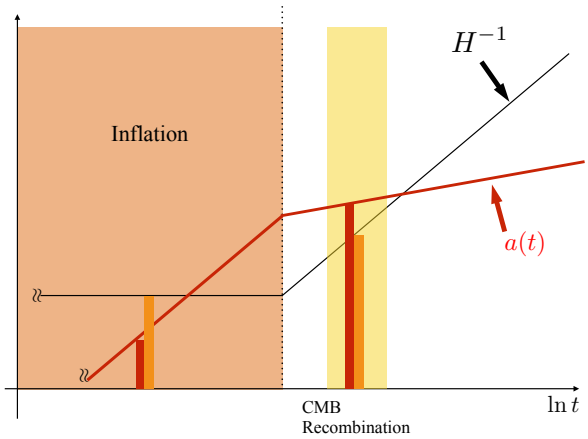

Figure 2.2.2: The time growth of the scale factor and the Hubble horizon when inflation is introduced. While inflation is occurring, H^{-1} is a constant while decreasing a flip the magnitude relation. This can explain the homogeneity and isotropy of the universe.

As described above, two problems of Friedmann cosmology are solved by adding the phase when the universe goes under accelerated expansion before decelerated expansion.

2.2.2 Slow-roll conditions

As we saw in the previous section, assuming that the universe experienced accelerated expansion in the very early epoch, the problems of Friedmann cosmology, Horizon Problem and Flatness Problem, can be solved. In this section we will see how to realize such accelerated expansion. From this section , we will use the notation $M_{pl}^2 = (8\pi G)^{-1}$ (M_{pl} is called the reduced Planck mass).

First we Introduce ϕ as a scalar field and whose action is given by

$$\int \sqrt{-g}\left(\frac{M_{pl}^2}{2}R - \frac{1}{2}(\partial\phi)^2 - V(\phi)\right). \tag{2.2.10}$$

This scalar field ϕ is called an inflaton and $V(\phi)$ is the potential of the

inflaton. Adapting FLRW metric, we can derive following equation from the 00 component of the Einstein equation

$$3M_{pl}^2 H^2 = \frac{1}{2}\dot{\phi}^2 + V \tag{2.2.11}$$

On the other hand, when we vary the action with the inflaton field ϕ, the equation of motion of ϕ follows

$$\ddot{\phi} + 3H\dot{\phi} + V' = 0. \tag{2.2.12}$$

Here, prime represents the differentiation with respect to inflaton ϕ.

Now, how is the acceleration expansion condition $-\dot{H}/H^2 < 1$ expressed using these two equations? Taking the time derivative of both sides of (2.2.11),

$$6M_{pl}^2 \dot{H} H = \dot{\phi}\ddot{\phi}. \tag{2.2.13}$$

Using the expression (2.2.12) to right hand side,

$$6M_{pl}^2 H\dot{H} = -3H\dot{\phi}^2. \tag{2.2.14}$$

Here we used the fact that the potential V does not depend on time explicitly, and so the condition $-\dot{H}/H^2 < 1$ can be rewritten as

$$-\frac{\dot{H}}{H^2} = \frac{\dot{\phi}^2}{2M_{pl}^2 H^2} = \frac{3\dot{\phi}^2}{2(\frac{1}{2}\dot{\phi}^2 + V)} < 1. \tag{2.2.15}$$

Thus, the condition (2.2.15) is satisfied if $\frac{1}{2}\dot{\phi}^2 \ll V$, that means, the potential is dominant in the energy density compared with the kinetic energy.

On the other hand, if ϵ grows with time and becomes larger than unity immediately, it will not get enough expansion. Therefore we need another condition on the growth rate of ϵ. We define,

$$\eta \equiv \frac{1}{2}\frac{d}{dN}\ln\epsilon = \frac{\dot{\epsilon}}{2\epsilon H} \tag{2.2.16}$$

The condition for decreasing the time change of ϵ is $|\eta| < 1$. However, this condition can also be rewritten as a condition for the dynamics of ϕ using the field equation and the Friedmann equation (2.2.16),

$$\begin{aligned}\eta = \frac{1}{2}\frac{d}{dN}\ln\epsilon = \frac{1}{2H}\frac{d}{dt}\ln\epsilon = \frac{1}{2H}\frac{d}{dt}\left[\ln(-\dot{H}) - 2\ln H\right] \\ = \frac{\ddot{H}}{2H\dot{H}} - \frac{\dot{H}}{H^2}.\end{aligned} \tag{2.2.17}$$

Using this expression and (2.2.14),

$$M_{pl}^2\ddot{H} = -\ddot{\phi}\dot{\phi}. \tag{2.2.18}$$

and this is calculated from (2.2.14),

$$\eta = \frac{\ddot{\phi}}{H\dot{\phi}} - \epsilon \tag{2.2.19}$$

Since $\epsilon < 1$, the condition for $|\eta| < 1$ is corresponding to $|\ddot{\phi}| \ll H|\dot{\phi}|$.

From the above, the condition for accelerated expansion $\epsilon < 1$ is $\frac{1}{2}\phi^2 \ll V$, the condition for acceleration expansion is $|\eta| < 1$ Is rewritten as $|\ddot{\phi}| \ll H|\dot{\phi}|$. These two conditions are called slow-roll conditions. Under these conditions, the expression (2.2.11) (2.2.12) are given as

$$3M_{pl}^2H^2 = V, \qquad 3H\dot{\phi} = -V'. \tag{2.2.20}$$

Now we can determine how the scale factor $a(t)$ evolves under the conditions (2.2.20). We impose the slow-roll conditions, and so the time evolution of the inflaton is very slow. Therefore, the growth of the potential is small and V can be regarded as almost constant. That means $H \sim$ Const. and in this situation the time evolution of the scale factor a follows

$$\frac{\dot{a}}{a} = H(\sim \text{Const}) \quad \Rightarrow \quad \dot{a} = Ha \quad \Rightarrow \quad a(t) = e^{Ht}. \tag{2.2.21}$$

When we introduce the action of inflaton and realize accelerated expansion by

imposing slow-roll conditions then the universe expands exponentially. This class of inflation is called slow-roll inflation and a lot of models have been proposed in last decades. Therefore, we have to discriminate each model and to confirm what kinds of models can fit to observational results in some way. In next chapter, we focus such method, namely cosmological perturbation.

Chapter 3

Primordial curvature perturbation

In this chapter, we will review cosmological perturbation theory and learn how to compute primordial curvature perturbation generated by inflation. In inflationary cosmology, it is one of the most powerful and informative way to discriminate each inflation model by comparing theoretically predicted primordial curvature perturbation and observed CMB temperature fluctuation.

3.1 Quantum Fluctuations during Inflation

We introduced slow-roll inflation in the previous chapter, but we did not see any specific inflation model. In the past few decades, huge numbers of inflation models which could realize the accelerated expansion have been proposed. Therefore, we have to verify these models in some way and determine models that can explain the observational results. In this chapter, first we will review cosmological perturbation in which we add a tiny perturbation to homogeneous and isotropic background. We can see how this perturbation variables and inflation models are related. The goal of this chapter is to find how to verify each inflation models by comparing the primordial density fluctuation with the temperature fluctuation of the CMB.

Cosmological Perturbation

In this section we introduce small perturbations to the homogeneous and isotropic background which we have worked on so far. After that, we will learn how each perturbation variables are transformed with respect to coordinate transformation.

The basic concept of cosmological perturbation is as follows. We divide arbitral quantities $X(t, \mathbf{x})$ into a homogeneous and isotropic part $\bar{X}(t)$ that does not depend on space coordinate and a part which depends on all of spacetime coordinates,

$$\delta X(t, \mathbf{x}) \equiv X(t, \mathbf{x}) - \bar{X}(t). \tag{3.1.1}$$

This class of perturbation is called linear perturbation. In the first order of this perturbation, the Einstein equation is schematically written as

$$\delta G_{\mu\nu} = (M_{pl})^{-2} \delta T_{\mu\nu}. \tag{3.1.2}$$

We will discuss the perturbation to the Einstein tensor which corresponds to Metric Perturbation and Matter Perturbation which is related to the energy momentum tensor.

Metric Perturbation

In the ideal homogeneous and isotropic universe, inflaton ϕ and metric $g_{\mu\nu}$ depend only on the time coordinate t. We can decompose ϕ and $g_{\mu\nu}$ into background part and small deviation part from background like following.

$$\phi(t, \mathbf{x}) = \bar{\phi}(t) + \delta\phi(t, \mathbf{x}), \qquad g_{\mu\nu}(t, \mathbf{x}) = \bar{g}_{\mu\nu}(t) + \delta g_{\mu\nu}(t, \mathbf{x}). \tag{3.1.3}$$

On the other hand, the perturbed metric $g_{\mu\nu}(t, \mathbf{x})$ can be expressed by each components with introducing arbitral functions.

$$
\begin{aligned}
ds^2 &= g_{\mu\nu}dx^\mu dx^\nu && (3.1.4)\\
&= -(1+2\Phi)dt^2 + 2aB_i dx^i dt + a^2[(1-2\Psi)\delta_{ij} + E_{ij}]dx^i dx^j && (3.1.5)
\end{aligned}
$$

Here, Φ, Ψ are called scalar perturbation. B_i and E_{ij} are also decomposed into scalar, vector, and tensor type perturbations,

$$
B_i \equiv \partial_i B - S_i, \quad \text{where} \quad \partial^i S_i = 0. \tag{3.1.6}
$$

$$
E_{ij} \equiv 2\partial_{ij}E + 2\partial_{(i}F_{j)} + h_{ij}, \qquad \text{where} \quad \partial^i F_i = 0, , \quad h^i_i = \partial^i h_{ij} = 0. \tag{3.1.7}
$$

From this decomposition, B, S is also called scalar perturbation, and S_i, F_i are called vector type perturbation and h_{ij} is called tensor type perturbation. Regarding vector perturbation, we can easily derive its evolution equation but we only obtain decaying solution of vector perturbation unless we consider special cases. Thus, in this thesis, we focus on scalar and tensor perturbation only.

Now we can see the transformation laws of each scalar perturbation Φ, B, E, Ψ with respect to the coordinate transformation t and x^i. Using arbitral functions $\alpha(x), \beta(x)$, they are given by,

$$
\begin{aligned}
t &\to t + \alpha, \\
x^i &\to x^i + \delta^{ij}\beta_{,j}.
\end{aligned} \tag{3.1.8}
$$

then, each perturbed quantities are transformed as

$$
\begin{aligned}
\Phi &\to \Phi - \dot{\alpha}, \\
B &\to B + a^{-1}\alpha - a\dot{\beta}, \\
E &\to E - \beta, \\
\Psi &\to \Psi + H\alpha.
\end{aligned}
$$

These are the transformation laws of each component of the perturbation to the metric.

Matter Perturbation

Next, we see the perturbation to the energy momentum tensor. Let each of the components of the energy momentum tensor be the unperturbed part of energy density $\bar{\rho}$, the unperturbed part of pressure $\bar{p}$ and the quantities with δ be the corresponding perturbation of each components.

$$\begin{aligned} T^0_0 &= -(\bar{\rho} + \delta\rho), \\ T^0_i &= (\bar{\rho} + \bar{p})av_i, \\ T^i_0 &= -(\bar{\rho} + \bar{p})(v^i - B^i)/a, \\ T^i_j &= \delta^i_j(\bar{p} + \delta p) + \Sigma^i_j. \end{aligned}$$

Here, v_i is defined as the spatial velocity $v_i \equiv u^i/u^0$ with the unit vector normalized as $u^\mu u_\nu = -1$. $\Sigma^i_{\ j}$ represents the anisotropic component of the stress tensor. ρ is energy density, p is pressure and q is defined as $(\delta q)_{,i} = (\bar{\rho} + \bar{p})$. For each quantities, we get the following.

$$\begin{aligned} \delta\rho &\to \delta\rho - \dot{\bar{\rho}}\alpha, \\ \delta p &\to \delta p - \dot{\bar{p}}\alpha, \\ \delta q &\to \delta q + (\bar{\rho} + \bar{p})\alpha. \end{aligned}$$

These are the transformation laws of each perturbed components of the energy momentum tensor.

Gauge Choice

So far we have considered transformation laws like (3.1.8) with respect to coordinate transformation. In general relativity, it is required that the theory is invariant under general coordinate transformation, and so the functions α, β can be any function. That is why, we need to pay much attention to *"what kind of gauge do we take?"* To see this problem, as an example, let us consider a completely homogeneous and isotropic universe that is not perturbed at all. Perfectly homogeneous and isotropic universe the energy density is free from spatial coordinates $\rho(t, \mathbf{x}) = \rho(t)$. Here we consider the coordinates transformations (3.1.8) $\tilde{t} = t + \alpha(t, \mathbf{x})$, then it gives a new coordinate system. $\rho(t) + \delta\rho(t(\tilde{t}, \mathbf{x}))$ $(\tilde{t}, \mathbf{x})$, the homogeneity and isotropy are lost and it looks like a perturbed universe. In fact, however, since we assumed that the universe is completely homogeneous and isotropic, we realize that this perturbed universe is not a physical one but simply due to coordinate transformation.

As described above, in cosmological perturbation, "apparent" perturbation caused by coordinate transformation (it is local transformations, and sometimes it is called gauge transformations) and true perturbation with actual fluctuation of energy density are can be mixed up. Therefore, we need to be careful not to be confused with them.

There are two well-established solutions to this problem. One is a gauge fixing method. In this method, we impose some conditions on each transformation function of gauge transformation and adopts only those which satisfy the conditions. This is Although it is a familiar method also in electromagnetism and the like, in the perturbation cosmology the relationship between a variable obtained by fixing a certain gauge and another variable obtained by another gauge fixing becomes very complicated, It will be difficult to guide many. The other is a method of gauge invariant perturbation theory that defines gauge invariant variables by taking appropriate linear combination of the perturbation variables defined above. In this method, once a gauge invariant variable is defined, no matter how coordinate transformation is performed

Since their expressions do not change, concerning this variable, it becomes unnecessary to worry about "apparent perturbation" or "true perturbation" as mentioned above. Because of this usefulness, we will adopt the gauge invariant perturbation theory in this thesis. We will see details of this method below.

Gauge-invarinat Variables

As we saw in the previous subsection, if we can define quantities which do not change its expression by coordinate transformation, the Gauge Choice problem is solved. We define such quantities by taking the appropriate combination of perturbation variables we have seen so far. First, we introduce so-called comoving curvature perturbation which is defined as,

$$\mathcal{R} \equiv \Psi - \frac{H}{\bar{\rho} + \bar{p}} \delta q. \tag{3.1.9}$$

The transformation of $\mathcal{R}$ follows from the transformation laws of $\Psi, \delta\rho, \delta p, \delta q$,

$$\begin{aligned} \mathcal{R} \to \tilde{\mathcal{R}} &= \Psi + H\alpha - \frac{H}{\bar{\rho} + \bar{p}} (\delta q + (\bar{\rho} + \bar{p})\alpha) \\ &= \Psi + H\alpha - \frac{H}{\bar{\rho} + \bar{p}}\ \delta q - H\alpha \\ &= \Psi - \frac{H}{\bar{\rho} + \bar{p}}\ \delta q. \end{aligned} \tag{3.1.10}$$

From above computation, it turns out that $\mathcal{R}$ is gauge invariant. Δq is also related to T^0_i component of the energy momentum tensor and $T^0_i = \partial_i \delta q$. On the other hand, in inflation, T^0_i can be expressed in terms of inflaton ϕ. Since it is $T^0_i = -\dot{\bar{\phi}} \partial_i \delta\phi$, we can rewrite q with respect to ϕ,

$$\mathcal{R} = \Psi + \frac{H}{\dot{\bar{\phi}}} \delta\phi. \tag{3.1.11}$$

In the frame which observers move together with the inflaton ϕ (comoving coordinate of the inflaton), we find $\delta\phi = 0$ and $\mathcal{R} = \Psi$. On the other hand, calculating the three-dimensional spational scalar curvature ${}^{(3)}R$ in perturbed

FLRW metric, we yield ${}^{(3)}R = 4\nabla^2\Psi/a^2$.

Therefore, $\mathcal{R}$ is directly related to three-dimensional space curvature in the comoving coordinate of the inflaton. This is why $\mathcal{R}$ is called comoving curvature perturbation.

Next we introduce uniform-density curvature perturbation as yet another important gauge invariant variable. This is defined as follows.

$$-\zeta \equiv \Psi + \frac{H}{\dot{\bar{\rho}}}\delta\rho. \tag{3.1.12}$$

As with the case of $\mathcal{R}$, we can also confirm that it is invariant to coordinate transformation by using the transformation laws of Ψ, ρ.

$$\begin{aligned} -\zeta \to -\tilde{\zeta} &= \Psi + H\alpha + \frac{H}{\dot{\bar{\rho}}}(\delta\rho - \dot{\bar{\rho}}\alpha) \\ &= \Psi + \frac{H}{\dot{\bar{\rho}}}\delta\rho + H\alpha - H\alpha \\ &= \Psi + \frac{H}{\dot{\bar{\rho}}}\delta\rho. \end{aligned} \tag{3.1.13}$$

The reason why this ζ is called uniform-densisty curvature perturbation is almost the same as comoving curvature perturbation. In a constant time hypersurface of uniform-density ($\delta\rho = 0$), we obtain $-\zeta = \Psi$ and again this Ψ is directly related to the three-dimensional space curvature $\mathcal{R}$.

By using the first order perturbed equation, we obtain the relationship between the Fourier components of $\mathcal{R}$ and ζ,

$$-\zeta_{\mathbf{k}} = \mathcal{R}_{\mathbf{k}} + \frac{k^2}{(aH)^2}\frac{2\bar{\rho}}{3(\bar{\rho}+\bar{p})}\Psi_{\mathrm{B}}. \tag{3.1.14}$$

It is understood that there is a relation that. k^2 is the wave number in Fourier space, which corresponds to the scale (mode) of interest in real space. In addition, Ψ_{B} introduced here is called Bardeen potential and is defined as follows: [27].

$$\Psi_{\rm B} \equiv \Psi + a^2 H(\dot{E} - B/a) \tag{3.1.15}$$

When $k^{-1} \gg (aH)^{-1}$ in the second term of the expression (3.1.14), that is, when the mode of interest is sufficiently larger than comoving hubble This is called superhorizon mode or superhorizon scale), the second term can be ignored, The result is $-\zeta \sim \mathcal{R}$. In superhorizon scale, ζ and $\mathcal{R}$ match. Therefore, for the correlation function to be computed later (eg 2 point correlation function) $\langle\zeta\zeta\rangle$ and $\langle\mathcal{R}\mathcal{R}\rangle$ matches.

3.1.1 Quantum Fluctuations in Inflationary Universe

In this section we quantize the gauge-invariant perturbation $\mathcal{R}$ (or ζ) considered in the previous section. We trace the procedure used in the quantum field theory and calculate the power spectrum of the fluctuation generated during inflation. Since curvature perturbation is almost constant outside of Horizon, this power spectrum is often evaluated at the timing just when fluctuation crosses Horizon (called Horizon crossing or Horizon exit). The outline to calculate power spectrum is following.

1. Consider the case of perturbed action (2.2.10), and expand action up to the second order. In particular, we need to pay attention to terms up to the second order of $\mathcal{R}$.

2. We derive the equation of motion of $\mathcal{R}$.

3. Performing the Fourier transform. The equations of each mode of $\mathcal{R}$ are complicated. In order to solve these equations approximately, we rely on the slow-roll conditions.

4. Quantizing $\mathcal{R}$ with the canonical commutation relation. This is one of the boundary condition (normalization condition) for determining the solution.

5. Define the vacuum to be consistent with UV side (*i.e.* the vacuum well inside the Horizon). This makes it possible to completely determine the mode function.

6. From the calculation of the two-point function of v, find the power spectrum of curvature fluctuation.

The outline of this calculation is similar for tensor perturbation h_{ij}.

Scalar Perturbations

We start with calculation of scalar perturbation. The starting action is the same as (2.2.10),

$$\int \sqrt{-g}\left(\frac{1}{2}R - \frac{1}{2}(\partial\phi)^2 - V(\phi)\right). \tag{3.1.16}$$

(In this calculation, we adopt the unit system $M_{pl} = 1$). In this action (2.2.10) we consider perturbation on FLRW metric. Especially since we are interested in $\mathcal{R}$,we will adopt the following gauge.

$$\delta\phi = 0, \quad g_{ij} = a^2\left[(1-2\mathcal{R})\delta_{ij} + h_{ij}\right], \quad \partial_i h_{ij} = h^i_i = 0. \tag{3.1.17}$$

This is the comoving gauge of the inflaton mentioned before. By adopting this gauge, we do not need to think about the fluctuation of the inflaton, and there is an advantage that the scalar perturbation Ψ is identical to $\mathcal{R}$. Other scalar perturbations such as Φ, B are related to $\mathcal{R}$ by the Einstein equation but we can prove that they do not have any kinetic terms and just give constraint equations. Thus we concentrate on $\mathcal{R}$ only.

After a long but straightforward calculation (see Appendix A for details of this calculation), The actions up to the second order of $\mathcal{R}$ are given by

$$S_{(2)} = \frac{1}{2}\int d^4x a^3 \frac{\dot{\phi}^2}{H^2}\left[\dot{\mathcal{R}}^2 - a^{-2}(\partial_i\mathcal{R})^2\right]. \tag{3.1.18}$$

Here we introduce a variable called Mukhanov-Sasaki variable for simplification of the symbol. This is defined as follows.

$$v \equiv zR, , \qquad \text{where} \qquad z^2 \equiv a^2 \frac{\dot{\phi}^2}{H^2} = 2a^2\epsilon. \tag{3.1.19}$$

Rewriting (3.1.18) using this variable, we get

$$S_{(2)} = \frac{1}{2}\int d\tau d^3x \left[(v')^2 + (\partial_i v)^2 + \frac{z''}{z}v^2\right], \qquad (...)' \equiv \partial_\tau(...). \tag{3.1.20}$$

Here, we replaced the time variable t with the conformal time τ defined by $d\tau = dt/a$.

Since action (3.1.20) is now obtained, we can derive the equation of motion of v.

$$v'' - \left(\partial^i\partial_i + \frac{z''}{z}\right)v = 0. \tag{3.1.21}$$

Performing Fourier transformation and rewriting (3.1.21) into the expression of each mode.

$$v_k'' + \left(k^2 - \frac{z''}{z}\right)v_k = 0. \tag{3.1.22}$$

Here, v_k is defined by the following Fourier transformation.

$$v(\tau, \mathbf{x}) = \int \frac{d^3k}{(2\pi)^3} v_{\mathbf{k}}(\tau) e^{i\mathbf{k}\cdot\mathbf{x}} \tag{3.1.23}$$

It is difficult to solve this equation (3.1.22) analytically. However, when the background spacetime is under de Sitter expansion, like inflation, it is possible to obtain an approximated analytical solution with the slow-roll conditions. We will see it later sections.

Quantization

Here we consider quantization v with the same procedure as when we quantize a scalar field. First, performing plane-wave expansion of v,

$$v \quad \rightarrow \quad \hat{v} = \int \frac{d\mathbf{k}^3}{(2\pi)^3} \left[v_k(\tau)\hat{a}_{\mathbf{k}} e^{i\mathbf{k}\cdot\mathbf{x}} + v_k^*(\tau)\hat{a}_{\mathbf{k}}^\dagger e^{-i\mathbf{k}\cdot\mathbf{x}} \right]. \tag{3.1.24}$$

As we do in the scalar field quantization, the Fourier component $v_{\mathbf{k}}$ of v is decomposed as follows.

$$v_{\mathbf{k}} \quad \rightarrow \quad \hat{v}_{\mathbf{k}} = v_k(\tau)\hat{a}_{\mathbf{k}} + v_{-k}^*(\tau)\hat{a}_{-\mathbf{k}}^\dagger, \tag{3.1.25}$$

Creation and annihilation operators $\hat{a}_{\mathbf{k}}, \hat{a}_{\mathbf{k}}^\dagger$

$$[\hat{a}_{\mathbf{k}}, \hat{a}_{\mathbf{k}'}^\dagger] = (2\pi)^3 \delta(\mathbf{k} - \mathbf{k}'). \tag{3.1.26}$$

It satisfies the exchange relationship that $v_{\mathbf{k}}$ is

$$\langle v_k, v_k \rangle \equiv i(v_k^* v_k' - v_k^{*\prime} v_k) = 1. \tag{3.1.27}$$

This is equivalent to imposing a canonical commutation relation on v and its canonical conjugate variable v'. In order to solve (3.1.22), two boundary conditions of v_k are required. However, the normalization condition (3.1.27) gives one of the conditions. Another boundary condition is obtained from a vacuum choice. In the next section we will discuss this point.

Boundary Conditions and Bunch-Davies Vacuum

Using the annihilation operator $\hat{a}_{\mathbf{k}}$ as defined in the previous section, a vacuum state is defined as,

$$\hat{a}_{\mathbf{k}}|0\rangle = 0. \tag{3.1.28}$$

It seems one of a natural choice. However, the story is not so simple. For example, just replace $(\partial^i\partial_i + z''/z)$ in the expression (3.1.21) as $\omega^2(\tau)$

$$v'' - \omega^2(\tau)v = 0. \tag{3.1.29}$$

This can be interpreted as the case in which the frequency of the harmonic oscillator is not constant and it is a function of τ. When the frequency is constant, we can define a proper variable and its canonical conjugate to do with quantum mechanics $\hat{a}_{\mathbf{k}}, \hat{a}^\dagger_{\mathbf{k}}$ is expressed in a linear combination is the only one. However, when the frequency is not constant and it is a certain function as it is now, ambiguity corresponding to that remains, and as a result, the above expression is not determined uniquely. Since this situation actually occurs in (3.1.21) (3.1.22), we have to choose a vacuum considering this situation [24].

The simplest way to make it easier for subsequent discussions is to place $\tau \to -\infty$ and $\hat{a}_{\mathbf{k}}|0\rangle = 0$. In $\tau \to -\infty$ any scale is inside enough of the comoving hubble and in this limit it is $k^{-1}\ ll(aH)^{-1}$, and so the expression (3.1.22)

$$v_k'' + k^2 v_k = 0. \tag{3.1.30}$$

This is a simple plane wave equation and its solution is given by $v_k \propto e^{-ik\tau}$. From the discussion on how to choose a vacuum like this one more boundary condition was obtained for v_k.

$$\lim_{\tau\to-\infty} v_k = \frac{e^{-ik\tau}}{\sqrt{2k}} \tag{3.1.31}$$

However, the factor $(\sqrt{2k})^{-1}$ was attached for the convenience of later standardization.
Now we have two boundary conditions (3.1.27) (3.1.31) for the expression (3.1.22), and so in principle v_k can be completely determined.

Solutions in de Sitter limit

Even though the boundary conditions are obtained, it is not easy to find a general analytical solution of (3.1.22). Next we address approximate analytical solutions here by taking de Sitter limit ($\epsilon \to 0$).

First we focus the term z''/z in (3.1.22). This term becomes ($H = $ Const.) in de Sitter limit.

$$z'' = \frac{1}{H}\left(a''\dot{\phi} + a\dot{\phi}' + a'\dot{\phi}' + a\dot{\phi}''\right). \tag{3.1.32}$$

On the other hand, as we saw in Chapter 2, in order to get accelerated expansion, the motion of inflaton must satisfy the slow-roll conditions. Thus all the second, third and forth terms in the parenthesis of the right hand side of (3.1.32) can be ignored. Therefore we get,

$$\frac{z''}{z} = \frac{a''}{a}. \tag{3.1.33}$$

Since in de Sitter limit $H \sim$ Const.,

$$\begin{aligned} a'' =& a\frac{d}{dt}\left(a\frac{da}{dt}\right) = a\frac{d}{dt}(a^2 H) = 2a^2\dot{a}H \\ \Rightarrow & \frac{a''}{a} = 2a^2H^2 \end{aligned} \tag{3.1.34}$$

Furthermore, in de Sitter limit $a \propto e^{Ht}$. Thus by integrating $d\tau = dt/a$,

$$\tau = \int \frac{dt}{a} = \int e^{-Ht}dt = -\frac{1}{aH} \tag{3.1.35}$$

after all, we can derive

$$\frac{z''}{z} = \frac{a''}{a} = \frac{2}{\tau^2}. \tag{3.1.36}$$

Substituting this for (3.1.22),

$$v_k'' + \left(k^2 - \frac{2}{\tau^2}\right)v_k = 0 \tag{3.1.37}$$

However, the general solution of this equation is following.

$$v_k = \alpha \frac{e^{-ik\tau}}{\sqrt{2k}} \left(1 - \frac{i}{k\tau}\right) + \beta \frac{e^{ik\tau}}{\sqrt{2k}} \left(1 + \frac{i}{k\tau}\right). \tag{3.1.38}$$

Here,α, β are arbitral constants. ((3.1.38)) is directly assigned to (3.1.37), it is confirmed that it is a solution). We determine this indefinite constant α, β by two boundary conditions (3.1.27) (3.1.31). The result is $\alpha = 1, \beta = 0$.

Based on the above discussion, the form of the mode function v_k in de Sitter limit was completely determined.

$$v_k = \frac{e^{-ik\tau}}{\sqrt{2k}} \left(1 - \frac{i}{k\tau}\right) \tag{3.1.39}$$

3.1.2 Power Spectrum of curvature perturbation

Now we can calculate the Power Spectrum with the concrete form of the mode function at de Sitter limit. For convenience of calculation we introduce $\hat{\psi}_{\mathbf{k}} \equiv a^{-1}\hat{v}_{\mathbf{k}}$. Using the expansion with the creation/annihilation operator of $\hat{v}_{\mathbf{k}}$,

$$\begin{aligned} \langle \hat{\psi}_{\mathbf{k}}(\tau)\hat{\psi}_{\mathbf{k}'}(\tau)\rangle &= (2\pi)^3\delta(\mathbf{k}+\mathbf{k}')\frac{|v_k(\tau)|^2}{a^2} \\ &= (2\pi)^3\delta(\mathbf{k}+\mathbf{k}')\frac{H^2}{2k^3}(1+k^2\tau^2). \end{aligned} \tag{3.1.40}$$

On the superhorizon scale $|k\tau| = |k/aH| \ll 1$, it reduces to

$$\langle \hat{\psi}_{\mathbf{k}}(\tau)\hat{\psi}_{\mathbf{k}'}(\tau)\rangle \to (2\pi)^3\delta(\mathbf{k}+\mathbf{k}')\frac{H^2}{2k^3}. \tag{3.1.41}$$

$$\langle \hat{\psi}_{\mathbf{k}}(\tau)\hat{\psi}_{\mathbf{k}'}(\tau)\rangle = (2\pi)^3\delta(\mathbf{k}+\mathbf{k}')P_\psi(k), \qquad \Delta^2_\psi(k) \equiv \frac{k^3}{2\pi^2}P_\psi(k) \tag{3.1.42}$$

Here we introduce P_ψ, Δ^2_ψ above and the dimension less power spectrum Δ^2_ψ is expressed as

$$\Delta_{\psi}^2 = \left(\frac{H}{2\pi}\right)^2 \tag{3.1.43}$$

the relationship between v and $\mathcal{R}$ is (3.1.19). Therefore the two-point function of the mode function of $calR$ is finally given by the following equation.

$$\langle \mathcal{R}_{\mathbf{k}} \mathcal{R}_{\mathbf{k}'} \rangle = (2\pi)^3 \delta(\mathbf{k} + \mathbf{k}') \frac{H_*^2}{2k^3} \frac{H_*^2}{\dot{\phi}_*^2} \tag{3.1.44}$$

Here, $*$ means the values evaluated at the Horizon crossing point. Besides, introducing $\Delta_{\mathcal{R}}, P_{\mathcal{R}}$ as follows,

$$\langle \mathcal{R}_{\mathbf{k}} \mathcal{R}_{\mathbf{k}'} \rangle = (2\pi)^3 \delta(\mathbf{k} + \mathbf{k}') P_{\mathcal{R}}(k), \qquad \Delta_{\mathcal{R}}^2(k) \equiv \frac{k^3}{2\pi^2} P_{\mathcal{R}}(k) \tag{3.1.45}$$

we can again define dimension less power spectrum $\Delta_{\mathcal{R}}^2(k)$ as

$$\Delta_{\mathcal{R}}^2(k) = \frac{H_*^2}{(2\pi)^2} \frac{H_*^2}{\dot{\phi}_*^2}. \tag{3.1.46}$$

This is the way of calculating the power spectrum of the curvature fluctuation for the scalar perturbation. The point is that we assumed slow-roll inflation to get this result. When calculating Power Spectrum for inflation model other than slow-roll, we have to follow the time evolution of Mukhanov variable v more precisely but in many cases we can not calculate it analytically. In such a case it is necessary to numerically calculate the time evolution of v but we will not go into the details here.

Tensor Perturbations

Next, we address the calculation of the tensor perturbation. The procedure of calculation is almost same with the case of scalar perturbation. First as well as in scalar perturbation, expand action (3.1.16) to second order of h_{ij} (3.1.17).

$$S_{(2)} = \frac{1}{8}\int d\tau dx^3 a^2 \left[(h'_{ij})^2 - (\partial_l h_{ij})^2\right]. \tag{3.1.47}$$

but this is almost same as the action of the massless scalar field in the FLRW spacetime.

Expanding h_{ij} as follows,

$$h_{ij} = \int \frac{d^3k}{(2\pi)^3} \sum_{s=+,\times} \epsilon^s_{ij}(k) h^s_{\mathbf{k}}(\tau) e^{i\mathbf{k}\cdot\mathbf{x}}. \tag{3.1.48}$$

Here, ϵ_{ij} satisfies $\epsilon_{ii} = k^i \epsilon_{ij} = 0$ and $\epsilon^s_{ij}(k)\epsilon^{s'}_{ij}) = 2\delta_{ss'}$. $s = +, \times$ correspond to two modes of gravitational wave, $+$ is called E mode, $\times$ is called B mode. Substituting the expansion of h_{ij} to (3.1.47) and performing x integration, we get

$$S_{(2)} = \sum_s \int d\tau d\mathbf{k} \frac{a^2}{4} \left[h^{s\prime}_{\mathbf{k}} h^{s\prime}_{\mathbf{k}} - k^2 h^s_{\mathbf{k}} h^s_{\mathbf{k}}\right]. \tag{3.1.49}$$

Here we define the new variable $v^s_{\mathbf{k}}$ as we did in the scalar case.

$$v^s_{\mathbf{k}} \equiv \frac{a}{2} h^s_{\mathbf{k}} \tag{3.1.50}$$

By rewriting (3.1.49) using this variable,

$$S_{(2)} = \sum_s \frac{1}{2} \int d\tau d^3\mathbf{k} \left[(v^{s\prime}_{\mathbf{k}})^2 - \left(k^2 - \frac{a''}{a}\right)(v^s_{\mathbf{k}})^2\right]. \tag{3.1.51}$$

Also in this action de Sitter limit

$$\frac{a''}{a} = \frac{2}{\tau^2}, \tag{3.1.52}$$

can be applicable. Here we can find that (3.1.51) looks two-copy of scalar perturbation.

Quantization

As mentioned above, since $h^s_{\mathbf{k}}$ can be regarded as a massless scalar field in FLRW space-time, we can use $\hat{\psi}_{\mathbf{k}}$ introduced in the case of scalar perturbation,

$$h^s_{\mathbf{k}} = 2\psi^s_{\mathbf{k}} = 2\psi_{\mathbf{k}}, \qquad \psi_{\mathbf{k}} \equiv \frac{v_{\mathbf{k}}}{a}. \tag{3.1.53}$$

Now we can use the formula of the power spectrum calculated for $\psi_{\mathbf{k}}$. Since $\Delta^2_\psi = (H/2\pi)^2$, power spectrum of the tensor perturbation Δ^2_h simply multiplied factor 4.

$$\Delta^2_h(k) = 4\left(\frac{H_*}{2\pi}\right)^2 \tag{3.1.54}$$

In the following sections, we will use the expression $\Delta_{\mathcal{R}} \equiv \Delta_s$ for scalar perturbation and $\Delta^2_t \equiv 2\Delta^2_h$ for tensor perturbation.

Energy Scale of Inflation and Lyth Bound

Here we introduce tensor-to-scalar ratio r, which is an important parameter for evaluating inflation model.

$$r \equiv \frac{\Delta^2_t(k)}{\Delta^2_s(k)} \tag{3.1.55}$$

This is the ratio of the tensor perturbation and the scalar perturbation created by inflation. Since generated perturbations are different from each inflation model. Thus we can evaluate the model by comparing it with CMB temperature fluctuation.

By setting the value of r, we can estimate the energy scale of inflation. The typical size of Δ^2_s is $\sim 10^{-9}$. On the other hand, using (3.1.54) and the Friedmann equation (2.2.20) with slow-roll approximation, we obtain $\Delta_t \propto H^2 \sim V$. By using this relationship, the energy scale at which inflation

have occurred is given as

$$V^{1/4} \sim \left(\frac{r}{0.01}\right)^{1/4} 10^{16}\text{GeV}. \tag{3.1.56}$$

For example, let us consider $r \sim 0.1$. $(r/0.01)^{1/4}$ is not too large to change the order of magnitude, $V^{1/4} \sim 10^{16}$GeV and the scale of Inflation is estimated to be about GUT scale.

In addition, we can estimate the extent of the inflaton field ϕ inflation between Inflation using r. (3.1.46) (3.1.54) r,

$$\begin{aligned} r = \frac{\Delta_t^2(k)}{\Delta_s^2(k)} = \frac{2\Delta_h^2(k)}{\Delta_{\mathcal{R}}^2(k)} &= 8\left(H^2 \cdot \frac{\dot{\phi}^2}{H^4}\right) \\ &= 8\left(\frac{1}{H^2}\left(\frac{d\phi}{dt}\right)^2\right) \\ &= 8\left(\frac{1}{H^2}\left(\frac{dN}{dt}\frac{d\phi}{dN}\right)^2\right) = 8\left(\frac{d\phi}{dN}\right)^2. \end{aligned} \tag{3.1.57}$$

We used that $N = \ln(a_f/a_i) = \int_i^f (da/a) = \int H dt$. If we revive M_{pl} (3.1.57) for understanding of the scale,

$$\frac{\Delta\phi}{M_{pl}} = \int_{N_f}^{N_i} dN \sqrt{\frac{r}{8}}. \tag{3.1.58}$$

Here, $\Delta\phi$ represents how much the inflaton has valid during inflation. As long as the slow-roll condition are satisfied, r does not change so much and is considered to be almost constant. Thus, (3.1.58) can be rewritten as follows [28].

$$\frac{\Delta\phi}{M_{pl}} = \int_{N_f}^{N_i} dN \sqrt{\frac{r}{8}} \sim \sqrt{\frac{r}{8}} \int_{N_f}^{N_i} dN = \sqrt{\frac{r}{8}} \cdot 60 \sim \mathcal{O}(1) \times \left(\frac{r}{0.01}\right)^{1/2}. \tag{3.1.59}$$

From this rough estimation, if r is greater than 0.01, it is $\Delta\phi > M_{pl}$, which

means that the excursion of inflaton is greater than the Plank scale. This type of Inflation models is called large field Inflation. A model such as $\Delta\phi < M_{pl}$ is called small field inflation. In this paper we mainly focus on the large field type Inflation model.

Relations between power spectrum and inflaton potential

In this section we will see the relationship between power spectrums Δ_s, Δ_t and the potential of inflaton. The goal of this chapter is to evaluate and verify each inflation model by comparing power spectrum and temperature fluctuation of CMB. Since most terms other than the potential term are common in most slow-roll inflation models, the characteristics of models are reflected in the potential. Therefore, if a relationship between power spectrum and potential is obtained, we can immediately discriminate each model or put constraints from CMB observation.

First of all, power spectrum of scalar perturbation was derived as

$$\Delta_s = \frac{H^2}{(2\pi)^2}\frac{H^2}{\dot{\phi}^2} \tag{3.1.60}$$

On the other hand, the slow-roll parameter ϵ introduced in Chapter 2 (2.2.1) is defined as $\epsilon = -\dot{H}/H^2$. In addition, $\dot{H}$ has been calculated under slow-roll conditions (2.2.14) and $\dot{H} = -\dot{\phi}^2/2M_{pl}^2$. Therefore, Δ_s can be represented by ϵ,

$$\Delta_s^2 = \frac{1}{8\pi^2}\frac{H^2}{M_{pl}^2}\frac{1}{\epsilon} \tag{3.1.61}$$

Using this equation and (3.1.54), we can see that r is represented only by the slow-roll parameter ϵ.

$$r = \frac{\Delta_t^2}{\Delta_s^2} = 16\epsilon \tag{3.1.62}$$

We can express ϵ with the potential using the (2.2.14) and (2.2.20) under slow-roll conditions.

$$\begin{aligned}\epsilon = -\frac{\dot{H}}{H^2} = \frac{1}{2M_{pl}^2}\left(\frac{\dot{\phi}}{H}\right)^2 &= \frac{1}{2M_{pl}^2}\left(\frac{3H\dot{\phi}}{3H^2}\right)^2 \\ &= \frac{1}{2M_{pl}^2}\left(\frac{-V'}{V/M_{pl}^2}\right)^2 = \frac{M_{pl}^2}{2}\left(\frac{V'}{V}\right)^2.\end{aligned} \tag{3.1.63}$$

this final expression

$$\epsilon_{\mathrm{v}} \equiv \frac{M_{pl}^2}{2}\left(\frac{V'}{V}\right)^2 \tag{3.1.64}$$

It should be noted that $\epsilon \sim \epsilon_{\mathrm{v}}$ is only available when the slow-roll condition is satisfied.

From the above discussion, we can represent the power spectrum of each scalar and tensor now with potential and ϵ_{v}.

$$\Delta_s^2 \sim \frac{1}{24\pi^2}\frac{V}{M_{pl}^4}\frac{1}{\epsilon_{\mathrm{v}}}, \qquad \Delta_t^2 \sim \frac{2}{3\pi^2}\frac{V}{M_{pl}^4} \tag{3.1.65}$$

Also, in slow-roll approximation, r is expressed as

$$r \sim 16\epsilon_{\mathrm{v}} \tag{3.1.66}$$

This is the relationship between the potential of power spectrum, r and inflaton that these were desired.

The relationship between e -folding N and ϵ_{v} is also derived. Since $dN = -Hdt$,

$$dN = -Hdt = -\frac{H}{\dot{\phi}}d\phi = -\frac{3H^2}{3\dot{H}\phi}d\phi \sim \frac{1}{M_{pl}^2}\frac{V}{V'}d\phi, \tag{3.1.67}$$

According to the definition of ϵ_{v},

$$N = \int_{\phi_f}^{\phi_*} \frac{d\phi}{M_{pl}} \frac{1}{\sqrt{2\epsilon_{\rm v}}}. \tag{3.1.68}$$

Scale-Dependence

The scale dependence of power spectrum is also an important index in verifying inflation models called spectral index.

$$n_s - 1 \equiv \frac{d\ln\Delta_s^2}{d\ln k}, \qquad n_t \equiv \frac{d\ln\Delta_t^2}{d\ln k}. \tag{3.1.69}$$

For example, for the scalar perturbation, this can be rewritten as follows.

$$\begin{aligned} \frac{d\ln\Delta_s^2}{d\ln k} &= \frac{d\ln\Delta_s^2}{dN} \times \frac{dN}{d\ln k} \\ &= \left(2\frac{d\ln H}{dN} - \frac{d\ln\epsilon}{dN}\right) \times \frac{dN}{d\ln k}. \end{aligned} \tag{3.1.70}$$

The first term in parentheses on the right-hand-side is simply -2ϵ. The second term in parenthesis can be written as follows

$$\frac{d\ln\epsilon}{dN} = 2(\epsilon - \eta), \qquad \text{where} \qquad \eta = -\frac{d\ln H_{,\phi}}{dN} \tag{3.1.71}$$

On the other hand, with respect to $dN/d\ln k$, if we remember that this mode satisfies the relationship o$k = aH$ when the mode k we are interested in is Horizon exit,

$$\frac{dN}{d\ln k} = \left[\frac{d\ln k}{dN}\right]^{-1} = \left[1 + \frac{d\ln H}{dN}\right]^{-1} \sim 1 + \epsilon. \tag{3.1.72}$$

We used $dN = d\ln a$ here. From the above, the spectral index n_s of the scalar perturbation is calculated by using the slow-roll parameter

$$1 - n_s \sim 4\epsilon - 2\eta \tag{3.1.73}$$

Similar results can be derived for spectral index n_t. Since it is $\Delta_t^2 \propto H^2$, we obtain

$$\begin{aligned}\frac{d\ln\Delta_t^2}{d\ln k} &= \frac{d\ln\Delta_t^2}{dN}\times\frac{dN}{d\ln k} \\ &\sim 2\frac{\ln H}{dN}\times(1+\epsilon) \quad = -2\epsilon(1+\epsilon)\sim -2\epsilon.\end{aligned} \tag{3.1.74}$$

We neglected terms that are second order of ϵ here . From this, n_t is given by

$$n_t \sim -2\epsilon \tag{3.1.75}$$

Under the slow-roll condition as described above, ϵ is $\epsilon \sim \epsilon_{\rm v}$. On the other hand, η is expressed as,

$$\eta \sim \eta_{\rm v} - \epsilon_{\rm v}, \qquad \text{where} \qquad \eta_{\rm v} \equiv M_{pl}^2\frac{V''}{V} \tag{3.1.76}$$

Therefore, we can write the spectral index with $\epsilon_{\rm v}, \eta_{\rm v}$,

$$1 - n_s \sim 6\epsilon_{\rm v} - 2\eta_{\rm v}, \qquad n_t \sim -2\epsilon_{\rm v}. \tag{3.1.77}$$

Since $\epsilon_{\rm v}, \eta_{\rm v}$ can be written with potential and its derivative, we now have an expression that evaluates the spectral index using potentials. From (3.1.66) and (3.1.77), we can immediately find a relationship between r and n_t

$$r = -8n_t \tag{3.1.78}$$

In this section the relationships between the inflaton potential $V(\phi)$ and n_s, n_t, r are clarified. Now, by comparing the observed values from CMB temperature fluctuation and theoretical calculation, we can test each inflation model. This can be done in the following procedure. First choose a certain scale k_0 (for example, $k_0 = 0.002\text{Mpc}^{-1}$) for Planck collaboration, expand the fluctuation Power Spectrum around k_0.

$$\begin{aligned}\ln\Delta_s(k) &= \ln\Delta_s(k_0) + (n_s-1)\ln(k/k_0) + \mathcal{O}((\ln(k/k_0))^2) \\ \ln\Delta_t(k) &= \ln\Delta_t(k_0) + n_t\ln(k/k_0) + \mathcal{O}((\ln(k/k_0))^2)\end{aligned} \tag{3.1.79}$$

Here, the theoretical unknown quantities are $\Delta_s(k_0), \Delta_t(k_0), n_s, n_t$. However, we have the relations (3.1.78) and $\Delta_t/\Delta_s = r$. Thus, in fact, there are three independent quantities.

By comparing theoretical estimate from each model and observational results of CMB temperature fluctuation, we can decide whether each model can explain observation facts or not.

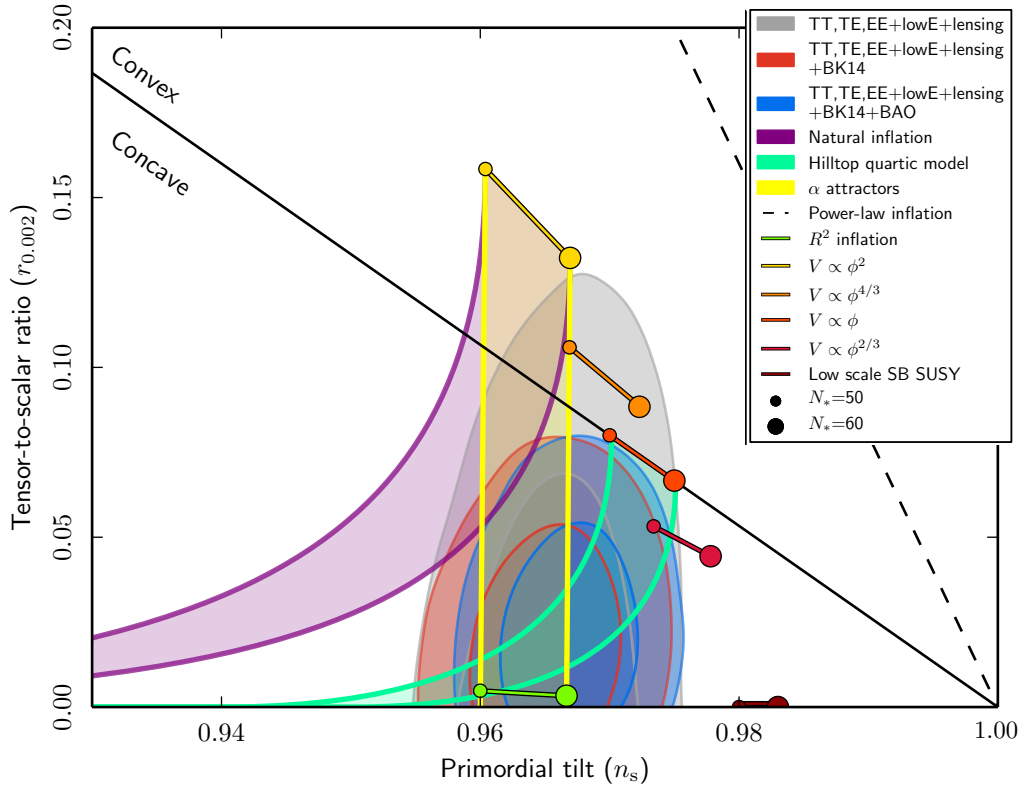

Figure 3.1.1: Constraints on spectral index n_s and tensor-to-scalar ratio r(*Planck collaboration, 2018*)

3.2 Single-field v.s. Multi-field

In multi-field inflation, unlike the case of single-field, we have to pay attention to the following points. ζ was defined as $-\zeta = \Psi + \frac{H}{\dot{\rho}}\delta\rho$. Here if there is a relationship $\delta\rho = \delta p$, this fluctuation is called adiabatic in analogy with thermodynamics. However, we can rewrite $\delta\rho$ as follows.

$$\delta\rho = \delta p - \dot{p}\,\Gamma, \qquad \text{where} \qquad \Gamma \equiv \frac{\delta p}{\dot{p}} - \frac{\delta\rho}{\dot{\rho}} \tag{3.2.1}$$

The condition of adiabatic fluctuation is $\Gamma = 0$. Again by analogy with thermodynamics, let us define the "generalized adiabatic condition" as follows.

$$\Gamma_{xy} = 0, \qquad \text{where} \qquad \Gamma_{xy} \equiv \frac{\delta x}{\dot{x}} - \frac{\delta y}{\dot{y}} \tag{3.2.2}$$

Where x, y can be any quantities which can be expressed by inflatons. In the case of single-field, we can calculate Γ_{xy} using relations like $\delta x = (\partial x/\partial\phi)\delta\phi$. Thus we can show that $\Gamma_{xy} = 0$ in single-field cases. In other words, we can conclude that fluctuations generated by single-field inflation are adiabatic fluctuations.

On the other hand, in the case of multi-field, for example in two-field case, ϕ, χ are taken as x, y, then $\Gamma_{\phi\chi} = \delta\phi/\dot{\phi} - \delta\chi/\dot{\chi}$, and in general this is non-zero. Therefore, in the case of multi-field, non-adiabatic fluctuation should also be considered, and also we need to take into accounts the interaction between an adiabatic part and a non-adiabatic part.

To see the concrete situation, let us consider giving perturbation: Q in a certain path on the field space as shown in Fig. 3.2.1. In single-field inflation, inflaton goes only along a one-dimensional path, and its fluctuation is adiabatic. However in multi-field cases, as shown in the figure, we can decompose Q with Q_{ad} in the direction along the trajectory and Q_s in the direction perpendicular to the trajectory.

$$\begin{aligned} Q_{ad} &= \cos\theta\delta\phi + \sin\theta\delta\chi \\ Q_s &= -\sin\theta\delta\phi + \cos\theta\delta\chi \end{aligned} \tag{3.2.3}$$

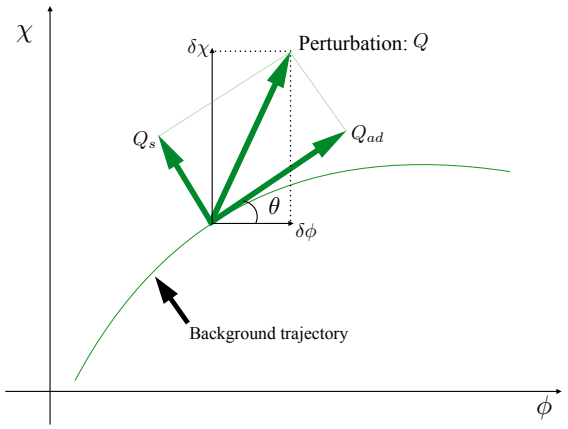

Figure 3.2.1: The schematic picture of the decomposition of a perturbation Q.

Where θ is the angle between Q_{ad} and $\delta\phi$, or same meaning, $\tan\theta = \delta\chi/\delta\phi = \dot{\chi}/\dot{\phi}$. Q_s is $\Gamma_{\phi\chi} = \frac{\delta\phi}{\dot{\phi}} - \frac{\delta\chi}{\dot{\chi}}$, and so it can be interpreted as the entropy fluctuation.

ζ is represented by $-\zeta = \frac{H}{\dot{\rho}}\delta\rho$ on the spatially flat time constant surface, $\Psi = 0$. Using inflaton ϕ, we can express ζ as $-\zeta = \frac{H}{\dot{\phi}}\delta\phi$. In the case of two-field inflation, we have $\dot{\rho} = \sqrt{\dot{\phi}^2 + \dot{\chi}}$. And also, the adiabatic part of $\delta\rho$ is given by Q_{ad} of (3.2.3). Therefore,

$$\zeta = -\frac{H}{\sqrt{\dot{\phi}^2 + \dot{\chi}^2}} Q_{ad} \tag{3.2.4}$$

Interestingly, in the case of single-field, we can find that $\dot{\zeta} \sim \mathcal{O}\left(\frac{k}{aH}\right)^2$, and tis means after Horizon exit ζ is constant on the superhorizon scale. However, in the case of multi-field we obtain,

$$\dot{\zeta} = -2\frac{H\dot{\theta}}{\sqrt{\dot{\phi}^2 + \dot{\chi}^2}} Q_s + \mathcal{O}\left(\frac{k}{aH}\right)^2, \tag{3.2.5}$$

and it turns out that ζ evolves over time after the Horizon exit. Especially, according to the expression (3.2.5), entropy transfer is obtained by evolution

of θ (which directly connects to bending degree of the inflaton trajectory in the field space) and that fluctuation turns to be the adiabatic fluctuation.

Chapter 4

δN formalism

4.1 Separate Universe approach and δN formalism

In order to determine ζ and its correlation functions we make use of the separate Universe approach and the δN formalism [13, 14, 11, 10, 53, 54]. The separate Universe approach corresponds to the leading order approximation in a gradient expansion. One first assumes that the characteristic length scale of spatial variations, L, is longer than the Hubble scale, namely $\xi = 1/(HL) \ll 1$. Associating a factor of ξ with spatial gradients appearing in the field equations, one can then perform an expansion in the parameter ξ. Neglecting terms of order ξ^2 and higher, one finds that the field equations take on exactly the same form as the background equations. In other words, separate super-Hubble sised patches are found to evolve as separate background Universes, differing only in their initial conditions. If we are interested in a comoving scale with wavenumber k, during inflation the parameter $\xi = k/(aH)$ will be decreasing exponentially with time. As such, the separate Universe approach will become applicable after the Horizon-crossing time, which is defined as the time at which $k = aH$.

Making use of the flat gauge, corresponding to $\psi = C_i = 0$, the validity of the separate Universe approach in the case of multiple scalar fields has been confirmed explicitly to all orders in perturbation theory by Sugiyama

et al. [54]. β^i and $\dot{h}_{ij}^{(T)}$ were shown to decay away on super-horizon scales, such that the field equations indeed take on exactly the same form as the background equations, namely

$$\hat{H}^2 = \frac{1}{3M_{pl}^2}\left[\frac{1}{2}\partial_\tau\hat{\phi}^I\partial_\tau\hat{\phi}^J + V\left(\hat{\phi}^I\right)\right], \tag{4.1.1}$$

$$\mathcal{D}_\tau\partial_\tau\hat{\phi}^I + 3\hat{H}\partial_\tau\hat{\phi}^I + \mathcal{G}^{IJ}V_{,J}(\hat{\phi}^K) = 0 \tag{4.1.2}$$

where $\hat{H}(t,\boldsymbol{x}) = H(t)/\alpha(t,\boldsymbol{x})$ is the local Hubble expansion and $\partial_\tau = \partial/\partial\tau$, with $d\tau = \alpha(t,\boldsymbol{x})dt$. A result that proves very useful is that the local e-folding number is found to be unperturbed [13, 10], as

$$\hat{N} = \int \hat{H}d\tau = \int Hdt. \tag{4.1.3}$$

This can also be understood if, associated with the perturbed metric, we define the effective scale factor $\hat{a}(t,\boldsymbol{x}) = a(t)e^{\psi(t,\boldsymbol{x})}$. The local e-folding number is then given as

$$\hat{N} = \ln\left(\frac{\hat{a}}{\hat{a}_*}\right) = \psi - \psi_* + N, \tag{4.1.4}$$

and in the flat slicing, i.e. $\psi = \psi_* = 0$, this reduces to the background e-folding number. The e-folding number is thus a useful time parameter in the flat gauge, and given that the field equations (4.1.1) and (4.1.2) take on the same form as the background equations, we are able to write

$$\hat{\phi}^I(N,\boldsymbol{x}) = \phi^I(N,\phi_*^J(\boldsymbol{x})), \tag{4.1.5}$$

where $\phi^I(N,\phi_*^J(\boldsymbol{x}))$ is a solution of the background equations of motion with the spatially dependent initial conditions $\phi^I(t_*) = \phi_*^I(\boldsymbol{x})$.[1] In other words, the value of $\hat{\phi}^I$ at a given location $\boldsymbol{x}$ is found simply by solving the background equations of motion with the appropriate initial conditions for that location.

[1] In principle we also need to specify the initial field velocities, but we will assume that the slow-roll approximation is valid around the time of horizon crossing, such that field velocities are given in terms of the field values as in eq. (5.2.19).

Having outlined the separate Universe approach, we now wish to determine ζ, and for this we use the δN formalism [13, 14, 10, 54]. The basic idea of the δN formalism is that ζ on some final uniform density slice can be given in terms of the spatial fluctuations of the e-folding number between an initial spatially flat slice and the final uniform density slice. This can be understood if we look at the expression for the local e-folding number given in (4.1.4). Taking the initial slice to be flat and the final slice to be a constant density one, corresponding to $\psi_* = 0$ and $\psi = \zeta$, we find $\delta N = \hat{N} - N = \zeta$. Note that it does not matter exactly when we take the initial flat slice, as it is only important that $\psi_* = 0$. The only restriction is that t_* must be after the time at which the scales under consideration have left the horizon.

The next step in the δN formalism is to show that δN can be expanded in terms of the field perturbations on the initial flat slice, $\delta\phi^I_*(\boldsymbol{x})$. To see this, recall that in the context of the separate Universe approach the field equations take on exactly the same form as the background equations. As mentioned above, this means that the solutions for $\hat{\phi}^I(N, \boldsymbol{x})$ in the flat gauge are as given in eq. (4.1.5), i.e. they are solutions to the background equations but with the initial conditions varying from place to place. Similarly, it also means that the energy density on flat slices can be expressed as

$$\hat{\rho}(N, \boldsymbol{x}) = \rho(N, \phi^I_*(\boldsymbol{x})), \tag{4.1.6}$$

where $\rho(N, \phi^I_*(\boldsymbol{x}))$ is the density as determined by solving the background field equations with the spatially inhomogeneous initial conditions $\phi^I(t_*) = \phi^I_*(\boldsymbol{x})$. In general $\hat{\rho}(N, \boldsymbol{x})$ is not spatially homogeneous, and if we assume that the initial conditions at position $\boldsymbol{x}$ can be expanded about the initial conditions of the fiducial background trajectory as $\phi^I_*(\boldsymbol{x}) = \phi^I_* + \delta\phi^I_*(\boldsymbol{x})$, this leads to an expansion of the form

$$\hat{\rho}(N, \boldsymbol{x}) = \rho(N, \phi^I_*) + \rho_{,I}(N, \phi^J_*)\delta\phi^I_*(\boldsymbol{x}) + \frac{1}{2}\rho_{,IJ}(N, \phi^K_*)\delta\phi^I_*(\boldsymbol{x})\delta\phi^J_*(\boldsymbol{x}) + \dots, \tag{4.1.7}$$

where $\rho(N, \phi^I_*)$ is the density of the fiducial background trajectory, $\rho_{,I}(N, \phi^J_*) =$

$\partial\rho(N,\phi_*^J)/\partial\phi_*^I$ and similarly for $\rho_{,IJ}(N,\phi_*^K)$. At each location $\boldsymbol{x}$, we can then consider the shift along the local trajectory, δN, that is required to reach a constant density slice. In other words, at each location $\boldsymbol{x}$ we find the shift in N such that $\hat{\rho}(N+\delta N,\boldsymbol{x})=\rho(N,\phi_*^I)$. Given the form of the expansion for $\hat{\rho}(N,\boldsymbol{x})$ in eq. (4.1.7), solving $\hat{\rho}(N+\delta N,\boldsymbol{x})=\rho(N,\phi_*^I)$ gives rise to an expansion of the form

$$\zeta(N,\boldsymbol{x})=\delta N(N,\boldsymbol{x})=N_{,I}(N,\phi_*^J)\delta\phi_*^I(\boldsymbol{x})+\frac{1}{2}N_{,IJ}(\phi_*^K)\delta\phi_*^I(\boldsymbol{x})\delta\phi_*^J(\boldsymbol{x})+\cdots, \tag{4.1.8}$$

which is the famous δN expansion. As mentioned above, in principle the initial flat slice can be taken to be at any time after the scales under consideration have left the horizon, but in practice it is useful to choose it to coincide with the horizon crossing time, as expressions for the quantities $\delta\phi_*^I(\boldsymbol{x})$ and their correlations at this time are known [13, 56].

While the above form for the expansion of ζ is perfectly acceptable, in the case of a curved field space the field perturbations $\delta\phi_*^I(\boldsymbol{x})=\phi_*^I(\boldsymbol{x})-\phi_*^I$, which correspond to coordinate displacements, do not transform covariantly. In order to obtain an explicitly covariant expression for ζ we follow the discussion in [57], see also [58, 59]. For sufficiently small $\delta\phi_*^I(\boldsymbol{x})$, the two points in field space $\phi_*^I(\boldsymbol{x})$ and ϕ_*^I are connected by a unique geodesic that we take to be parameterised by λ. Normalising λ such that $\phi^I(\lambda=0)=\phi_*^I$, and $\phi^I(\lambda=1)=\phi_*^I(\boldsymbol{x})$, we can obtain a Taylor series expansion for $\delta\phi^I=\phi^I(\lambda=1)-\phi^I(\lambda=0)$ as

$$\delta\phi^I=\left.\frac{d\phi^I}{d\lambda}\right|_{\lambda=0}+\frac{1}{2}\left.\frac{d^2\phi^I}{d\lambda^2}\right|_{\lambda=0}+\cdots. \tag{4.1.9}$$

On the other hand, the geodesic satisfies

$$\mathcal{D}_\lambda\frac{d\phi^I}{d\lambda}\equiv\frac{d^2\phi^I}{d\lambda^2}+\Gamma^I_{JK}\frac{d\phi^J}{d\lambda}\frac{d\phi^K}{d\lambda}=0. \tag{4.1.10}$$

As such, introducing $\mathcal{Q}^I=d\phi^I/d\lambda|_{\lambda=0}$, which resides in the tangent space at $\phi^I(\lambda=0)$ and thus transforms covariantly, we can express $\delta\phi^I$ in terms of $\mathcal{Q}^I$ as

$$\delta\phi^I = \mathcal{Q}^I - \frac{1}{2!}\Gamma^I{}_{JK}\mathcal{Q}^J\mathcal{Q}^K + \cdots . \tag{4.1.11}$$

Inserting this relation into (4.1.8) we obtain

$$\zeta(N,\boldsymbol{x}) = N_{,I}(N,\phi_*^J)\mathcal{Q}_*^I(\boldsymbol{x}) + \frac{1}{2}\mathcal{D}_I\mathcal{D}_J N(N,\phi_*^K)\mathcal{Q}_*^I(\boldsymbol{x})\mathcal{Q}_*^J(\boldsymbol{x}) + \cdots , \tag{4.1.12}$$

which is now explicitly covariant.

The power spectrum and bispectrum of ζ

Having obtained an expansion for ζ in terms of the covariantised field perturbations on a flat slice at the horizon crossing time, we now turn to the correlation functions of ζ. Working in Fourier space, the two-point correlation function of ζ is parameterised as

$$\langle\zeta(\mathbf{k}_1)\zeta(\mathbf{k}_2)\rangle = (2\pi)^3\delta^3(\mathbf{k}_1+\mathbf{k}_2)P_\zeta(k_1) = (2\pi)^3\delta(\mathbf{k}_1+\mathbf{k}_2)\frac{2\pi^2}{k_1^3}\mathcal{P}_\zeta(k_1), \tag{4.1.13}$$

and the three-point correlation function is similarly parameterised as

$$\langle\zeta(\mathbf{k}_1)\zeta(\mathbf{k}_2)\zeta(\mathbf{k}_3)\rangle = (2\pi)^3\delta^3(\mathbf{k}_1+\mathbf{k}_2+\mathbf{k}_3)B_\zeta(k_1,k_2,k_3). \tag{4.1.14}$$

$P_\zeta(k)$ and $\mathcal{P}_\zeta(k)$ are the power spectrum and reduced power spectrum, respectively, while $B_\zeta(k_1,k_2,k_3)$ is the bispectrum. In both (4.1.13) and (4.1.14) the delta functions are a consequence of assuming statistical homogeneity, and the fact that P_ζ, $\mathcal{P}_\zeta$ and B_ζ depend only on the magnitudes of $\boldsymbol{k}_i$ is a consequence of assuming statistical isotropy. In relation to the three-point function, a useful parameter introduced to quantify the level of non-Gaussianity is f_{NL}, which is defined as

$$f_{\rm NL} = \frac{5}{6}\frac{B_\zeta(k_1,k_2,k_3)}{P_\zeta(k_1)P_\zeta(k_2) + \text{c.p.}}, \tag{4.1.15}$$

where c.p. denotes cyclic permutations of k_1, k_2 and k_3. Given the expansion for ζ in eq. (4.1.12), we see that the correlation functions of ζ can be expressed in terms of the correlation functions of the covariantised field perturbations on the initial flat slice, $\mathcal{Q}^I$. In particular, we have

$$\langle\zeta(\mathbf{k}_1)\zeta(\mathbf{k}_2)\rangle = N_{,I}N_{,J}\langle\mathcal{Q}^I_*(\mathbf{k}_1)\mathcal{Q}^J_*(\mathbf{k}_2)\rangle, \tag{4.1.16}$$

$$\begin{aligned}\langle\zeta(\mathbf{k}_1)\zeta(\mathbf{k}_2)\zeta(\mathbf{k}_3)\rangle = {} & N_{,I}N_{,J}N_{,K}\langle\mathcal{Q}^I_*(\mathbf{k}_1)\mathcal{Q}^J_*(\mathbf{k}_2)\mathcal{Q}^K_*(\mathbf{k}_3)\rangle \\ & + N_{,I}N_{,J}\mathcal{D}_K\mathcal{D}_L N\int\frac{d^3\mathbf{q}}{(2\pi)^3}\langle\mathcal{Q}^K_*(\mathbf{k}_1-\mathbf{q})\mathcal{Q}^I_*(\mathbf{k}_2)\rangle\langle\mathcal{Q}^L_*(\mathbf{q})\mathcal{Q}^J_*(\mathbf{k}_3)\rangle + \text{c.p}\,,\end{aligned} \tag{4.1.17}$$

where for brevity we drop the arguments of $N_{,I}$ and $\mathcal{D}_J\mathcal{D}_I N$. The contribution to the three-point correlation function of ζ coming from the first term involving the three-point correlation functions of $\mathcal{Q}^I$ is known to be unobservably small [60, 61], so in proceeding we choose to neglect it. As such, the only quantities required are the two-point correlation functions of $\mathcal{Q}^I$. At linear order in perturbations we have $\mathcal{Q}^I = \delta\phi^I$, and the two-point correlation functions of $\delta\phi^I$ in the case of a curved field space have been calculated in [13, 56]. The result at lowest order in slow-roll is

$$\langle\mathcal{Q}^I_*(\mathbf{k}_1)\mathcal{Q}^J_*(\mathbf{k}_2)\rangle = (2\pi)^3\delta^3(\mathbf{k}_1+\mathbf{k}_2)\frac{2\pi^2}{k_1^3}\left(\frac{H_*}{2\pi}\right)^2\mathcal{G}^{IJ}_*, \tag{4.1.18}$$

where recall that an asterisk now denotes that a quantity should be evaluated at the time of horizon crossing, namely $k_1 = a_*H_*$. Substituting this result into eqs. (4.1.16) and (4.1.17), expressions for $\mathcal{P}_\zeta(k_1)$ and f_{NL} are obtained as

$$\mathcal{P}_\zeta(k) = \left(\frac{H_*}{2\pi}\right)^2\mathcal{G}^{IJ}_* N_{,I}N_{,J}, \tag{4.1.19}$$

$$f_{NL} = \frac{5}{6}\frac{N^{,I}N^{,J}\mathcal{D}_I\mathcal{D}_J N}{\left(N^{,K}N_{,K}\right)^2}, \tag{4.1.20}$$

where the raised indices in the second expression are raised with $\mathcal{G}^{IJ}_*$.

In addition to the above two observables, we also consider the tilt of the power spectrum, n_s, and the tensor-to-scalar ratio, r. The tilt of the power

spectrum is defined through the relation

$$\mathcal{P}_\zeta(k) = A_s \left(\frac{k}{k_p}\right)^{n_s-1}, \tag{4.1.21}$$

where k_p is some pivot scale and A_s gives the magnitude of $\mathcal{P}_\zeta$ at the pivot scale. The scale dependence of $\mathcal{P}_\zeta$ as given in eq. (4.1.19) appears through its dependence on quantities evaluated at the horizon crossing time of the comoving scale k. We do not present a detailed derivation here, but the final result is given as [13]

$$n_s = 1 - 2\epsilon_* - 2\frac{1 + N_{,I}\left(\frac{1}{3}R^{IJKL}\frac{V_{,J}V_{,K}}{V^2} - \frac{\mathcal{D}^I\mathcal{D}^L V}{V}\right)_* N_{,L}}{N^{,M}N_{,M}}, \tag{4.1.22}$$

where, R^{IJKL} is the curvature tensor constructed from $\mathcal{G}_{IJ}$. Note that A_s is found simply by taking $k = k_p$ in eq. (4.1.19).

Finally, the tensor-to-scalar ratio is defined as the ratio between the power spectra of tensor and scalar perturbations. In particular, if we parameterise the power spectrum of tensor perturbations as

$$\mathcal{P}_T(k) = A_T \left(\frac{k}{k_p}\right)^{n_T}, \tag{4.1.23}$$

then we have $r = A_T/A_s$. It can be shown that $A_T = 8(H_*/(2\pi))^2/M_{pl}^2$, see e.g. [62], such that we obtain

$$r = \frac{8}{M_{pl}^2 N^{,I} N_{,I}}. \tag{4.1.24}$$

4.2 Transport method

In this section, we introduce an extended version of the δN formalism so called the trans port method. This has been discussed in [15, 16, 17, 18]. In Fig.4.2.1, we can see the basic idea of the transport method.

In terms of δN formalism, we need to compute $\frac{\partial N}{\partial \phi_*^a}$ and $\frac{\partial^2 N}{\partial \phi_*^a \partial \phi_*^b}$. To do so, we need to estimate the difference of N between the background trajectory

and the subtrajectory, and the difference should be evaluated on the uniform density slice. Thus, in the straightforward way of the δN formalism, we should have consider numbers of subtrajectories. However, in the transport method, we do not need subtrajectories anymore. In this method, first we consider the derivative $\frac{\partial N}{\partial \varphi^a}$ on the uniform density slice. Here, $\delta\varphi^a$ is a small displacement on the uniform density slice. In fact, we can always calcurate $\frac{\partial N}{\partial \varphi^a}$ analitically on every uniform density slices. Moreover, we introduce the gauge transformation from the displacement on the uniform density slice, $\delta\varphi^\alpha$ to that of on the constant N slice, $\delta\phi^a$. That means we introduce the gauge transformation Γ^α_a, Γ^α_{ab} as,

$$\frac{\partial N}{\partial \phi^a_*} = \frac{\partial N}{\partial \varphi^\alpha}\Gamma^\alpha_a. \tag{4.2.1}$$

and

$$\frac{\partial^2 N}{\partial \phi^a_* \partial \phi^b_*} = \frac{\partial N}{\partial \varphi^\alpha}\Gamma^\alpha_{ab} + \frac{\partial^2 N}{\partial \varphi^\alpha \partial \varphi^\beta}\Gamma^\alpha_a \Gamma^\beta_b. \tag{4.2.2}$$

According to this expression, to obtain $\frac{\partial N}{\partial \varphi^a_*}$, we have to determine $\frac{\partial N}{\partial \varphi^a}$ and Γ^α_a, respectively.

Let us first discuss the concrete form of $\frac{\partial N}{\partial \varphi^a}$. We introduced this as a differentiation on the uniform density slice ($\delta\rho = 0$). Thus we have

$$\rho_N \delta N + \frac{\partial \rho}{\partial \varphi^\alpha}\delta\varphi^\alpha + \frac{\partial \rho}{\partial \varphi^\alpha_N}\delta\varphi^\alpha_N = 0 \tag{4.2.3}$$

Using Friedmann equeation, we can derive the form of

$$\delta N = \frac{1}{2\epsilon}\left(\frac{V_\alpha}{V}\delta\varphi^\alpha + \frac{1}{3-\epsilon}\varphi^\alpha_N \delta\varphi^\alpha_N(N, \vec{x})\right), \tag{4.2.4}$$

$$\frac{\partial N}{\partial \varphi^\alpha} = \frac{1}{2\epsilon}\frac{V_\alpha}{V}, \quad \frac{\partial N}{\partial \varphi^\alpha_N} = \frac{\varphi^\alpha_N}{2\epsilon(3-\epsilon)} \tag{4.2.5}$$

In addition, we can obtain second derivatives

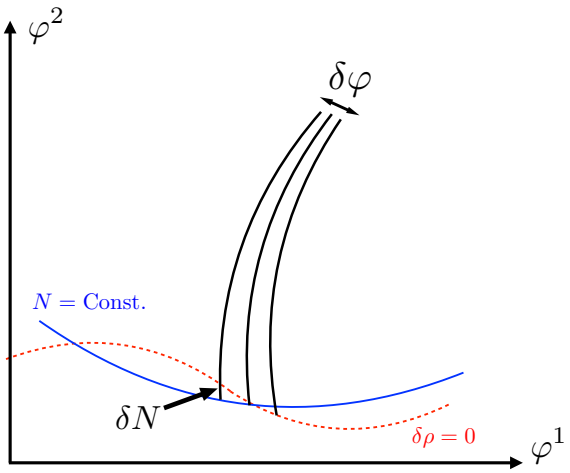

Figure 4.2.1: The schematic figure of the transport method. The red dashed line represents the uniform density slice, and the blue solid line represents the constant N slice. In the δN formalism, the constant N slice is not necessarily to correspond to a slice on which slow roll conditions are violated. The essential idea is to estimate curvautre perturbation on the unifrom density slice.

$$\frac{\partial^2 N}{\partial\varphi^\alpha \partial\varphi^\beta} = \frac{1}{2\epsilon}\left[\frac{V_{\alpha\beta}}{V} - \left(1+\frac{\eta}{2\epsilon}\right)\frac{V_\alpha V_\beta}{V^2}\right], \tag{4.2.6}$$

$$\frac{\partial^2 N}{\partial\phi^\alpha \partial\varphi_N^\beta} = -\frac{3-\epsilon+\eta/2}{2\epsilon^2(3-\epsilon)}\frac{V_\alpha}{V}\varphi_N^\beta, \tag{4.2.7}$$

$$\frac{\partial^2 N}{\partial\varphi_N^\alpha \partial\varphi_N^\beta} = \frac{1}{2\epsilon(3-\epsilon)}\left[\delta_{\alpha\beta} - \frac{6-3\epsilon+\eta/2}{\epsilon(3-\epsilon)}\varphi_N^\alpha.\varphi_N^\beta\right] \tag{4.2.8}$$

Next we determine Γ^α_a and Γ^α_{ab}. Here, just for simplicity, we introduce $\varphi^\alpha_N = \mathcal{U}^\alpha$ which is defined as

$$\mathcal{U}^\alpha = \phi^\alpha_N, \quad \alpha = 1\cdots M \tag{4.2.9}$$

$$\mathcal{U}^\alpha = -(3-\epsilon)\left(\phi^{\alpha \bmod M} + \frac{V_{\alpha \bmod M}}{V}\right), \quad \alpha = M+1\cdots 2M \tag{4.2.10}$$

Where M is the number of inflatons. Expanding φ^α_N with respect to $\delta\varphi$, we obtain

$$\delta\varphi^\alpha_N = \mathcal{U}^\alpha_\beta \delta\varphi^\beta + \frac{1}{2}\mathcal{U}^\alpha_{\beta\gamma}\delta\varphi^\beta\delta\varphi^\gamma \tag{4.2.11}$$

On the other hand, by the difenition of the gauge transfromation Γ^α_a and Γ^α_{ab},

$$\delta\varphi^\alpha = \Gamma^\alpha_b \delta\phi^b_* + \frac{1}{2}\Gamma^\alpha_{ab}\delta\phi^a_*\delta\phi^b_* \tag{4.2.12}$$

Taking N derivative of (4.2.12), and compaire it with (4.2.11), we can find the defferential equations which Γ^α_a and Γ^α_{ab} obey.

$$\frac{d}{dN}\Gamma^\alpha_a = \mathcal{U}^\alpha_\beta \Gamma^\beta_a \tag{4.2.13}$$

$$\frac{d}{dN}\Gamma^\alpha_{ab} = \mathcal{U}^\alpha_\beta \Gamma^\beta_{ab} + \mathcal{U}^\alpha_{\beta\gamma}\Gamma^\beta_a\Gamma^\gamma_b \tag{4.2.14}$$

Solving these equations, we can determine the gauge transformtions along the background tarjectory, and we yield $\frac{\partial N}{\partial\varphi^\alpha}$ which is defined on each uniform density slices. Combining these equations, we can calcurate $\frac{\partial N}{\partial\phi^a}$ much more efficiently than the normal δN formalism.

Part II

Multi-field Inflation Models

Chapter 5

Multi-field effects in a simple extension of R^2 inflation

5.1 Introduction for this model

In this chapter, we study a type of $R^2 + m^2\phi^2$ models as an example of two-field inflation models, i.e., the system containing a Ricci scalar squared term and a canonical scalar field with quadratic mass term. In the Einstein frame this model takes the form of a two-field inflation model with a curved field space, and under the slow-roll approximation contains four free parameters corresponding to the masses of the two fields and their initial positions. We investigate how the inflationary dynamics and predictions for the primordial curvature perturbation depend on these four parameters. Our analysis is based on the δN formalism, which allows us to determine predictions for the non-Gaussianity of the curvature perturbation as well as for quantities relating to its power spectrum. Depending on the choice of parameters, we find predictions that range from those of R^2 inflation to those of quadratic chaotic inflation, with the non-Gaussianity of the curvature perturbation always remaining small. Using our results we are able to put constraints on the masses of the two fields.

Because recent cosmic microwave background (CMB) observations are in good agreement with the predictions of inflation, and the data is now precise,

we can constrain individual models of inflation [46] by using those observational data. While observations are still perfectly consistent with single-field inflation, in the context of high-energy particle physics theories there is strong motivation to consider multi-field models. For instance, when compactifying superstring theory or supergravity on to four dimensions, many scalar/pseudo-scalar fields usually appear, such as moduli and axions. It is thus important to determine the observable consequences of multi-field inflation models and how they, and the theories in which they are embedded, can be constrained by current and future observations. In relation to this there are perhaps two key features that distinguish multi-field models from single field models. The first is that the curvature perturbation on constant density slices, ζ, is not necessarily conserved on super-horizon scales, and the second is that its statistical distribution may deviate from a Gaussian one. In the case of single-field inflation, Maldacena's consistency relation dictates that the non-Gaussianity of ζ in the squeezed limit should be unobservably small, which is a consequence of the fact that ζ is conserved on super-horizon scales in single-field inflation models [12]. This suggests that if a relatively large non-Gaussianity were to be observed, this would be a strong indication that multiple fields were present during inflation. Even if not observed, however, it is still important to determine the implications of this for multi-field models. While current constraints on non-Gaussianity from the CMB are relatively weak, future large scale structure surveys promise to improve these constraints considerably, see e.g. [47]. In light of the above, it is clear that in looking to test any multi-field model of inflation one will need to be able to calculate how the curvature perturbation evolves on super-horizon scales and how much its statistical distribution deviates from a Gaussian one.

In this work we consider a simple multi-field extension of so-called R^2 inflation, also sometimes referred to as Starobinsky inflation [48]. In its Jordan frame representation, the original model consists of a modified gravity sector containing a term proportional to R^2, and the inflationary predictions are in very good agreement with observations [46]. In trying to embed this model in a more fundamental framework such as a supergravity, however, it is natural to expect the appearance of additional scalar degrees of freedom

(see e.g. [49]) and an important question is then how much the inflationary predictions are affected by these additional degrees of freedom. As a toy model, here we consider adding a canonical scalar field with quadratic mass term to the original Jordan frame action, which is the same model as considered in [50]. Similar models have also been considered in [51, 52]. Re-writing the model as a scalar-tensor theory of gravity plus additional scalar, and transforming to the Einstein frame, this model takes the form of a two-field inflation model with a non-flat field space. One of the fields, often referred to as the scalaron, corresponds to the additional scalar degree of freedom associated with the R^2 term in the original action, and the second is simply the field we have introduced by hand. In addition to the non-flat field space, the potential in the Einstein frame also contains interactions between the two fields.

In analyzing the inflationary predictions of this model we make use of the separate Universe approach and δN formalism [13, 14, 11, 10, 53, 54]. Due to the non-flat field space and interaction terms in the potential, it is not possible to calculate $\delta N (= \zeta)$ analytically, and so we rely on numerical calculations. Making the slow-roll approximation, such that only the initial field positions need to be specified in solving the inflationary dynamics, the model essentially contains four parameters: the masses of the two fields and their initial positions. We explore how the inflationary dynamics and predictions for the correlation functions of ζ depend on these four parameters, and using current observational data we put constraints on the masses of the two fields.

This chapter is organised as follows. In Sec. 5.2, we explain the concrete set-up of our model and present the background field equations. In Sec. 5.3 we briefly describe our numerical method and present the results of our analysis. Our findings are then summarised in Sec. 5.4.

5.2 Set-up and background equations

The model we consider contains an R^2 term and an additional scalar field χ with a canonical kinetic term. We further assume that the potential for the χ field is a simple quadratic. The action of this model is thus given by

$$S_J = \int d^4x\sqrt{-\tilde{g}}\left[\frac{M_{pl}^2}{2}\tilde{R} + \frac{\mu}{2}\tilde{R}^2\right] + \int d^4x\sqrt{-\tilde{g}}\left[-\frac{1}{2}\tilde{g}^{\mu\nu}\partial_\mu\chi\partial_\nu\chi - \frac{1}{2}m_\chi^2\chi^2\right]. \tag{5.2.1}$$

Here the subscript J denotes the Jordan frame, $\tilde{g}_{\mu\nu}$ is the Jordan frame metric, $\tilde{R}$ is the Ricci scalar constructed from $\tilde{g}_{\mu\nu}$ and its derivatives, $M_{pl} = 1/\sqrt{8\pi G}$ is the reduced Planck mass, where G is Newton's gravitational constant, and μ is a dimensionless parameter. In analyzing the above model it is useful to re-write it as a model containing two scalar fields and a canonical Einstein-Hilbert term, which can be achieved as follows, see e.g. [55]. First we introduce the auxiliary field φ, and consider the action

$$S_{J\,\mathrm{Grav}} = \frac{M_{pl}^2}{2}\int d^4x\sqrt{-\tilde{g}}\left(f(\varphi) + f_{,\varphi}(\varphi)(R-\varphi)\right), \tag{5.2.2}$$

where $f(\varphi) = \varphi + \mu\varphi^2/M_{pl}^2$ and $f_{,\varphi} = df/d\varphi$. Minimizing this action with respect to φ gives the constraint

$$\frac{2\mu}{M_{pl}^2}(R-\varphi) = 0, \tag{5.2.3}$$

which for non-zero μ gives $\varphi = R$. On substituting $\varphi = R$ into (5.2.2) we recover the gravitational part of (5.2.1), which confirms the equivalence of these two actions. Next we introduce $e^{2\alpha\phi} = 1 + 2\mu\varphi/M_{pl}^2$ with $\alpha = 1/(\sqrt{6}M_{pl})$, such that (5.2.2) takes the form

$$S_{J\,\mathrm{Grav}} = \int d^4x\sqrt{-\tilde{g}}\left(\frac{M_{pl}^2}{2}e^{2\alpha\phi}\tilde{R} - \tilde{V}(\phi)\right), \qquad \tilde{V}(\phi) = \frac{M_{pl}^4}{8\mu}\left(e^{2\alpha\phi}-1\right)^2. \tag{5.2.4}$$

Thus we have re-written the gravitational part of the action given in eq. (5.2.1) as a scalar-tensor theory with a non-minimal coupling between the scalar field ϕ and gravity. Note, however, that there is no kinetic term for the ϕ field in this representation. Finally we make a conformal transformation of the metric, expressing the Jordan frame metric $\tilde{g}_{\mu\nu}$ in terms of the so-called Einstein frame metric $g_{\mu\nu}$ as

$$g_{\mu\nu} = \Omega^2 \tilde{g}_{\mu\nu}, \qquad \text{where} \qquad \Omega^2 = e^{2\alpha\phi}. \tag{5.2.5}$$

On doing so we find that the total action takes the form

$$S_E = \int d^4x\sqrt{-g}\left[\frac{M_{pl}^2}{2}R - \frac{g^{\mu\nu}}{2}(\partial_\mu\phi)(\partial_\nu\phi) - \frac{1}{2}g^{\mu\nu}e^{-2\alpha\phi}(\partial_\mu\chi)(\partial_\nu\chi) - V(\phi,\chi)\right], \tag{5.2.6}$$

with

$$V(\phi,\chi) = \frac{3}{4}m_\phi^2 M_{pl}^2(1-e^{-2\alpha\phi})^2 + \frac{1}{2}m_\chi^2 e^{-4\alpha\phi}\chi^2. \tag{5.2.7}$$

Here we introduced $m_\phi^2 = M_{pl}^2/(6\mu)$ and the subscript E denotes the Einstein frame. The label 'Einstein frame' is appropriate given that the gravity part of the action now takes the canonical Einstein-Hilbert form, which is somewhat easier to analyze than the gravity sector of the original action (5.2.1). Note, however, that reducing the gravity sector to the canonical Einstein-Hilbert form has come at the cost of introducing the additional scalar degree of freedom ϕ — often referred to as the scalaron — and interaction terms between the two fields ϕ and χ, which appear in the second term of the potential and in the kinetic term of χ.

Using a more abstract notation, the action (5.2.6) can be re-written in the form of a non-linear sigma model as

$$S_E = \int d^4x\sqrt{-g}\left[\frac{M_{pl}^2}{2}R - \frac{1}{2}\mathcal{G}_{IJ}g^{\mu\nu}\partial_\mu\phi^I\partial_\nu\phi^J - V(\phi^I)\right]. \tag{5.2.8}$$

In our case the Latin indices I and J take on the values ϕ and χ, with $\phi^\phi = \phi$ and $\phi^\chi = \chi$. $\mathcal{G}_{IJ}$ is interpreted as the metric on field space, and in our case

the components are given as

$$\mathcal{G}_{\phi\phi} = 1, \quad \mathcal{G}_{\chi\chi} = e^{-2\alpha\phi}, \quad \mathcal{G}_{\phi\chi} = \mathcal{G}_{\chi\phi} = 0. \tag{5.2.9}$$

Varying the action (5.2.8) with respect to $g_{\mu\nu}$, assuming a Friedmann-Lemaitre-Robertson-Walker (FLRW) metric of the form $g_{\mu\nu} = \text{diag}(-1, a^2(t), a^2(t), a^2(t))$ and taking the scalar fields to be homogeneous, namely $\phi^I = \phi^I(t)$, we obtain the Friedmann equation

$$H^2 = \frac{1}{3M_{pl}^2}\left[\frac{1}{2}\mathcal{G}_{IJ}\dot{\phi}^I\dot{\phi}^J + V(\phi^I)\right], \tag{5.2.10}$$

and the continuity equation

$$\dot{H} = -\frac{1}{2M_{pl}^2}\mathcal{G}_{IJ}\dot{\phi}^I\dot{\phi}^J, \tag{5.2.11}$$

where $H = \dot{a}/a$ and an overdot denotes taking the derivative with respect to time. The equations of motion for the homogeneous fields ϕ^I are given as

$$\mathcal{D}_t\dot{\phi}^I + 3H\dot{\phi}^I + \mathcal{G}^{IJ}V_{,J} = 0, \tag{5.2.12}$$

where $V_{,J} = \partial V/\partial\phi^J$ and we have introduced the covariant time derivative $\mathcal{D}_t$ that acts as $\mathcal{D}_t X^I = \dot{X}^I + \Gamma^I_{\ JK}\dot{\phi}^J X^K$, with the Christoffel symbols $\Gamma^I_{\ JK}$ being constructed from $\mathcal{G}_{IJ}$ and its derivatives (see Appendix for details). In our case, the equations of motion for ϕ and χ are given as

$$\ddot{\phi} + 3H\dot{\phi} + \alpha e^{-2\alpha\phi}\dot{\chi}^2 + V_{,\phi} = 0, \tag{5.2.13}$$

$$\ddot{\chi} + 3H\dot{\chi} - 2\alpha\dot{\phi}\dot{\chi} + e^{2\alpha\phi}V_{,\chi} = 0. \tag{5.2.14}$$

In the context of inflation, it is useful to define the slow-roll parameters $\epsilon = -\dot{H}/H^2$ and $\eta = \dot{\epsilon}/(\epsilon H)$. In order to obtain quasi-exponential inflation we require $\epsilon \ll 1$, and the condition $\eta \ll 1$ ensures that inflation lasts for long enough.[1] The amount of inflation is parameterised in terms of the e-folding

[1]Strictly speaking η can be negative. So we take slow-roll to mean that $|\eta| \ll 1$.

number N defined as

$$N(t, t_*) = \int_{t_*}^{t} H(t)dt = \ln\left(\frac{a(t)}{a(t_*)}\right), \tag{5.2.15}$$

where t_* is the initial time, and observational constraints dictate that $N \sim 60$. In terms of the scalar fields, we have

$$\epsilon = \frac{1}{2M_{pl}^2}\frac{\mathcal{G}_{IJ}\dot{\phi}^I\dot{\phi}^J}{H^2} \qquad \text{and} \qquad \eta = 2\epsilon + 2\frac{\mathcal{G}_{IJ}\dot{\phi}^I\mathcal{D}_t\dot{\phi}^J}{H\mathcal{G}_{KL}\dot{\phi}^K\dot{\phi}^L}. \tag{5.2.16}$$

The slow-roll condition $\epsilon \ll 1$ thus implies that

$$H^2 \simeq \frac{V(\phi^I)}{3M_{pl}^2}. \tag{5.2.17}$$

Given that $\epsilon \ll 1$, the condition $\eta \ll 1$ implies that

$$\frac{\mathcal{G}_{IJ}\dot{\phi}^I\mathcal{D}_t\dot{\phi}^J}{H\mathcal{G}_{KL}\dot{\phi}^K\dot{\phi}^L} \ll 1. \tag{5.2.18}$$

In the single-field case, where we can always redefine the field such that $\mathcal{G}_{\phi\phi} = 1$, this reduces to $\ddot{\phi} \ll H\dot{\phi}$, which allows us to neglect the acceleration term in the equation of motion for ϕ. In the multi-field case with a curved field space, however, the situation is not so simple, as the above condition only constrains the component of $\mathcal{D}_t\dot{\phi}^I$ along the background trajectory. Nevertheless, we assume that the magnitude of the acceleration vector $\mathcal{D}_t\dot{\phi}^I$ is much smaller than the magnitude of the velocity vector $H\dot{\phi}^I$, namely $(\mathcal{G}_{IJ}\mathcal{D}_t\dot{\phi}^I\mathcal{D}_t\dot{\phi}^J)^{1/2} \ll H(\mathcal{G}_{IJ}\dot{\phi}^I\dot{\phi}^J)^{1/2}$. By the Cauchy-Schwarz inequality, this will guarantee that condition (5.2.18) is satisfied. If we further assume that the field basis is such that $|\mathcal{D}_t\dot{\phi}^I| \ll |H\dot{\phi}^I|$ for all I, where here by $|X^I|$ we mean the magnitude of the Ith component of X^I, then the equations of motion (5.2.12) reduce to

$$3H\dot{\phi}^I \simeq -\mathcal{G}^{IJ}V_{,J}, \tag{5.2.19}$$

meaning that we are in an attractor regime where the field velocities are given as functions of the field positions. Using the slow-roll equations (5.2.17) and

(5.2.19) we can then derive consistency conditions for the potential and its derivatives. Namely, we find

$$\epsilon \simeq \epsilon_V = \frac{M_{pl}^2}{2}\frac{\mathcal{G}^{IJ}V_{,I}V_{,J}}{V^2} \ll 1, \qquad \eta \simeq \eta_V = 4\epsilon_V - \frac{M_{pl}^4}{\epsilon_V}\frac{\mathcal{D}_K V_{,J}\mathcal{G}^{KL}V_{,L}\mathcal{G}^{JM}V_{,M}}{V^3} \ll 1, \tag{5.2.20}$$

where $\mathcal{D}_K V_{,J} = V_{,JK} - \Gamma^L_{JK}V_{,L}$ is the covariant derivative of $V_{,J}$. The first condition $\epsilon_V \ll 1$ thus puts a constraint on the first derivatives of V, while the condition $\eta_V \ll 1$ constrains the second derivatives of V. In particular, assuming $\epsilon_V \ll 1$, the condition $\eta_V \ll 1$ will be satisfied if we assume that all the eigenvalues of the field-space tensor $\eta^I_{\ J}$ are small, where $\eta^I_{\ J}$ is defined as

$$\eta^I_{\ J} \equiv M_{pl}^2\frac{\mathcal{G}^{IK}\mathcal{D}_J V_{,K}}{V}. \tag{5.2.21}$$

Provided the number of fields is not too large, the Eigenvalues of $\eta^I_{\ J}$ will in turn be small if $\eta^I_{\ J} \ll 1$ for all I and J. Note that the quantity $\eta^I_{\ J}$ corresponds to the covariant Hessian of the potential divided by $V/M_{pl}^2 \simeq 3H^2$, and the covariant Hessian of the potential contributes to the effective mass matrix of field fluctuations about the background trajectory, see e.g. [13]. As such, the condition $\eta^I_{\ J} \ll 1$ will constitute part of the sufficient condition for the effective mass of field fluctuations to be small compared to the Hubble scale.

5.3 Numerical analysis and results

As can be seen from the expressions given in eqs. (4.1.19), (4.1.20), (4.1.22) and (4.1.24), the observables $\mathcal{P}_\zeta$, n_s, r and f_{NL} for a given inflationary trajectory can be determined with knowledge of the background dynamics alone, which is one of the very appealing aspects of the δN formalism. In particular, we require the background quantities H, ϵ, $\mathcal{G}_{IJ}$ and V evaluated at the horizon-crossing time of the comoving scale under consideration, as well as the derivatives of the e-folding number up to a constant density surface with respect to the field values at the horizon crossing time, $N_{,I}$ and $\mathcal{D}_J\mathcal{D}_I N$. For a

restricted class of potentials and field-space metrics it is possible to determine the derivatives of N analytically if the slow-roll equations of motion (5.2.19) are assumed to hold throughout inflation, see e.g. [76, 77, 78, 79, 80], but in general one has to resort to numerical calculations. The model we are considering contains both a non-trivial field-space metric and interaction terms in the potential, meaning that the derivatives of N cannot be determined analytically. We thus have to take a numerical approach, the method of which we now briefly explain.

Our code is based on the finite difference method. We first consider a background trajectory with the initial conditions (ϕ_*, χ_*), and assume that the scale under consideration left the horizon as the trajectory passed through this point. Evolving along the trajectory, at any later time of interest t, we can determine the number of e-foldings since the horizon-crossing time, $N(t, \phi_*, \chi_*)$, and the density at that time, $\rho(t, \phi_*, \chi_*)$. Next we consider another trajectory with displaced initial conditions, e.g. $(\phi_* + \Delta\phi, \chi_*)$. Evolving along this trajectory we determine the time $\tilde{t} = t + \delta t$ at which the density of the displaced trajectory coincides with $\rho(t, \phi_*, \chi_*)$, namely $\rho(\tilde{t}, \phi_* + \Delta\phi, \chi_*) = \rho(t, \phi_*, \chi_*)$. We then determine the number of e-foldings that have elapsed on the perturbed trajectory from the initial time up to the time $\tilde{t}$, $N(\tilde{t}, \phi_* + \Delta\phi, \chi_*)$. This is the number of e-foldings up to the constant density surface, and the derivative of N with respect to ϕ_* is then given as

$$N_{,\phi_*} = \frac{N(\tilde{t}, \phi_* + \Delta\phi, \chi_*) - N(t, \phi_*, \chi_*)}{\Delta\phi}. \tag{5.3.1}$$

The same procedure applies for determining $N_{,\chi_*}$, and can be extended to calculate the second-order derivatives $N_{,\phi_*\phi_*}$, $N_{,\chi_*\chi_*}$ and $N_{,\phi_*\chi_*} = N_{,\chi_*\phi_*}$. In all our calculations we assume that the slow-roll field equations (5.2.17) and (5.2.19) are a good approximation at the time of horizon crossing. The initial field velocities are thus determined through eq. (5.2.19) and do not need to be specified independently. Nevertheless, we do solve the full equations of motion eq. (5.2.12) when calculating the derivative of N. This allows for the possibility that the slow-roll approximation breaks down later on during the super-horizon evolution. We have worked with 32-digit precision.

Note that the time t in the above discussion can be any time after the horizon crossing time, so by varying t we can determine the evolution of ζ. If we are interested in determining ζ at the end of inflation, then we take t to be the time at which $\epsilon \simeq 1$. As discussed at the end of the previous section, if an adiabatic limit has not been reached by the end of inflation then it is necessary to follow the evolution of ζ through (p)reheating and until an adiabatic limit is reached and ζ becomes conserved. However, the evolution of ζ through (p)reheating is beyond the scope of this work, and we restrict our attention to the evolution of ζ up until the end of inflation.

In proceeding, rather than working with the parameters m_ϕ and m_χ, we instead introduce the mass ratio defined as

$$R_{\rm mass} \equiv \frac{m_\chi}{m_\phi}. \tag{5.3.2}$$

This allows an overall m_ϕ^2 to be factored out of the potential, namely

$$V(\phi,\chi) = m_\phi^2 \mathcal{V}(\phi,\chi), \qquad \mathcal{V}(\phi,\chi) = \frac{3}{4}M_{pl}^2(1-e^{-2\alpha\phi})^2 + \frac{1}{2}R_{\rm mass}^2 e^{-4\alpha\phi}\chi^2. \tag{5.3.3}$$

If we then introduce the re-scaled time parameter $\tilde{\tau} = m_\phi t$, we find that the background field equations reduce to

$$\mathcal{D}_{\tilde{\tau}}\phi^I_{\tilde{\tau}} + 3\mathcal{H}\phi^I_{\tilde{\tau}} + \mathcal{G}^{IJ}\mathcal{V}_{,J} = 0, \tag{5.3.4}$$

$$\mathcal{H}^2 = \frac{1}{3M_{pl}^2}\left[\frac{1}{2}\mathcal{G}_{IJ}\phi^I_{\tilde{\tau}}\phi^J_{\tilde{\tau}} + \mathcal{V}(\phi^I)\right], \tag{5.3.5}$$

where a subscript $\tilde{\tau}$ denotes taking the derivative with respect to $\tilde{\tau}$, e.g. $\phi^I_{\tilde{\tau}} = d\phi^I/d\tilde{\tau}$, $\mathcal{H} = a_{\tilde{\tau}}/a$ and $\mathcal{D}_{\tilde{\tau}}X^I = X^I_{\tilde{\tau}} + \Gamma^I_{JK}\phi^J_{\tilde{\tau}}X^K$. As such, we see that the mass m_ϕ drops out of the field equations. In particular, this means that the solution for $\mathcal{H}$ as a function of $\tilde{\tau}$ will be independent of m_ϕ. If we then consider the definition of the e-folding number, we have

$$N = \int_{t_*}^{t} H dt = \int_{\tilde{\tau}_*}^{\tilde{\tau}} \mathcal{H} d\tilde{\tau}, \tag{5.3.6}$$

from which we conclude that the e-folding number is independent of the overall mass scale m_ϕ. This in turn means that the derivatives of N, required in calculating $\mathcal{P}_\zeta$, n_s, r and f_{NL}, will also be independent of m_ϕ. Given the expressions for n_s, r and f_{NL}, we thus find that they are all independent of m_ϕ. The only observable that depends on m_ϕ is $\mathcal{P}_\zeta$, as this depends on the overall normalization of H_*^2.[2] Explicitly, we have

$$\mathcal{P}_\zeta(k) = m_\phi^2 \left(\frac{\mathcal{H}_*}{2\pi}\right)^2 \mathcal{G}_*^{IJ} N_{,I} N_{,J}, \tag{5.3.7}$$

which means that we are able to determine the quantity $\mathcal{P}_\zeta/m_\phi^2$ without knowing m_ϕ.

Using this new parameterization, the free parameters of the theory (assuming slow-roll at horizon crossing) are m_ϕ, $R_{\rm mass}$, ϕ_* and χ_*. We will now consider how the infationary dynamics and predictions for ζ depend on these parameters.

Background trajectories

In light of the preceding discussion, we see that the shape of trajectories in field space will be independent of m_ϕ. As such, the only remaining parameters are $R_{\rm mass}$, ϕ_* and χ_*. Broadly speaking, we are interested in the three regimes $R_{\rm mass} > 1$, $R_{\rm mass} \sim 1$ and $R_{\rm mass} < 1$, and in Fig. 5.3.1 we plot example trajectories for the representative values $R_{\rm mass} = 5,\ 1,\ 1/5$. In each case we consider the three sets of initial conditions $(\phi_*/M_{pl}, \chi_*/M_{pl}) = (6, 3)$, $(\phi_*/M_{pl}, \chi_*/M_{pl}) = (5, 3)$ and $(\phi_*/M_{pl}, \chi_*/M_{pl}) = (6, 1.5)$, and each trajectory is evolved until inflation ends. When interpreting the trajectories, one has to be careful to recall that it is not only the potential shape that is important, as the effect of the non-flat field space must also be taken into account. In this model, for example, we have $\mathcal{G}^{\chi\chi} = e^{2\alpha\phi}$. Given that the slow-roll equation of motion for χ takes the form $3H\dot{\chi} \simeq -\mathcal{G}^{\chi\chi} V_{,\chi}$, we can expect that

[2] Another way to see the independence of m_ϕ is to write the field equations of motion directly in terms of the time parameter N. On doing so, the potential only appears in the combination $V_{,I}/V$, meaning that the overall factor of m_ϕ^2 drops out.

for super-Planckian values of ϕ the velocity is enhanced compared to what we would naively expect from the gradient of the potential alone. Nevertheless, the trajectories in Fig. 5.3.1 qualitatively agree with our naive expectation.

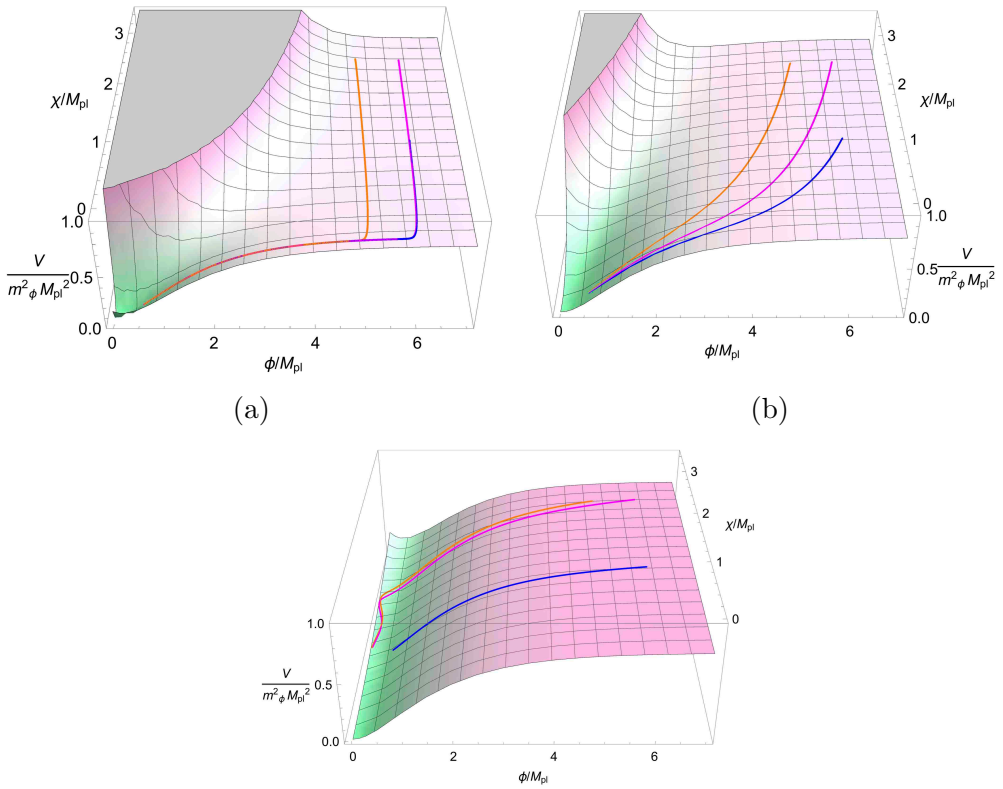

Figure 5.3.1: Examples trajectories for three different values of $R_{\rm mass}$. We show the cases a) $R_{\rm mass} = 5.0$, b) $R_{\rm mass} = 1.0$, and c) $R_{\rm mass} = 0.2$. For each value of $R_{\rm mass}$ three trajectories are plotted, with the initial conditions given as $(\phi_*/M_{pl}, \chi_*/M_{pl}) = (6.0, 3.0)$ (magenta line), $(\phi_*/M_{pl}, \chi_*/M_{pl}) = (5.0, 3.0)$ (orange line) and $(\phi_*/M_{pl}, \chi_*/M_{pl}) = (6.0, 1.5)$ (blue line).

In the case $R_{\rm mass} = 5$ we find that the trajectories first rapidly evolve in the χ direction, with most of inflation then taking place as the trajectory proceeds along the local minimum at $\chi = 0$. Given that the potential reduces to the single-field R^2 potential at $\chi = 0$, we expect the last stage of inflation to be indistinguishable from the original R^2 model. At the level of perturbations, as the trajectory evolves along the local minimum we expect

that ζ should be conserved and that isocurvature perturbations will decay, such that an adiabatic limit is approached. Recall that in the original R^2 inflation model approximately 60 e-foldings of inflation are obtained by taking $\phi_*/M_{pl} \simeq 5.5$. As such, in the large $R_{\rm mass}$ limit, if we take any set of initial conditions with $\phi_*/M_{pl} \sim 5.5$, the final stage of inflation along $\chi = 0$ will constitute the whole observable part of inflation, and we thus expect that predictions for ζ and its statistical properties will be indistinguishable from the original R^2 model.

In the case $R_{\rm mass} = 1$, the trajectories are less trivial, in the sense that they continue to turn throughout the evolution. Correspondingly, we expect that ζ will continue to evolve throughout inflation. It is in this parameter region that an adiabatic limit may not be reached by the end of inflation, and ζ may continue to evolve through the (p)reheating epoch. If this is the case, then the correlation functions of ζ that we find at the end of inflation should not be directly compared with observations.

Finally, in the case $R_{\rm mass} = 1/5$, the trajectories are again as expected, with essentially two stages of inflation taking place. Initially the trajectories evolve in the ϕ direction, with the potential profile in the ϕ direction being very similar to that of the original R^2 inflation model. In the cases of the orange and magenta trajectories, they then turn and inflation proceeds as they evolve essentially in the χ direction but while oscillating about the local minimum located close to but not exactly at $\phi = 0$. For this choice of $R_{\rm mass}$, these trajectories do not appear to fully relax to the bottom of the local minimum before the end of inflation, and so we might expect that ζ is still evolving. In the case of the blue trajectory, due to the smaller initial position $\chi_*/M_{pl} = 1.5$, we find that there is no second stage of inflation driven by the χ field.

A feature that it is common to all choices of $R_{\rm mass}$ is that for $\chi = 0$ both the potential and $V_{,\phi}$ reduce to those of R^2 inflation, while $V_{,\chi} = 0$. Consequently, trajectories with $\chi_* = 0$ will evolve purely in the ϕ direction, and we expect that predictions for ζ will coincide with those of R^2 inflation.

As we move to non-zero values of χ, deviations from the R^2 potential depend on $R_{\rm mass}$, ϕ and χ. For super-Planckian values of ϕ satisfying $2\alpha\phi \gg$

1, such that $e^{-2\alpha\phi} \ll 1$, deviations from the R^2 potential are suppressed by a factor of $e^{-4\alpha\phi}$, and will therefore be negligible for sufficiently large values of ϕ. This feature can be seen in all panels of Fig. 5.3.1. In order for the χ-field contribution to the potential to dominate at some super-Planckian value of ϕ, one would require $R_{\rm mass}^2\chi^2 \gg 3M_{pl}^2 e^{4\alpha\phi}/2$, i.e. $R_{\rm mass}$ or χ must be very large. However, in such a parameter region we find that $\epsilon_\phi \equiv M_{pl}^2(V_{,\phi}/V)^2/2 \simeq 8M_{pl}^2\alpha^2 > 1$, such that $\epsilon_V = \epsilon_\phi + \epsilon_\chi > 1$, where $\epsilon_\chi \equiv M_{pl}^2 e^{2\alpha\phi}(V_{,\chi}/V)^2/2$, i.e. the slow-roll approximation breaks down.

Note that although the potential reduces to $m_\chi^2\chi^2/2$ if we take $\phi = 0$, due to the interaction term we do not have $V_{,\phi} = 0$ when $\phi = 0$. As such, even if we start with $\phi_* = 0$, we do not necessarily obtain chaotic inflation along the χ direction. Indeed, $\dot{\phi}$ is positive along the axis $\phi = 0$, and if we calculate ϵ_ϕ we again find $\epsilon_\phi = 8M_{pl}^2\alpha^2 > 1$, such that $\epsilon_V > 1$ and the slow-roll approximation is violated. Nevertheless, in the limit $R_{\rm mass} \ll 1$, with appropriate initial conditions we do find that the final stages of inflation essentially coincide with quadratic chaotic inflation driven by the χ field. As can be seen in the third panel of Fig 5.3.1, for small values of $R_{\rm mass}$ and sufficiently super-Planckian initial conditions for ϕ and χ, we obtain two stages of inflation. The first stage is driven by ϕ, and once ϕ reaches its minimum the second stage is driven essentially by χ. The minimum of the potential in the ϕ direction lies on the curve defined by

$$\frac{2}{3}R_{\rm mass}^2\frac{\chi^2}{M_{pl}^2} = e^{2\alpha\phi} - 1. \tag{5.3.8}$$

As such, if $R_{\rm mass}$ is small enough to ensure that $R_{\rm mass}\chi/M_{pl} \ll \sqrt{3/2}$, we find that the minimum lies very close to the χ axis, with $\phi/M_{pl} \ll \sqrt{3/2}$. In the same limit $R_{\rm mass}\chi/M_{pl} \ll \sqrt{3/2}$, we find that along the minimum with respect to ϕ the potential and its derivative with respect to χ are approximately given as

$$V|_{V,\phi=0} \simeq \frac{1}{2}m_\chi^2\chi^2, \qquad V_{,\chi}|_{V,\phi=0} \simeq m_\chi^2\chi, \tag{5.3.9}$$

i.e. they coincide with the case of a quadratic mass term for the χ field. Con-

sequently, in the limit $R_{\rm mass} \ll 1$, or more precisely $R_{\rm mass} \ll \sqrt{3/2}M_{pl}/\chi_*$, once the ϕ field has evolved to its minimum we expect quadratic chaotic inflation driven by χ to take place. If we require that this stage of chaotic inflation lasts for approximately 60 e-foldings, then this means we require $\chi_* \simeq 15.5 M_{pl}$, which in turn gives the condition $R_{\rm mass} \ll \sqrt{3/2}/15.5 \simeq 0.08$. In analogy with the large $R_{\rm mass}$ limit, we find that for $R_{\rm mass} \ll 0.08$ the whole of the observable period of inflation will essentially coincide with quadratic chaotic inflation driven by χ if we take any initial conditions with $\chi_* \sim 15.5 M_{pl}$. At the level of perturbations, in analogy with the large $R_{\rm mass}$ case, as the trajectory evolves along the the local minimum close to $\phi = 0$ we expect that ζ will be conserved and that isocurvature perturbations decay, such that an adiabatic limit is approached.

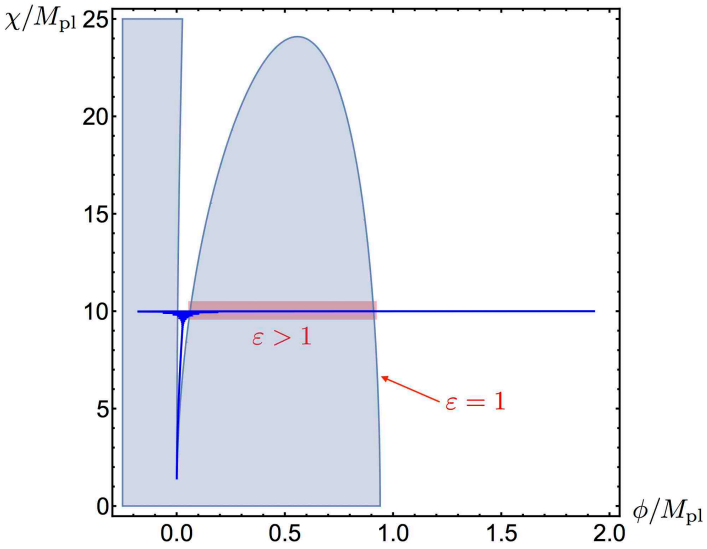

Figure 5.3.2: An example trajectory for $R_{\rm mass} = 0.02$ and $(\phi_*/M_{pl}, \chi_*/M_{pl}) = (2.0, 10.0)$. The region with $\epsilon_V > 1$ is shaded in blue. The trajectory consists of two inflationary stages separated by a non-inflationary stage.

Given that the mass ratio $R_{\rm mass} = 0.2$ considered in Fig. 5.3.1 is not so small, in Fig. 5.3.2 we plot an example trajectory for the case $R_{\rm mass} = 0.02$ and the initial conditions $(\phi_*/M_{pl}, \chi_*/M_{pl}) = (2.0, 10.0)$. We also show the region where $\epsilon_V > 1$. Similar to the case $R_{\rm mass} = 0.2$ considered in Fig. 5.3.1,

the trajectory first evolves in the ϕ direction and the potential profile essentially coincides with R^2 inflation. Intermediately, when ϕ drops below M_{pl}, one thus finds that ϵ_V becomes greater than unity and inflation temporarily ceases. However, once the trajectory reaches the local minimum, ϵ_V once again becomes less than unity and inflation recommences, with the subsequent trajectory evolving essentially in the χ direction. It is thus important when considering small values of $R_{\rm mass}$ that we do not terminate our integration of the trajectory prematurely, in order not to miss the second stage of inflation. Note that there is a period during which the ϕ field oscillates about its minimum, and during this period one might expect the ϕ field to decay into any matter fields to which it is coupled, including the χ field. Indeed, due to the non-minimal coupling of ϕ to the Ricci scalar in the Jordan frame, we expect there to at least be gravitationally induced couplings between ϕ and any other matter fields present, see e.g. [81, 82]. However, in the following we neglect the possible decay of the ϕ field, postponing a careful consideration of this effect to future work.

Evolution of perturbations

Having given some example background trajectories, we now consider the evolution of ζ, or more precisely its correlation functions. As discussed above, in single field inflation we know that ζ is conserved on superhorizon scales, while in multi-field inflation it is sourced by isocurvature perturbations if the trajectory in field space deviates from a geodesic, see e.g. [65, 66].

Perhaps the most interesting evolution of ζ and its correlation functions is observed in the case of small $R_{\rm mass}$. As an example, we consider the parameters $R_{\rm mass} = 0.1$ and $(\phi_*/M_{pl}, \chi_*/M_{pl}) = (5, 8)$. The background trajectory for this choice of parameters is shown in Fig. 5.3.3. Given that $R_{\rm mass} \ll 1$, we see that the trajectory first evolves in the ϕ direction, before moving along the local minimum that runs almost parallel to the χ axis. In total there are approximately 60 e-foldings of inflation, with the turn occurring at $N \sim 45$. In the left panel of Fig. 5.3.4 we plot the evolution of the power spectrum, normalised by the final value. As expected, it remains

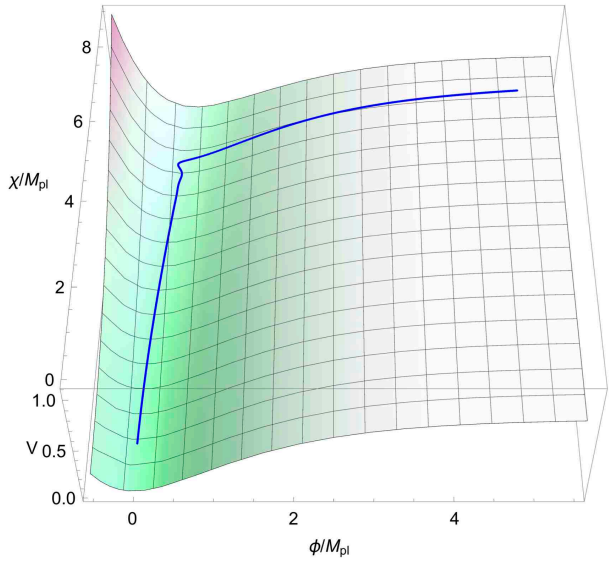

Figure 5.3.3: An example trajectory with $R_{\rm mass} = 0.1$ and initial conditions $(\phi_*/M_{pl}, \chi_*/M_{pl}) = (5.0, 8.0)$. Inflation lasts for a total of 58 e-foldings.

constant for the first 40 e-folds, and is then sourced by isocurvature modes as the trajectory turns at around $N \sim 45$. Given the relatively large mass hierarchy, $\mathcal{P}_\zeta$ is seen to oscillate as the trajectory oscillates about the local minimum, before again approaching a constant as an essentially single-field limit is reached.

In the right panel of Fig. 5.3.4 we show the evolution of $f_{\rm NL}$ for the same trajectory. Up until the turn it is negligibly small, with $f_{NL} \sim \mathcal{O}(10^{-2})$. During the turn and subsequent oscillations we find that f_{NL} also oscillates, with a peak amplitude of $f_{NL} \simeq 0.35$. In the final stage, however, f_{NL} relaxes back down to an unobservably small value of $\mathcal{O}(10^{-2})$. The behaviour of the power spectrum and f_{NL} in this example are qualitatively very similar to that observed in double quadratic inflation models, see e.g. [76, 83, 84] and references therein.

We have also considered the evolution of $\mathcal{P}_\zeta$ and f_{NL} in the other regimes $R_{\rm mass} > 1$ and $R_{\rm mass} \sim 1$. For trajectories with $R_{\rm mass} > 1$, such as those shown in the first panel of Fig. 5.3.1, due to the fact that the trajectories quickly evolve to the ϕ axis and reach an effectively single-field trajectory

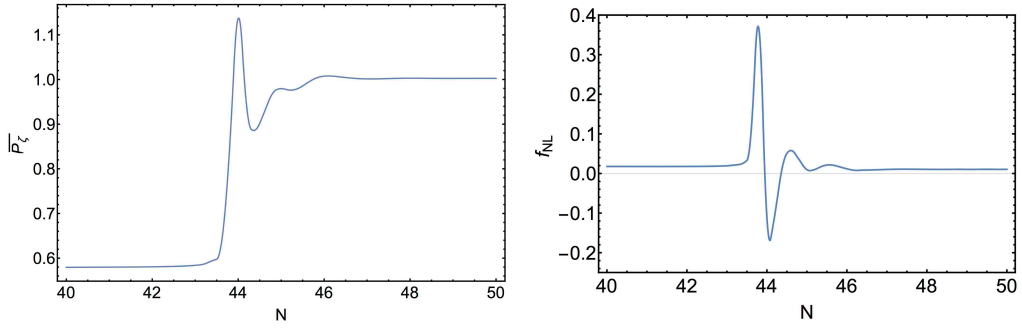

Figure 5.3.4: Evolution of the normalised power spectrum $\overline{P}_\zeta = P_\zeta(N)/P_\zeta(N_{\rm final})$ (left panel) and f_{NL} (right panel) for the example trajectory plotted in Fig. 5.3.3.

along the ϕ axis, we find that $\mathcal{P}_\zeta$ and f_{NL} also quickly reach constant values, with $f_{NL} \sim \mathcal{O}(10^{-2})$. Note that the background trajectories shown in the first panel of Fig. 5.3.1 do not oscillate about the ϕ axis, and correspondingly we find that $\mathcal{P}_\zeta$ and f_{NL} also do not oscillate before settling to their constant values. For trajectories with $R_{\rm mass} \sim 1$, such as those shown in the second panel of Fig. 5.3.1, we find that the evolution of $\mathcal{P}_\zeta$ and f_{NL} is much more gradual, with f_{NL} remaining $\mathcal{O}(10^{-2})$ throughout the evolution.

Exploring and constraining parameter space

Having looked at representative example trajectories in the three regimes $R_{\rm mass} < 1$, $R_{\rm mass} \sim 1$ and $R_{\rm mass} > 1$, we now proceed to put constraints on the parameters m_ϕ and $R_{\rm mass}$. In doing so we consider thirty-one different mass ratios in the range $10^{-3} \leq R_{\rm mass} \leq 10^3$, distributed evenly over $\log R_{\rm mass}$. For each value of $R_{\rm mass}$ we then consider a 50×50 grid of initial conditions (ϕ_*, χ_*), with ϕ_* spanning the range $0 \leq \phi_* \leq 6M_{pl}$ and χ_* spanning the range $0 \leq \chi_* \leq 16M_{pl}$.[3] Next we neglect any points on the grid for which either $\epsilon_V > 1$ or $|\eta_V| > 1$, i.e. we require that the slow-roll approximation is valid at the horizon-crossing time. For the remaining points

[3]From our knowledge of the R^2 and quadratic chaotic inflation models, we know that taking $\phi_* > 6$ or $\chi_* > 16$ will always give $N_{\rm total} > 60$, but observationally we are only interested in the last 60 e-folds of inflation. Hence our choice of maximum ϕ_* and χ_*.

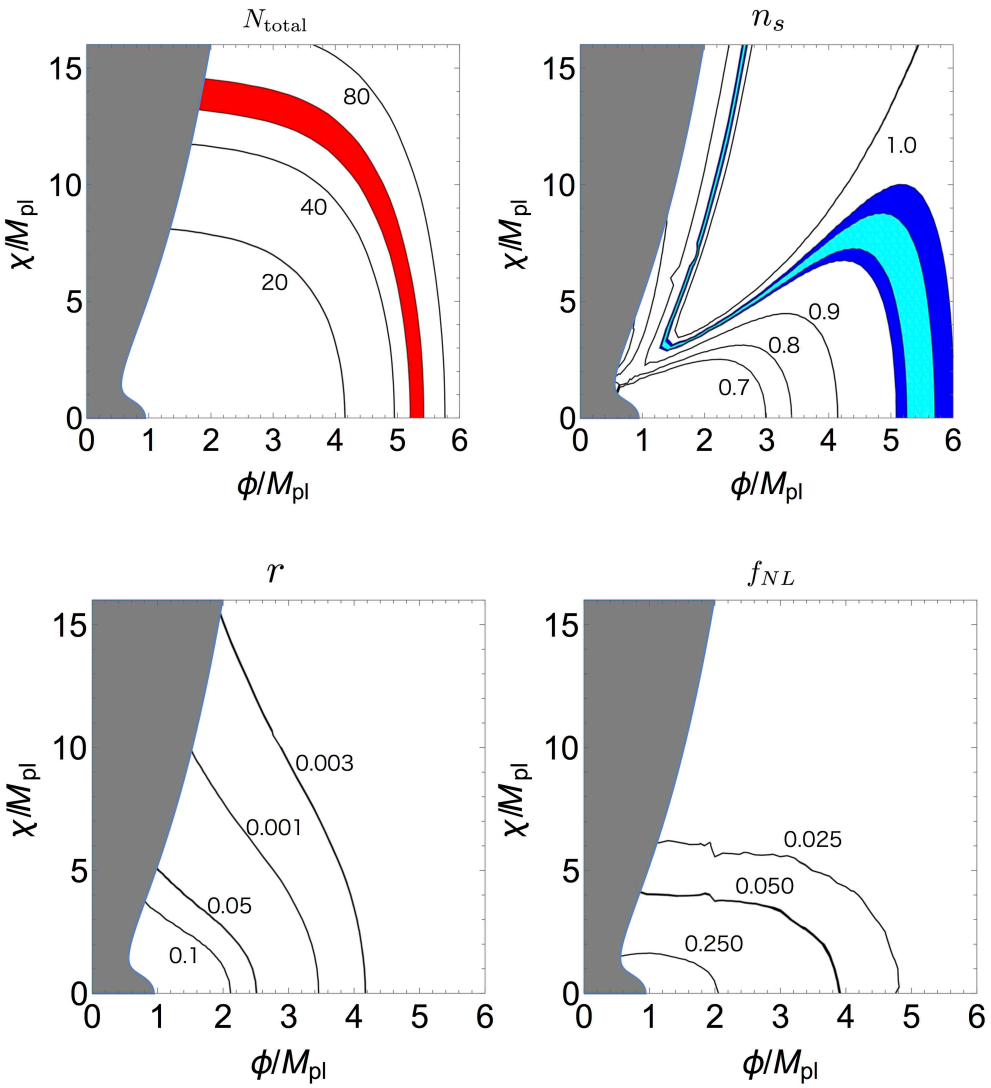

Figure 5.3.5: Predictions in the ϕ_*–χ_* plane for the e-folding number N (upper left), spectral tilt n_s (upper right), tensor-to-scalar ratio r (lower left) and non-Gaussianity parameter $f_{\rm NL}$ (lower right) for the case $R_{\rm mass} = 1.0$. The red shaded region in the upper left plot shows the initial conditions for which $50 < N_{\rm total} < 60$. Here $N_{\rm total}$ is the total amount of e-foldings from the horizon exit to the end of inflation. The light blue (dark blue) shaded region in the upper right plot indicates the range of initial conditions for which n_s lies within 1-σ (2-σ) of the observed value. The grey shaded region in all plots corresponds to where $\epsilon_V > 1$.

we are then able to determine N, $\mathcal{P}_\zeta/m_\phi^2$, n_s, r and f_{NL} without needing to specify m_ϕ. Neglecting points that do not give $50 < N_{\rm total} < 60$, for each of the remaining points we perform a chi-squared analysis to determine the range of m_ϕ for which the predictions for $\mathcal{P}_\zeta$, n_s, r and f_{NL} lie within 1- and 2-σ of the observed values summarised at the end of chapter 4. At this point, for every observationally allowed set of initial conditions (ϕ_*, χ_*) we have a maximum and minimum allowed m_ϕ. To find the overall maximum and minimum allowed values of m_ϕ for a given $R_{\rm mass}$, we must then take the maximum of all the maxima and the minimum of all the minima. Note that for any value of $R_{\rm mass}$ we are guaranteed to find a non-vanishing allowed range of m_ϕ, as we will always recover the predictions of R^2 inflation if we take $\chi_* = 0$.

As an example, in Fig. 5.3.5 we show the predictions for N, n_s, r and f_{NL} in the ϕ_*–χ_* plane for the case $R_{\rm mass} = 1$. In the plot of N we highlight in red the region for which $50 < N_{\rm total} < 60$. Similarly, in the plot of n_s we highlight in light- and dark-blue the regions that fall within 1- and 2-σ of the observed value. For all values of ϕ_* and χ_* we find that r and f_{NL} are consistent with observational constraints. In Fig. 5.3.6 we combine the constraints coming from N and n_s, which allows us to determine the region in the ϕ_*–χ_* plane in which the horizon exit point must lie. The intersection of the red shaded region with the ϕ axis corresponds to the initial conditions for R^2 inflation. As we move away from the ϕ axis we see that there is quite an extended region that remains in agreement with observations. Interestingly, there is another small allowed region towards the top left-hand corner of the ϕ_*–χ_* plane.

The obtained constraints on m_ϕ as a function of $R_{\rm mass}$ are shown in Fig. 5.3.7. In the limits of both small and large $R_{\rm mass}$ we find that the allowed range is consistent with that of R^2 inflation, for which slow-roll estimates give $m_\phi \simeq (1.2\text{–}1.4) \times 10^{-5} M_{pl}$ for $N_{\rm total} = 50$–60. In the large $R_{\rm mass}$ limit this has a relatively simple interpretation. As the χ field becomes more massive one approaches a limit in which all slow-roll trajectories satisfiying $\epsilon_V, |\eta_V| \ll 1$ at horizon crossing and giving $50 < N_{\rm total} < 60$ correspond to effecitvely single-field trajectories that evolve along the ϕ axis, where the

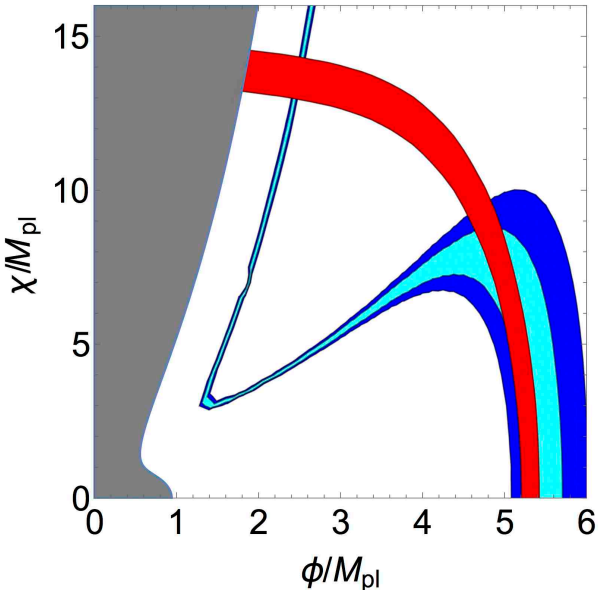

Figure 5.3.6: Combined constraints in the ϕ_*–χ_* plane for the case $R_{\rm mass} = 1$. The red shaded region corresponds to the constraint $50 < N_{\rm total} < 60$, while the light- and dark-blue regions correspond to the 1- and 2-σ observational constraints on n_s given at the end of chapter 4. Predictions for r and $f_{\rm NL}$ are consistent with observations for all sets of initial conditions. The grey shaded region corresponds to where $\epsilon_V > 1$.

potential reduces to that of R^2 inflation. We can see from Fig. 5.3.7 that such a limit is reached for $R_{\rm mass} \sim 10$. In the small $R_{\rm mass}$ limit the situation is less clear. The fact that the allowed range of m_ϕ approaches a constant can be understood as follows. So long as $R_{\rm mass}$ is smaller than some critical value — which our results suggest is around $R_{\rm mass} \simeq 10^{-2}$ — one finds that for a given set of initial conditions the last 60 e-foldings of inflation is well approximated by a stage of R^2 inflation followed by a stage of quadratic chaotic inflation, as was observed in Fig. 5.3.2. The fact that the allowed range of m_ϕ coincides with that of R^2 inflation, however, is not so obvious. As χ_* is increased from 0 to $16M_{pl}$ (and ϕ_* is correspondingly adjusted to give the desired number of e-foldings), we expect that predictions for $\mathcal{P}_\zeta$, r, n_s and f_{NL} will interpolate between those of R^2 inflation and those of quadratic chaotic inflation. While the latter are ruled out by observations,

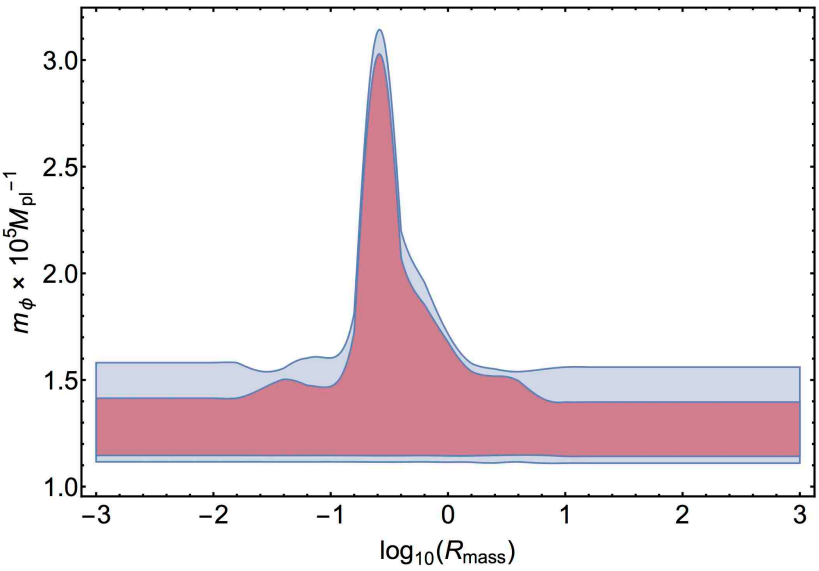

Figure 5.3.7: Allowed regions in the $R_{\rm mass}$–m_ϕ plane at 1-σ (red shaded region) and 2-σ (blue shaded region).

one might naively expect that intermediately there are values of χ_* that give predictions deviating from R^2 inflation but still in agreement with observations, which in turn would naively alter the allowed range of m_ϕ. However, our results suggest that the allowed range of m_ϕ is essentially unaffected.

For intermediate values of $R_{\rm mass}$ the obtained bounds on m_ϕ are found to deviate from those of R^2 inflation. As we can see in Fig. 5.3.7, the allowed range of m_ϕ has a peak of $m_\phi \simeq 3 \times 10^{-5} M_{pl}$ at around $\log_{10}(R_{\rm mass}) \simeq -0.5$ ($R_{\rm mass} \simeq 0.3$). However, one must bear in mind that for some of the trajectories in this parameter range an adiabatic limit will not have been reached by the end of inflation. As such, it may be that the constraints in this region would change if effects of the (p)reheating epoch were taken into account.

Using the definition of $R_{\rm mass}$, we can use the above constraints on m_ϕ to also put bounds on m_χ as a function of $R_{\rm mass}$. The results are shown in Fig. 5.3.8a. Similarly, recall that in the Jordan frame representation of this model one has the parameter μ instead of m_ϕ, see eq. (5.2.1). Given

that these two parameters are related as $m_\phi^2 = M_{pl}^2/(6\mu)$, we can re-express our constraints on m_ϕ as constraints on μ, and the results are shown in Fig. 5.3.8b. In the original R^2 inflation model, slow-roll estimates determine that in order to satisfy observational constraints one requires $\mu \simeq (0.9\text{–}1.2) \times 10^9$ for $N_{\rm total}$=50–60 [85, 86], which is consistent with our constraints. In the multi-field extension of R^2 inflation that we have considered, we find the allowed range of μ to be $\mu \simeq (0.2\text{–}1.3) \times 10^9$.

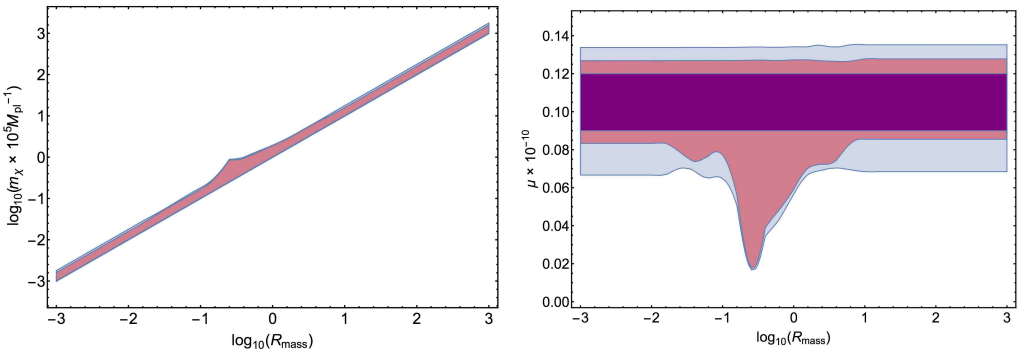

(a) (b)

Figure 5.3.8: (a) Allowed regions in the $R_{\rm mass}$–m_χ plane at 1-σ (red shaded region) and 2-σ (blue shaded region). (b) Allowed regions in the $R_{\rm mass}$–μ plane at 1-σ (red shaded region) and 2-σ (blue shaded region). The purple-shaded region shows $\mu = (0.9\text{–}1.2) \times 10^9$, which corresponding to the case of the original R^2 inflation model with $N_{\rm total} = 50\text{–}60$.

5.4 Summary of this model

In this chapter we have considered a two-field inflation model based on a simple multi-field extension of R^2 inflation. In addition to a term proportional to R^2, the Jordan frame action contains a canonical scalar field χ with quadratic mass term. On re-writing the model as a scalar-tensor theory and making a conformal transformation into the Einstein frame, the model takes the form of a two-field inflation model with a non-flat field space as shown in eq. (5.2.6). The first field, ϕ, corresponds the additional degree of freedom associated with the R^2 term in the original action and is often referred to

as the scalaron. This field has a canonical kinetic term and its potential takes on the same form as in the original R^2 inflation model, approaching a constant for super-Planckian values of ϕ. The second field, χ, on the other hand, has a non-canonical kinetic term that depends exponentially on ϕ, and its quadratic mass term similarly contains an exponential coupling with ϕ.

Assuming that the slow-roll approximation is valid at horizon crossing, such that only the initial field positions have to be specified in solving for the inflationary dynamics, the four free parameters of the model are m_ϕ, $R_{\rm mass} = m_\chi/m_\phi$, ϕ_* and χ_*. In Sec. 5.3 we have explored how the inflationary dynamics and predictions for the correlation functions of ζ depend on these four parameters, both qualitatively and quantitatively.

For $R_{\rm mass} \sim 10$ we find that all slow-roll trajectories satisfying $\epsilon_V, |\eta_V| \ll 1$ at horizon crossing and giving $50 < N < 60$ follow an effectively single-field trajectory evolving along the local minimum of the potential at $\chi = 0$. Given that the potential coincides with that of the original R^2 inflation model along $\chi = 0$, the predictions for ζ and its correlation functions also coincide with the original model. In this region of parameter space observational constraints give $m_\phi \simeq (1.1\text{–}1.6) \times 10^{-5} M_{pl}$ at 2-σ.

For $R_{\rm mass} < 10^{-2}$ we find that inflationary trajectories consist of a stage of R^2 inflation driven by ϕ followed by a stage of quadratic chaotic inflation driven by χ. How the last observable 60 e-foldings of inflation are divided between these two stages depends on the initial conditions, and the predictions for ζ and its correlation functions thus range from those of R^2 inflation to those of quadratic chaotic inflation. Interestingly, however, we find that the final constraints on m_ϕ are very similar to those obtained in the large $R_{\rm mass}$ limit, namely they essentially coincide with the limits on m_ϕ obtained in the original R^2 model.

Finally, in the parameter region $R_{\rm mass} \sim 1$, we find that the constraints on m_ϕ are less tight, with $m_\phi \simeq (1.1\text{–}3.2) \times 10^{-5} M_{pl}$ at 2-σ. Here it is less easy to interpret the results, as the inflationary trajectories are truly multi-field in nature, with both ϕ and χ evolving throughout inflation in many cases and the dynamics very much depending on the initial conditions. Nevertheless, one can see that the net result of these multi-field effects is to increase the

allowed range of m_ϕ as compared to the original R^2 model, and in particular to allow for larger values of m_ϕ.

One issue that we have not fully addressed in this work is the possibility that ζ may continue to evolve after the end of inflation. If an adiabatic limit is not reached by the end of inflation then one should continue to follow the evolution of ζ through (p)reheating and until an adiabatic limit is reached. It is only the final ζ that should then be compared with observations. In the cases $R_{\rm mass} \gg 1$ and $R_{\rm mass} \ll 1$ the issue is naively not important, as we expect an adiabatic limit to be reached before the end of inflation for most inflationary trajectories. For $R_{\rm mass} \sim 1$, however, this is no longer the case, and so post-inflationary evolution of ζ may affect the constraints on m_ϕ in this region. We hope to address this issue in future work.

Chapter 6

Multi-Moduli inflation

6.1 Introduction for this model

In this chapter, we discuss a multi-field inflation model based on string compactification. String theory is formulated in 10 or 11 dimensions. Therefore, we need to compactify it on any internal manifolds to obtain four-dimensional effective theories. Associated with a compactification, a lot of scalar fields appear in four-dimensional theory, which are called moduli fields. To fix each physical constant and to avoid "fifth-force" interaction, we have to stabilize these moduli fields. This is so-called "The moduli stabilization problem" (for review, see [87, 88]).

On the other hand, inflation is one of the most promising paradigm in modern cosmology. The typical energy scale of inflation could be close to the Grand Unification scale or string scale. Thus, from the top-down viewpoint, it is natural to regard stabilized moduli as inflation fields. So far, numbers of works have been proposed which are based on moduli stabilization, but almost all model rely on tuning of parameters to realize single-field inflation. This is just because for simplicity of their models or lack of the way to analyze multi-field models. However, from the viewpoint of string compactification, it is ubiquitous to consider multi-field type inflation. In our work, we established the numerical framework to address analysis of multi-field dynamics, and applied it to the multi-field inflation model which is based on

string compactification and string loop corrections.

In analyzing the inflationary predictions of this model we make use of the δN formalism and the transport method developed in [15, 16, 17, 18]. Utilizing this method, we can analyze the inflation model with taking into account full multi-field effects such that isocurvature transfers in turning or oscillation trajectories.

This chapter is organized as follows. In section 6.2 we briefly review fibre inflation which is an inflation model based on moduli stabilization and string loop corrections. In section 6.3, we extend the fibre inflation to a multi-field model. We analyze this model with δN formalism in section 6.4. In particular, we discuss trajectory-dependence of inflationary predictions. Section 6.5 is devoted to summary of this model.

6.2 Fibre inflation

In the effective 4d supergravity, scalar potential is given by

$$V = e^K [K^{i\bar{j}} D_i W D_{\bar{j}} \overline{W} - 3|W|^2]. \tag{6.2.1}$$

Here, K is a Kähler potential, and W is a superpotential. D_i is the covariant derivative associated with Kähler metric, and defined as

$$D_i \equiv \partial_i + \partial_i K, \tag{6.2.2}$$

where the index i denote each scalar field.

Following Kallosh *et al.*[89], we take a superpotential of moduli T_i as follows:

$$W = \int G_3 \wedge \Omega + \sum_i A_i e^{-a_i T_i} = W_0 + \sum_i A_i e^{-a_i T_i}, \tag{6.2.3}$$

In general, T_i are complex fields, and here the first term comes from a combination of induced 3-form flux G_3 and the holomorphic 3-form Ω. Ω can be determined by the geometry of the internal space, and this term fixes complex structure moduli. The second term comes from non-perturbative

effects (e.g. gaugino condensation, or world sheet instanton) and it gives the potential of Käler moduli.

Following Large Volume Scenario, we take a Käler potential of the form,

$$K = -2\ln\left(\mathcal{V} + \frac{\xi}{2g_s^{3/2}}\right), \tag{6.2.4}$$

$\mathcal{V}$ is a volume of the internal space, and the second term in the parenthesis comes from α' correction which is a perturbative correction to the Kähler potential [90].

In the original paper of Fibre inflation, authors took a volume $\mathcal{V}$ as follows:

$$\begin{aligned}\mathcal{V} =& \lambda_1 t_1 t_2^2 + \lambda_s t_s^3 \\ =& \alpha\left(\sqrt{\tau_1}\tau_2 - \gamma\tau_s^{3/2}\right),\end{aligned} \tag{6.2.5}$$

where τ_i is the real part of T_i, and in this expression, τ_1, τ_2 and τ_s are 4-cycles of the internal manifold. τ_2 fixes overall volume, and τ_1 is much smaller than τ_2. Therefore, in terms of moduli, τ_1 is expected to be a dynamical field, and τ_s is a blow-up mode.

In Fibre inflation, they considered string-loop corrections to scalar potential which is given by

$$\delta V_{(g_s)} = \delta V^{KK}_{(g_s),\tau_1} + \delta V^{KK}_{(g_s),\tau_2} + \delta V^{W}_{(g_s),\tau_1\tau_2}, \tag{6.2.6}$$

and each term is expressed as

$$\delta V^{KK}_{(g_s),\tau_1} = g_s^2 \frac{\left(C_1^{KK}\right)^2}{\tau_1^2}\frac{W_0^2}{\mathcal{V}^2}, \tag{6.2.7}$$

$$\delta V^{KK}_{(g_s),\tau_2} = 2g_s^2 \frac{\left(C_2^{KK}\right)^2}{\tau_2^2}\frac{W_0^2}{\mathcal{V}^2}, \tag{6.2.8}$$

$$\delta V^{W}_{(g_s),\tau_1\tau_2} = -\left(\frac{2C_{12}^W}{t_*}\right)\frac{W_0^2}{\mathcal{V}^3}. \tag{6.2.9}$$

By using

$$\mathcal{V} \sim \alpha\sqrt{\tau_1}\tau_2 \quad \Rightarrow \quad \frac{1}{\tau_2} \propto \frac{\sqrt{\tau_1}}{\mathcal{V}}, \tag{6.2.10}$$

we can rewrite (6.2.8)

$$\delta V^{KK}_{(g_s),\tau_2} \propto \frac{\tau_1}{\mathcal{V}^2}\frac{W_0}{\mathcal{V}^2}. \tag{6.2.11}$$

Also, once we compute the intersection of τ_1 and τ_2, we can express (6.2.9) in terms of τ_1. According to (6.2.5),

$$\tau_1 = \frac{\partial \mathcal{V}}{\partial t_1} = (\lambda_1 t_2)\, t_2 \quad \text{and} \quad \tau_2 = \frac{\partial \mathcal{V}}{\partial t_2} = 2t_1\,(\lambda_1 t_2)\,, \tag{6.2.12}$$

and then, this implies that intersection t_* is given by

$$t_* = \sqrt{\lambda_1 \tau_1}. \tag{6.2.13}$$

Now (6.2.9) can be expressed as

$$\delta V^{W}_{(g_s),\tau_1\tau_2} \propto -\frac{1}{\mathcal{V}\sqrt{\tau_1}}\frac{W_0^2}{\mathcal{V}^2}. \tag{6.2.14}$$

In the end, we obtain the final expression of the string-loop corrections:

$$\delta V_{(g_s)} = \left(\frac{A}{\tau_1^2} - \frac{B}{\mathcal{V}\sqrt{\tau_1}} + \frac{C\tau_1}{\mathcal{V}^2}\right)\frac{W_0^2}{\mathcal{V}^2}, \tag{6.2.15}$$

In terms of the canonically normalized field φ,

$$\varphi = \frac{\sqrt{3}}{2}\ln\tau, \tag{6.2.16}$$

(6.2.15) becomes

$$\delta V_{(g_s)} = \frac{W_0^2}{\mathcal{V}^2}\left(Ae^{-2\kappa\varphi} - \frac{B}{\mathcal{V}}e^{-\kappa\varphi/2} + \frac{C}{\mathcal{V}^2}e^{\kappa\varphi}\right). \tag{6.2.17}$$

where $\kappa = \frac{2}{\sqrt{3}}$. Then, we obtain

$$V \simeq \frac{W_0^2}{\mathcal{V}^2}\left[(3-R) - 4\left(1+\frac{1}{6}R\right)e^{-\kappa\varphi/2} + \left(1+\frac{2}{3}R\right)e^{-2\kappa\varphi} + Re^{\kappa\varphi}\right] \tag{6.2.18}$$

In [93], the authors took $R = 10^{-3}$, and then the potential has a flat region which is suitable for inflation.

6.3 Multi-Moduli inflation

In the context of string compactification, especially Calabi-Yau compactification, it is more natural to consider multi-moduli in the effective theory, and it leads to multi-field type model-building of inflation. Motivated by this reason, we extend the fibre inflation theory to a multi-field version. First, we take following modulus dependence of the volume.

$$\begin{aligned}\mathcal{V} &= \lambda_1 t_1 t_2 t_3 + \lambda_s t_s^3 \\ &= \alpha\left(\sqrt{\tau_1\tau_2\tau_3} - \gamma\tau_s^{3/2}\right).\end{aligned} \tag{6.3.1}$$

We consider the case that τ_3 fixes the overall volume and τ_1 and τ_2 are dynamical. Again τ_s is the blow-up mode.

In this set up, we have following correction terms from string-loop corrections.

$$\delta V^{KK}_{(g_s),\tau_i} = g_s^2 \frac{\left(C_i^{KK}\right)^2}{\tau_i^2}\frac{W_0^2}{\mathcal{V}^2} \quad (i=1,2,3) \tag{6.3.2}$$

$$\delta V^{W}_{(g_s),\tau_1\tau_2} = g_s^2 \frac{\left(C_{12}^{KK}\right)^2}{\tau_1\tau_2}\frac{W_0^2}{\mathcal{V}^2} \tag{6.3.3}$$

$$\delta V^{W}_{(g_s),\text{intersection}} = -\left(\frac{C_{ij}^W}{t_{ij}^*}\right)\frac{W_0^2}{\mathcal{V}^3} \quad (i,j=1,2,3, i\neq j) \tag{6.3.4}$$

,and

$$\delta V^{W}_{(g_s),\tau_1\tau_2\tau_3} = -\left(\frac{C^{W}_{123}}{t^{*}_{123}}\right)\frac{W_0^2}{\mathcal{V}^3} \tag{6.3.5}$$

Eq.(6.3.2) is corresponding to a contribution from each moduli τ_i, and (6.3.3) comes from the cycle which is linear combination of τ_1 and τ_2. (6.3.4) and (6.3.5) come from intersections of each moduli. (6.3.4) corresponds to intersections of two of three moduli and, (6.3.5) corresponds to the intersection of all three moduli.

Combining all terms, the final expression is written as

$$\delta V_{(g_s)} = \left(\frac{C_1}{\tau_1^2} + \frac{C_2}{\tau_2^2} + \frac{C_3}{\tau_3^2} + \frac{C_4}{\tau_1\tau_2} - \frac{C_5}{t_{12}\mathcal{V}} - \frac{C_6}{t_{23}\mathcal{V}} - \frac{C_7}{t_{31}\mathcal{V}} - \frac{C_8}{t_{123}\mathcal{V}}\right)\frac{W_0^2}{\mathcal{V}^2}. \tag{6.3.6}$$

Here we can use the relation

$$\mathcal{V} \sim \alpha\sqrt{\tau_1\tau_2\tau_3}, \frac{1}{\sqrt{\tau_3}} \propto \frac{\sqrt{\tau_1\tau_2}}{\mathcal{V}}. \tag{6.3.7}$$

and compute t_{ij}, t_{123} from (6.3.1). Then we have

$$\delta V_{(g_s)} = \left(\frac{C_1}{\tau_1^2} + \frac{C_2}{\tau_2^2} + \frac{C_3(\tau_1\tau_2)^2}{\mathcal{V}^2} + \frac{C_4}{\tau_1\tau_2} - \frac{C_5}{\mathcal{V}\sqrt{\tau_1}} - \frac{C_6}{\mathcal{V}\sqrt{\tau_2}} - \frac{C_7}{\mathcal{V}^2}\sqrt{\tau_1\tau_2} - C_0\right)\frac{W_0^2}{\mathcal{V}^2}. \tag{6.3.8}$$

Here we used the fact $t_{123} = \lambda_1 = \text{const.}$ and replaced the C_8 term with another constant C_0.

Again using the canonically normalized field φ

$$\varphi_i = \frac{\sqrt{3}}{2}\ln\tau_i, \tag{6.3.9}$$

then we obtain the explicit form of the potential of Multi-moduli inflation,

$$
\begin{aligned}
V_{inf} &= V_0 + \delta V_{(g_s)} \\
&= V_0 + \frac{W_0^2}{\mathcal{V}^2} \times \\
&\left(C_1 e^{-2\kappa\varphi_1} + C_2 e^{-2\kappa\varphi_2} + \frac{C_3}{\mathcal{V}^2} e^{2\kappa(\varphi_1+\varphi_2)} + C_4 e^{-\kappa(\varphi_1+\varphi_2)} - \frac{C_5}{\mathcal{V}} e^{-\kappa\varphi_1/2} \right. \\
&\left. - \frac{C_6}{\mathcal{V}} e^{-\kappa\varphi_2/2} - \frac{C_7}{\mathcal{V}^2} e^{\kappa(\varphi_1+\varphi_2)/2} + C_0 \right).
\end{aligned}
\tag{6.3.10}
$$

Taking a similar choice of coefficients of each terms to fibre inflation, we set

$$
\begin{aligned}
V_{inf} \;\propto\; & 6(1+R) + (1+R)(e^{-2\kappa\varphi_1} + e^{-2\kappa\varphi_2}) - 4(1+R)(e^{-\kappa\varphi_1/2} + e^{-\kappa\varphi_1/2}) \\
& + (1+R)e^{-\kappa(\varphi_1+\varphi_2)} - Re^{-\kappa(\varphi_1+\varphi_2)} + Re^{2\kappa(\varphi_1+\varphi_2)}
\end{aligned}
\tag{6.3.11}
$$

Again taking $R = 10^{-3}$, the potential has a flat region. In this set up, there exist a lot of variations of trajectories of inflaton. Thus, we cannot apply the analysis which we used in cases of single-field inflation, and we need to take into accounts of multi-field effects.

6.4 Multi-field analysis and results

Using the transport method, we analyze this model shown in Eq.(6.3.10). One can immediately find that all trajectories on this potential are classified into two types. One type is like Fig.6.4.1. The trajectories showed in Fig. 6.4.1 behave like a single-field inflation at the beginning, and once they relax to the bottom of the potential ($\varphi_2 = 0$, in this case) they turn almost perpendicularly. After they turned, again they go down like a single-field inflation. For initial conditions such that we take in Fig. 6.4.1, all trajectories converge to the straight trajectory along φ_1-axi. This is one of an attractor trajectory in this potential.

For these kinds of trajectories in Fig. 6.4.1,the situation is similar to

double inflation models, and we can see the evolution of n_s, r, and $f_{\rm NL}$ in Fig. 6.4.2. Before turning points, some of trajectories yield values of ns and r which are far from the observationally-allowed values. However, after turning, the isocurvature perturbation is changed to the adiabatic curvature perturbation, and then almost all trajectories yield values of ns and r which are close to allowed value.

On the other hand, since the later stages of inflation is the same as essentially single-field inflation, $f_{\rm NL}$s are as small as those of single-field cases even though they have peaky futures and yield large non-Gaussianity $f_{\rm NL} \sim \mathcal{O}(1)$ intermediately. Hence, one can realize that if trajectories converge to the attractor, it is hopeless to find large non-Gaussianity. This is an important consequence for the trajectories shown in Fig.6.4.1

We show a different class of trajectories in Fig.6.4.3. For example, if inflation starts from $(\varphi_{1*}/M_{pl}, \varphi_{2*}/M_{pl}) = (5.0, 5.0)$, then we can find the trajectory becomes almost straight line. Thus, each quantities n_s, r and $f_{\rm NL}$ are almost constant during inflation. However, if inflation starts an initial point such that slightly deviated from on the straight line, for instance $(\varphi_{1*}/M_{pl}, \varphi_{2*}/M_{pl}) = (5.16, 5.0)$, then we see some non-trivial behaviors. In Fig.6.4.3, a blue trajectory start from $(5.1, 5.0)$, and it has no specific feature. It is almost the same as the one of single-field inflation. However, if we start $(5.16, 5.0)$(orange trajectory), first it goes down as same as straight line, but intermediately it deviates from that line. Moreover, near the end of inflation, the trajectory is bending and gives multi-field effects. In the end point of inflation, we have the times larger non-Gaussianity ($f_{\rm NL} \sim 0.23$) than that is predicted by single-field models. This is one of the interesting results of this model. In fact, similar analysis have already done in [59]. In addition, if inflation starts from $(5.2, 5.0)$(green trajectory), its motion is almost same with orange trajectory, and near the end of inflation, $f_{\rm NL}$ is enhanced. However, after the enhancement, this trajectory relax to the attractor trajectory and $f_{\rm NL}$ becomes small again $f_{\rm NL} \sim \mathcal{O}(10^{-2})$ in the end of inflation. This means that in order to obtain large non-Gaussianity, we need to tune the initial conditions, and it would be challenging to yield large $f_{\rm NL}$.

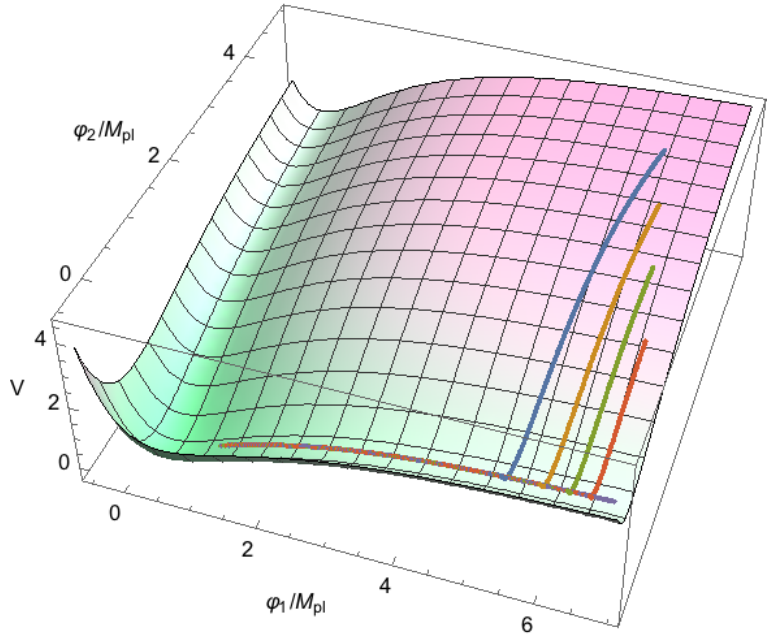

Figure 6.4.1: Examples of trajectories. Each initial conditions are $(\varphi_1/M_{\rm pl}, \varphi_2/M_{\rm pl}) = (6.0, 4.0)$ (blue), $(\varphi_1/M_{\rm pl}, \varphi_2/M_{\rm pl}) = (6.2, 3.2)$ (orange), $(\varphi_1/M_{\rm pl}, \varphi_2/M_{\rm pl}) = (6.4, 2.4)$ (green), $(\varphi_1/M_{\rm pl}, \varphi_2/M_{\rm pl}) = (6.5, 1.6)$ (red), $(\varphi_1/M_{\rm pl}, \varphi_2/M_{\rm pl}) = (6.8, 0.0)$ (purple). All trajectories roll down to the minimum of φ_2 direction, and in that stage, they are essentially the same as those of single-field inflation. After they turn, they become almost same single-field inflation.

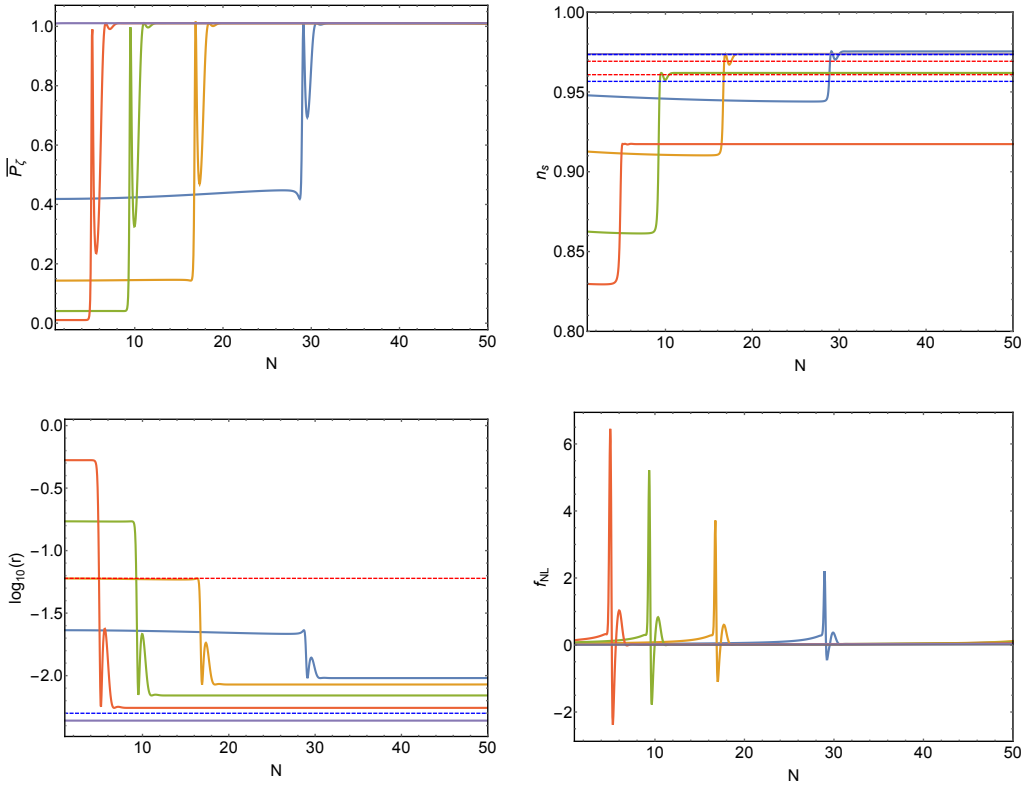

Figure 6.4.2: Superhorizon evolutions of the normalized power spectrum $(P_\zeta(N)/P_\zeta(N_{\rm final}))$, spectral index n_s (left-upper), tensor-scalar ratio r (right-upper), non-Gaussianity $f_{\rm NL}$ (left-bottom). All trajectories yield $n_s \sim 0.97$. Strictly speaking, however, all trajectories yield a bit too large n_s because the observational bound is $n_s = 0.965 \pm 0.0042(68\%\text{C.L.})$. Tensor-scalar ratios are small $r \sim \mathcal{O}(10^{-2})$ for all trajectories. At the first regime of inflation, all trajectories are almost straight, and so f_{NL} are as small as cases of single-field inflation($f_{NL} \sim \mathcal{O}(10^{-2})$). At the turning points, they are enhanced to $\mathcal{O}(10^{-1})$, and they may violate the Maldacena's consistency relation ($f_{NL} \sim (1 - n_s)$). However, after the turns, they become small again ($\sim \mathcal{O}(10^{-2})$) and they become horizon re-entry values.

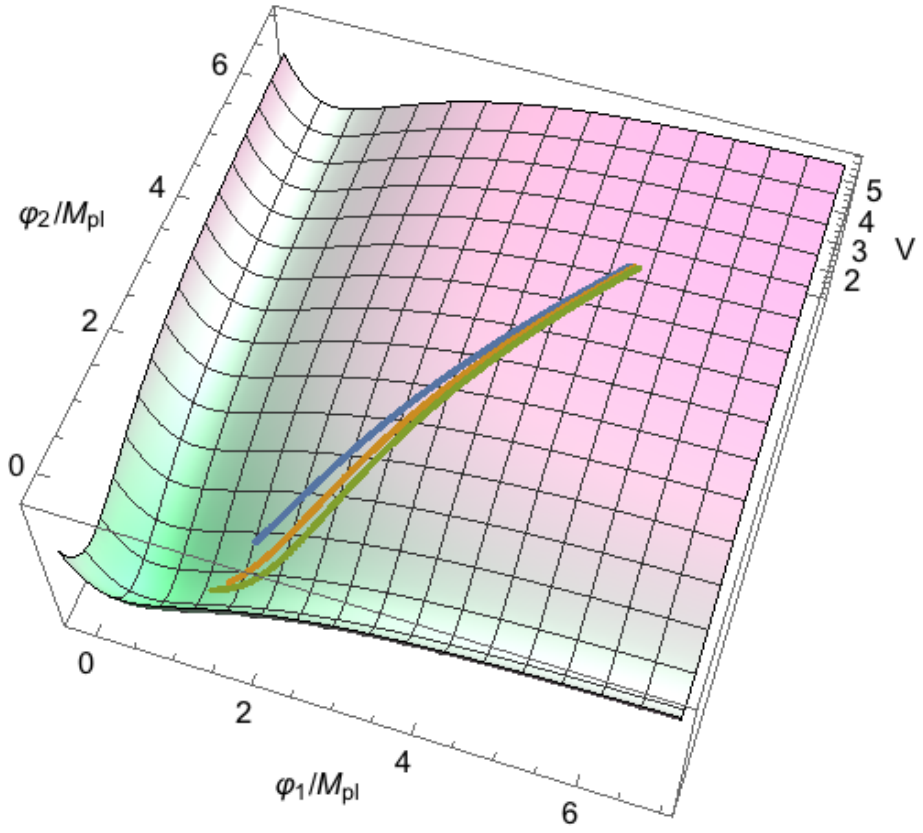

Figure 6.4.3: Examples of trajectories. $(\varphi_1/M_{\rm pl}, \varphi_2/M_{\rm pl}) = (5.0, 5.0 + 0.10)$ (blue), $(\varphi_1/M_{\rm pl}, \varphi_2/M_{\rm pl}) = (5.0, 5.0 + 0.16)$ (orange), $(\varphi_1/M_{\rm pl}, \varphi_2/M_{\rm pl}) = (5.0, 5.0 + 0.20)$ (green).

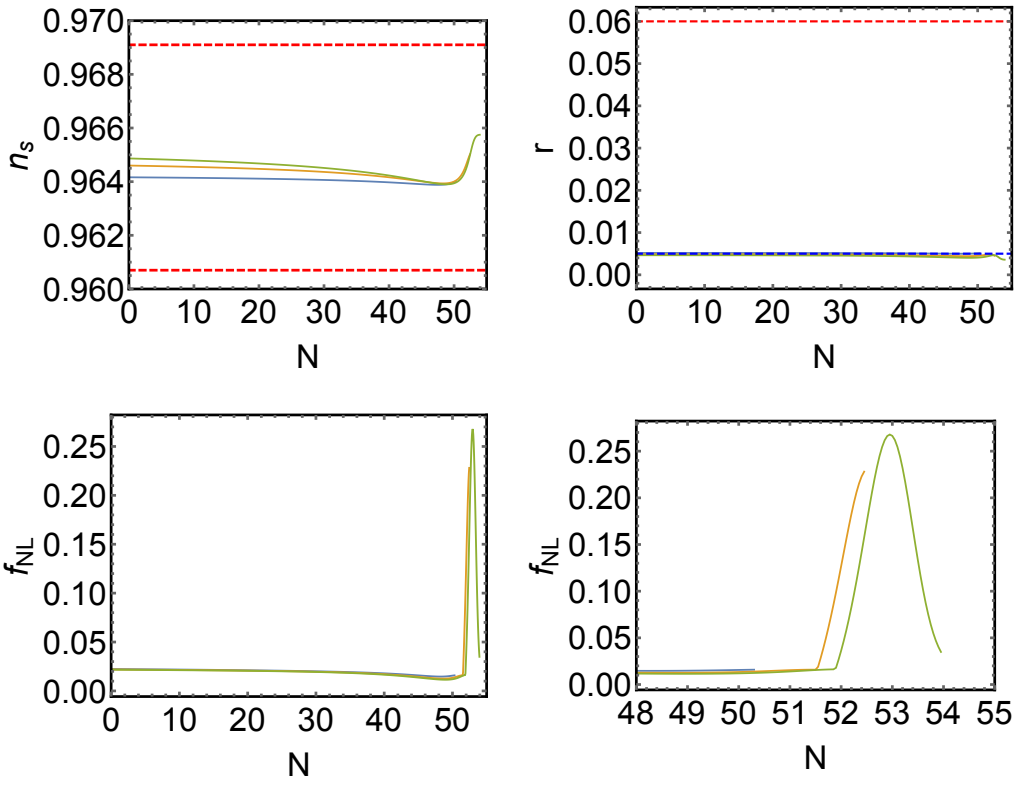

Figure 6.4.4: Superhorizon evolutions of spectral index n_s (left-upper) tensor-scalar ratio r (right-upper), non-Gaussianity $f_{\rm NL}$ (left-bottom) and close-up version of evolution of $f_{\rm NL}$ (N = 48-55).

Exploring and constraining field space

In Fig. 6.4.5, we show the predictions for N, n_s, r and $f_{\rm NL}$ in the $\varphi_1 - \varphi_2$ plane. We compute the predictions from 30×30 grid of initial points.

In the plot of e-folding number N, we highlight in red the region for which 50 ¡ N ¡ 60. Similarly, in the plot of n_s we highlight in cyan and blue the regions that yield within 1- and 2-σ of the observed value. The shape of the band of n_s is not so trivial. According to the expression of n_s, it contains second derivative of the potential, and it gives relatively larger negative contribution to n_s at around the regions which are close to φ_1 and φ_2 axes. That is why such a winding feature appears. In the plot of r, we draw the current observational bound on r with magenta line, $r < 0.07$. We can see that in the outside region of the magenta line, r falls to allowed value everywhere. For all initial points which yield enough e-folds, non-Gaussianity $f_{\rm NL}$ obtains small, and that magnitudes are almost same as that of single-field inflation models $f_{\rm NL} \sim \mathcal{O}(10^{-2})$. Therefore, we can conclude that every points which give enough e-folds predict the observationally-allowed values of r and $f_{\rm NL}$.

In Fig.6.4.6 we combine the constraints coming from N and n_s, which allows us to determine the region in the $\varphi_1 - \varphi_2$ plane in which the horizon exit point should be. It is reasonable that we find the allowed regions such that the intersections of the red shaded region with the axis. These regions approximately correspond to the initial conditions for single-field fibre inflation. A allowed region at around $(\varphi_1/M_{\rm pl}, \varphi_2/M_{\rm pl}) \sim (5.0, 5.0)$ is also natural because if inflation starts at this region, its trajectory becomes almost straight line. Thus, the predictions reduce to those of single-field fibre inflation. Moreover, there are non-trivial allowed regions such as around $(\varphi_1/M_{\rm pl}, \varphi_2/M_{\rm pl}) \sim (6.0, 1.0)$ and $(\varphi_1/M_{\rm pl}, \varphi_2/M_{\rm pl}) \sim (1.0, 6.0)$. That is coming from the non-trivial shape of the allowed region of n_s, and that winding future is originally coming from the tachyonic property of the inflaton potential.

6.5 Summary of this model

In this chapter, we have considered the two-field inflation model based on the string compactification and the moduli stabilization with the string loop corrections. The KKLT framework is known as the successful scenario to stabilize all moduli, and it is one of natural directions to use these stabilized moduli to be the inflaton fields. However, the scalar potential derived from the KKLT framework is not suitable for inflation since it is too steep to obtain the slow-roll for small field. Actually t should have become a run-away type potential at a large field value. One key idea to obtain a flat potential is to consider perturbative corrections. In particular, in the fibre inflation model, the string loop correction plays an important role to obtain a flat direction. In fact, this discussion is applicable to multiple moduli, and we have constructed an inflation potential in which two Kähler moduli have an exponentially flat direction. In multi-field inflation models, generally curvature perturbation is not conserved on the superhorizon scale. Thus, we need to estimate curvature perturbation not only at the beginning of the inflation, but also time-evolution of the adiabatic mode of the curvature perturbation fully in whole period of the inflation.

An important observable to discriminate single-field models from multi-field models is the non-Gaussianity of curvature perturbation. The Maldacena's consistency relation claims that in a single-field inflation, there is a special relationship between the spectral index n_s and the non-Gaussianity $f_{\rm NL}$ to be $f_{\rm NL} = \frac{5}{12}(1 - n_s)$. This means that the non-Gaussianity is as small as $\mathcal{O}(10^{-2})$ in single-field models. In contrast, there is a possibility that multi-field models may yield a relatively larger $f_{\rm NL}$.

According to our analysis, almost every trajectory of this model converges to an attractor trajectory. Once they converge to attractors, then they behave essentially like a single-field inflation. Hence, for such trajectories, we cannot expect to find any deviations from those in single-field cases. On the other hand, we have addressed another class of trajectories such that first it moves as just a straight line, but intermediately deviate from it and shows non-trivial multi-field effects at the end of inflation. For this kinds of

trajectories, we can find a significantly larger non-Gaussianity than that is predicted by single field models. In this work, we have surely found such a kind of trajectory, and it really yields a large non-gaussianity $f_{\rm NL} \sim 0.23$. While current constraints on non-Gaussianity from the CMB are still too weak to test the model, future observations are expected to considerably improve the constraints (see, e.g., Ref.[47]). This implies that we have a great possibility to test if inflation is really driven by multi-fields, and the results should provide rich information of new physics beyond the standard model to describe the early Universe.

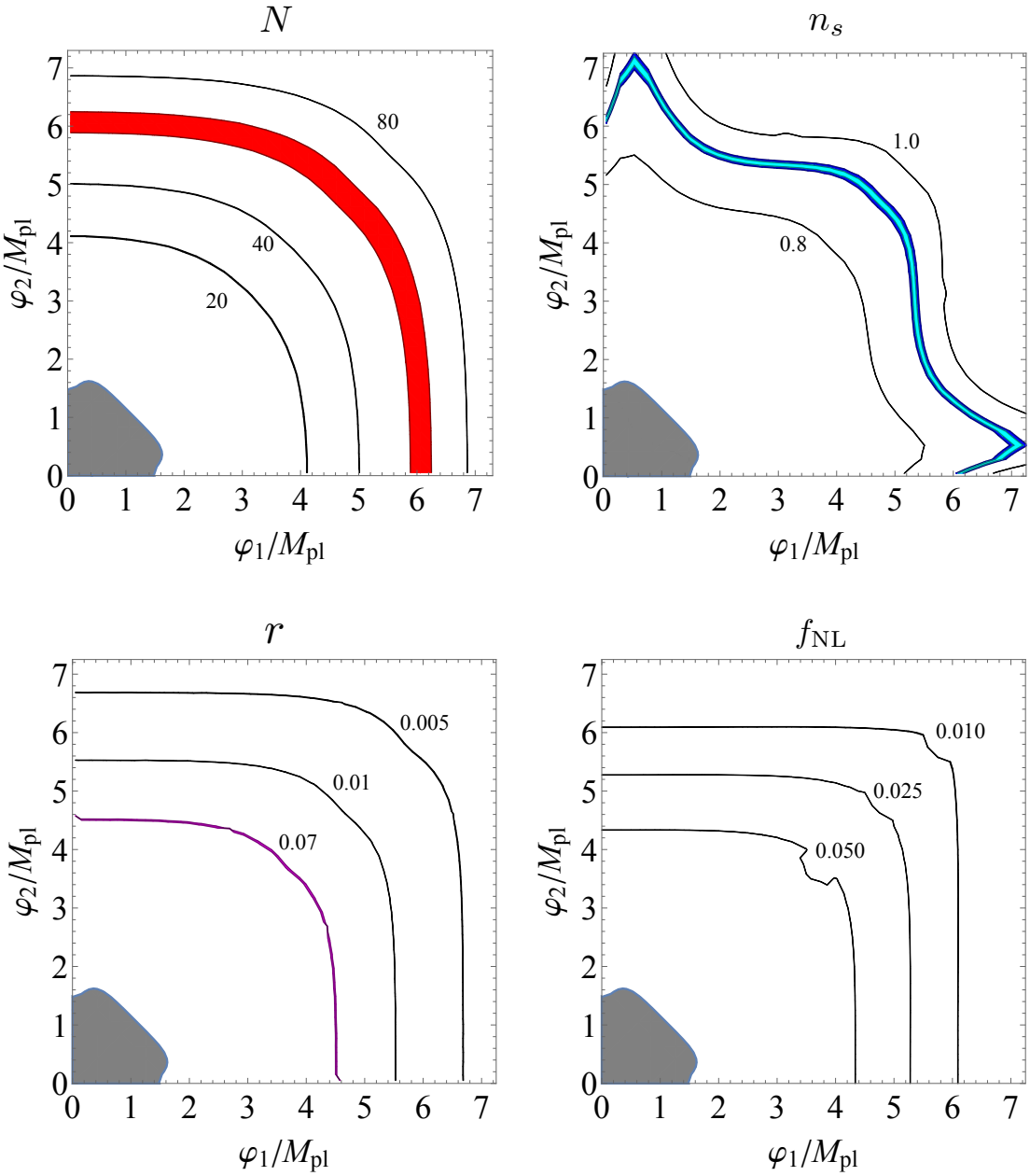

Figure 6.4.5: Results of the searches on the field search. Left-top : numbers of e-folds. The red band shows a region which yields $N = 50 - 60$. Right-top : spectral index n_s. The cyan and blue bands correspond to the region which gives n_s within 1-σ, and2-σ of the observed value, respectively. Left-bottom : tensor-to-scalar ratio. The magenta line shows current observational bound, $r < 0.07$. Right-bottom : non-Gaussianity. For all initial points which yield enough e-folds, $f_{\rm NL}$ becomes as small as $\mathcal{O}(10^{-2})$. The gray region in each panel corresponds to where $\epsilon > 1$, and slow-roll inflation does not occur.

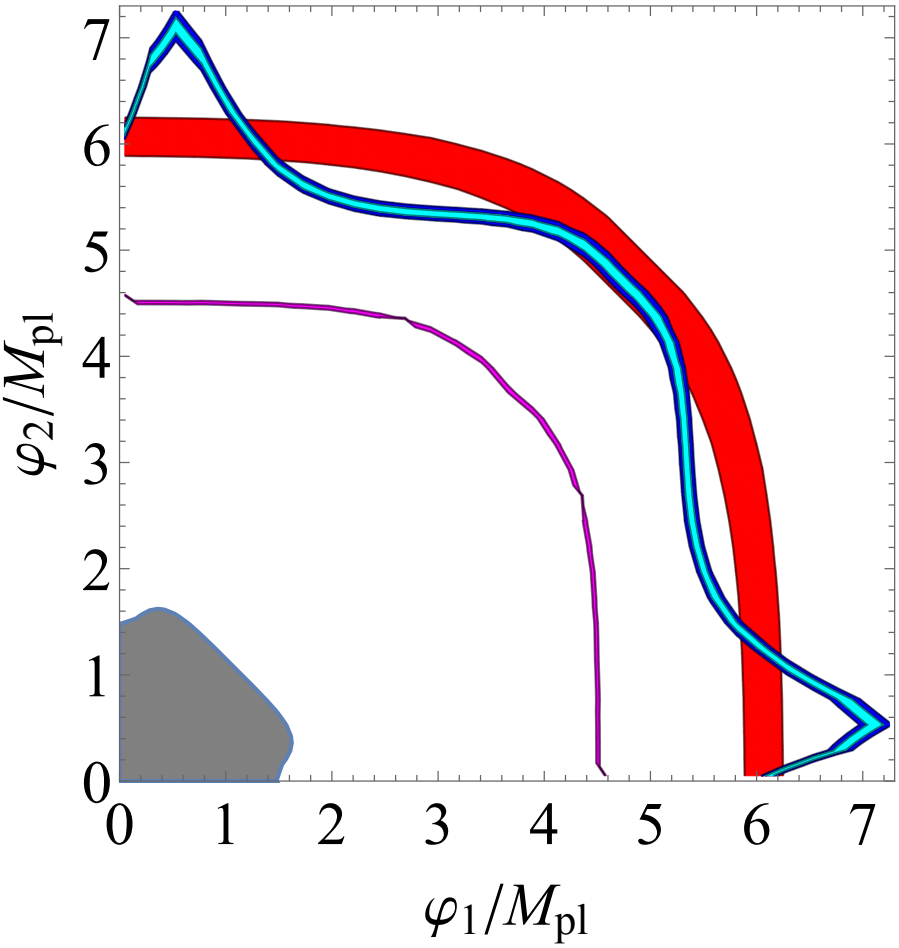

Figure 6.4.6: Combined constraints on the $\varphi_1 - \varphi_2$ plane. The red band corresponds to the range of the e-fold number $50 < N < 60$, while the cyan and blue regions correspond to the 1- and 2-σ observational constraints on n_s. The magenta line represents $r = 0.07$. The Gray shaded region corresponds to where $\epsilon > 1$

Chapter 7

Summary

In this thesis, I have discussed how to compute the observables related with curvature perturbation and putting constraints on inflation models by comparing them with observation, particularly focusing on the special techniques of the multi-field effects appeared in the multi-field inflation models. In terms of the buildings of inflation models based on superstring/supergravity, the multiple scalar fields naturally play roles of inflaton. In this sense multi-field models are attractive, and it is crucial to consider the multi-field effects to theoretically calculate the observables in the multi-field inflation models.

As we have seen in chapter 3, in cases of single-field inflation, the super-horizon mode of curvature perturbation is conserved during inflation. Thus, we just need to estimate perturbation only at the horizon exit point. On the other hand, in cases of multi-field models, because of the existence of the isocurvature modes, curvature perturbation can growth with time even after the modes exit the horizon. Hence we need to fully trace the time-evolution of curvature perturbation from the beginning to the end of inflation or a sufficiently later time until curvature perturbation becomes constant. To perform such an analysis we have introduced the δN formalism and the transport method in chapter 4. Our approaches by using these techniques are so helpful that we can compute curvature perturbation along the inflaton trajectory even in the multi-field models.

Using the δN formalism and the transport method, we have analyzed two

inflation models. In chapter 5, we have investigated a $R^2 + \chi^2$ model. In this model, performing conformal transformation, we find that this model has a Starobinsky-like asymptotic flat potential of scalaron, and χ has a non-canonical kinetic term and mixing terms with scalaron in the potential. We have traced the time-evolution of power spectrum and the non-linearity parameter of Non-Gaussianity $f_{\rm NL}$. Then, we have shown that in a certain parameter set, $f_{\rm NL}$ becomes large $f_{\rm NL} \sim \mathcal{O}(1)$ at the turning point of the trajectory of the fields. However, unfortunately we could not find a parameter set in which $f_{\rm NL}$ becomes large at the end of inflation with satisfying the observed values of N, n_s and r.

In chapter 6, we have worked on a two-field model based on string compactification, which can be called "Multi-Moduli inflation". To obtain four dimensional effective theory from 10 dimensional superstring/supergravity, we need to reduce the dimension of the spacetime. Associated with this dimensional reduction, moduli fields appear in its effective theory, and become good candidates for inflaton fields. We have extended a known moduli inflation model (Fibre inflation) to a multi-field model. We have searched model parameters, in particular the initial configuration of inflaton fields. Remarkably, we have found a set of initial conditions which yields the allowed value of N, n_s and r, and give significantly larger Non-Gaussianity ($f_{\rm NL} \sim 0.23$) than that predicted in the single-field models. Thus, when we observe $f_{\rm NL}$ of the order of the $\mathcal{O}(0.1)$ precision by using future-planning CMB projects, we will be able to test this type of multi-field models.

To summarize this thesis, with the approaches we have developed here, we can investigate various multi-field inflation models. In future, by comparing lots of theoretical predictions on the observables in inflation with new observational results, we expect that we can enjoy more rich insights into high-energy physics and physics in the beginning of the Universe.

Acknowledgments

First of all, I would like to show my greatest appreciation to my supervisor, Dr. Kazunori Kohri at SOKENDAI (the Graduate University for Advanced Studies) and at High Energy Accelerator Research Organization (KEK), whose enormous supports and a lot of insightful comments were necessary for the course of my study, and discussions with him have been always helpful for me. I have learned and acquired a lot of knowledge from him in the five years of my Ph.D. course.

My appreciation also goes to Prof. Takahiko Matsubara at SOKENDAI and at KEK, whose comments were innumerably valuable, and I received generous support from him. I am also indebted to Dr. Koutarou Kyutoku at SOKENDAI and at KEK, who always provided useful discussions and sincere encouragement.

I would also like to thank Prof. Joseph Conlon at The University of Oxford. To build our model of the inflation model based on string compactification, he gave enormous numbers of insightful comments and technical help about string theory and moduli stabilization.

Besides, I also grateful Dr. Mindaugas Karčiauskas at Jyvaskyla University and Dr. Jonathan White. They gave me great helped and provided significant contributions to our works.

Additionally, I am deeply grateful to the members of the Cosmophysics Group, KEK Theory Center: Dr. Takahiro Terada, Dr. Takafumi Kokubu, Dr. Sai Wang, Nagisa Hiroshima and Takuya Hasegawa. They gave me informative comments and warm encouragements in my daily life. Moreover, I would also like to thank Dr. Yoshihiko Oyama for his kind supports and

discussions in the first year of my Ph.D. course. In addition, I am also grateful to my friends who made my life in KEK enjoyable, Shingo Mori, Ryuji Motono and Katsumasa Nakayama.

Financially, I have been supported by JSPS Core-to-Core Program, Advanced Research Networks to stay and study in Institute of Cosmology and Gravitation, Portsmouth and by SOKENDAI internship program to study at The University of Oxford. Thanks to these support programs, I could have great chances to discuss physics and collaborate with researchers overseas.

Finally, I would also like to express my deepest gratitude to my family for their moral supports and warm encouragements for the whole of my Ph.D. years.

Appendix A

ADM decomposition and the action of $\mathcal{R}$

In this Appendix A, we derive the action up to the second order of the perturbation $\mathcal{R}$ using a method so-called Arnowit-Deser-Misner (ADM) formalism or ADM decomposition. The starting point is,

$$S = \int \sqrt{-g}\ d^4x \left[\frac{M_{pl}^2}{2} R - \frac{1}{2} g^{\mu\nu} \partial_\mu \phi \partial_\nu \phi - V \right].$$

The spatial component of the metric $g_{\mu\nu}$ in this action is the perturbed FLRW metric,

$$q_{ij} = a^2[(1 - 2\mathcal{R})\delta_{ij} + h_{ij}], \qquad \text{where} \ \ \partial_i h_{ij} = h^i{}_i = 0. \tag{A.0.1}$$

In particular, $\mathcal{R} = \Psi + \frac{H}{\dot{\phi}}\delta\phi$, and if we take a comoving gauge of ϕ it becomes $\mathcal{R} = \Psi$.

Here we introduce ADM decomposition. In this decomposition, we can express the line element ds as follows.

$$ds^2 = -N(\mathbf{x})^2 dt^2 + q_{ij}(N^i(\mathbf{x})dt + dx^i)(N^j(\mathbf{x})dt + dx^j). \tag{A.0.2}$$

Here, $N(\mathbf{x})$ is a Lapse function, $N^i(\mathbf{x})$ is a shift vector. In ADM decomposition, metric $g_{\mu\nu}$ is represented by the Lapse function and shift vector like

$$g_{\mu\nu} = \begin{pmatrix} -N^2 + h_{ij}N^iN^j & N_j \\ N_i & q_{ij} \end{pmatrix} \tag{A.0.3}$$

On the other hand, the inverse matrix $g^{\mu\nu}$ is given by

$$g^{\mu\nu} = \begin{pmatrix} -N^{-2} & N^{-2}N^j \\ N^{-2}N^i & q^{ij} - N^{-2}N^iN^j \end{pmatrix} \tag{A.0.4}$$

We can use these expressions for later calculation. Next let us calculate the inflaton part and Einstein-Hilbert part R separately.

First of all, the kinetic term of inflaton is given by

$$\begin{aligned} g^{\mu\nu}\partial_\mu\phi\partial_\nu\phi &= -N^{-2}\dot{\phi}^2 + 2N^{-2}N^i\dot{\phi}\partial_i\phi + (q^{ij} - N^{-2}N^iN^j)\partial_i\phi\partial_j\phi \\ &= -N^{-2}(\dot{\phi}^2 - 2\dot{\phi}N^i\partial_i\phi + N^iN^j\partial_i\phi\partial_j\phi) + q^{ij}\partial_i\phi\partial_j\phi \\ &= -N^{-2}(\dot{\phi} - N^i\partial_i\phi)^2 + q^{ij}\partial_i\phi\partial_j\phi. \end{aligned} \tag{A.0.5}$$

Next we address the Einstein-Hilbert part. For the later convenience, we define the scalar curvature R of 4-dimensional spacetime as $R^{(4)}$, and the scalar curvature of a constant 3-dimensional hypersurface of a certain time in the 4-dimensional time space is expressed as$R^{(3)}$,

$$R^{(3)} = R^{(4)} - K_{ij}K^{ij} + K^2. \tag{A.0.6}$$

Here, K_{ij} is called extrinsic curvature,

$$K_{ij} \equiv q_i^k q_j^l \nabla_k n_l. \tag{A.0.7}$$

n_l is defined as $n_l = N_l/\sqrt{N^iN_i}$, which is a unit normal vector of a constant surface for a certain time and $K = K^i{}_i$.

Furthermore, $\sqrt{-g}$ can be rewritten by the determinant of q_{ij},

$$\sqrt{-g} = \sqrt{q}N \tag{A.0.8}$$

To summarize (A.0.5), (A.0.6) and (A.0.8), we obtain

$$S = \int d^4x\sqrt{q}N[R^{(3)} + K_{ij}K^{ij} - K^2 + N^{-2}(\dot{\phi} - N^i\partial_i\phi)^2 - q^{ij}\partial_i\phi\partial_j\phi - 2V] \tag{A.0.9}$$

Here we calculate the extrinsic curvature using the concrete form of the metric $g_{\mu\nu}$ (A.0.2) ,

$$K_{ij} = N^{-1} \times \frac{1}{2}(\dot{q_{ij}} - \nabla_i N_j - \nabla_j N_i) \equiv N^{-1}E_{ij} \tag{A.0.10}$$

This E_{ij} represents the action,

$$S = \int d^4x\sqrt{q}[NR^{(3)}+N^{-1}(E_{ij}E^{ij}-E^2)+N^{-1}(\dot{\phi}-N^i\partial_i\phi)^2-Nq^{ij}\partial_i\phi\partial_j\phi-2NV] \tag{A.0.11}$$

Here, $E = E^i{}_i$.

From (A.0.11), we obtain the action of perturbation $\mathcal{R}$. The important point here is that there is a relationship $R^{(3)} = 4\nabla^2\mathcal{R}^{(3)}$.

(A.0.11) are varied by N, N_i, so that each equation is obtained. Since N, N_i do not have kinetic terms, these equations are not equations of motion but simply constraint conditions.

$$R^{(3)} - N(E_{ij}E^{ij} - E^2) - N^{-2}\dot{\phi}^2 - 2V = 0. \tag{A.0.12}$$

Next we consider the variance with respect to N_i, but the variance of $E_{ij}E^{ij}$ is similar to the field strength of the gauge field $F_{\mu\nu}F^{\mu\nu}$, which is similar to E_{ij}. For the variance of E^2, $\frac{\partial E^2}{\partial(\partial_i N_j)} = 2E\frac{\partial E}{\partial(\partial_i N_j)}$. When we use $E = \frac{1}{2}\dot{g_{ij}} - \nabla^i N_i$,

we obtain a term $2E\delta^i_j$. Therefore, the expression obtained by varying with N_i is

$$\nabla_i[N^{-1}(E^i_j - E\delta^i_j)] = 0. \tag{A.0.13}$$

Let us perturbe N, N^i, respectively to solve the two constraint equations (A.0.12) and (A.0.13).

$$\begin{aligned} N &= 1 + N_1, \\ N^i &= \partial^i\xi + N^i_T \qquad \text{where} \qquad \partial_i N^i = 0. \end{aligned} \tag{A.0.14}$$

(A.0.14) can be interpreted as expanding N, N^i to first order of $\mathcal{R}$. Using such a perturbative expansion, from (A.0.12),

$$N_1 = \frac{\dot{\mathcal{R}}}{H}. \tag{A.0.15}$$

and from (A.0.13),

$$\xi = -\frac{\dot{\mathcal{R}}}{H} + \frac{a^2}{H}\epsilon\chi \qquad \text{where} \qquad \partial^2\chi = \dot{\mathcal{R}}, \tag{A.0.16}$$

respectively.

By substituting these expressions, and performing partial integral, we obtain the second order action of $\mathcal{R}$,

$$S_{(2)} = \frac{1}{2}\int d^4x a^3 \frac{\dot{\phi}^2}{H^2}\left[\dot{\mathcal{R}}^2 - a^{-2}(\partial_i\mathcal{R})^2\right] \tag{A.0.17}$$

Appendix B

Conformal transformation and Starobinsky inflation

Conformal transformation for metric $g_{\mu\nu}$ is defined as,

$$\tilde{g}_{\mu\nu} = \Omega^2_{(x)} g_{\mu\nu} \tag{B.0.1}$$

this $\Omega_{(x)}$ is called a conformal factor. Let us consider how Ricci scalar is transformed for this conformal transformation. By converting from any arbitrary frame to another frame, the covariant derivative of a vector ω^ν is

$$\tilde{\nabla}_\mu \omega_\nu = \nabla_\mu \omega_\nu - C^\rho{}_{\mu\nu} \omega_\rho. \tag{B.0.2}$$

where $C^\rho{}_{\mu\nu}$ is defined as,

$$C^\rho{}_{\mu\nu} = \frac{1}{2} \tilde{g}^{\rho\sigma} (\nabla_\mu \tilde{g}_{\nu\sigma} + \nabla_\nu \tilde{g}_{\sigma\nu} - \nabla_\sigma \tilde{g}_{\mu\nu}) \tag{B.0.3}$$

note that this is not a Christoffel simbol.

Since $\nabla_\rho g_{\mu\nu} = 0$,

$$\nabla_\rho \tilde{g}_{\mu\nu} = \nabla_\rho (\Omega^2 g_{\mu\nu}) = 2\Omega g_{\mu\nu} \nabla_\rho \Omega \tag{B.0.4}$$

using this to $C^\rho{}_{\mu\nu}$ we have,

$$
\begin{aligned}
C^{\rho}{}_{\mu\nu} &= \Omega^{-1} g^{\rho\sigma}(g_{\mu\sigma}\nabla_{\nu}\Omega + g_{\nu\sigma}\nabla_{\nu}\Omega - g_{\mu\nu}\nabla_{\sigma}\Omega) \\
&= 2\delta^{\rho}{}_{(\mu}\nabla_{\nu)} \ln\Omega - g_{\mu\nu}g^{\rho\sigma}\nabla_{\sigma}\ln\Omega
\end{aligned}
\tag{B.0.5}
$$

The relationship between a curvature tensor $R_{\mu\nu\rho}{}^{\sigma}$ obtained from ∇_{μ} and $\tilde{\nabla}_{\mu}$ with curvature tensor $\tilde{R}_{\mu\nu\rho}{}^{\sigma}$ is

$$
\begin{aligned}
\tilde{R}_{\mu\nu\rho}{}^{\sigma} &= R_{\mu\nu\rho}{}^{\sigma} - (\nabla_{\mu}C^{\sigma}{}_{\nu\rho} - \nabla_{\nu}C^{\sigma}{}_{\mu\rho} - C^{\lambda}{}_{\rho\mu}C^{\sigma}{}_{\nu\lambda} + C^{\lambda}{}_{\rho\nu}C^{\sigma}{}_{\mu\lambda}) \\
&= R_{\mu\nu\rho}{}^{\sigma} - 2\nabla_{[\mu}C^{\sigma}{}_{\nu]\rho} + 2C^{\lambda}{}_{\rho[\mu}C^{\sigma}{}_{\nu]\lambda}.
\end{aligned}
\tag{B.0.6}
$$

Substituting (B.0.5) into (B.0.6),

$$
\begin{aligned}
\tilde{R}_{\mu\nu\rho}{}^{\sigma} =& R_{\mu\nu\rho}{}^{\sigma} + 2\delta^{\sigma}{}_{[\mu}\nabla_{\nu]}\nabla_{\rho}\ln\Omega - 2g^{\sigma\lambda}g_{\rho[\mu}\nabla_{\nu]}\nabla_{\lambda}\ln\Omega \\
&+ 2(\nabla_{[\mu}\ln\Omega)\delta^{\sigma}{}_{\nu]}\nabla_{\rho}\ln\Omega - 2(\nabla_{[\mu}\ln\Omega)g_{\mu]\rho}g^{\sigma\lambda}\nabla_{\lambda}\ln\Omega \\
&- 2g_{\rho[\mu}\delta^{\sigma}{}_{\nu]}g^{\alpha\beta}\nabla_{\alpha}\ln\Omega\nabla_{\beta}\ln\Omega
\end{aligned}
\tag{B.0.7}
$$

In the expression (B.0.7), we contract ν and σ. In the case of n dimensional spacetime, we obtain

$$
\begin{aligned}
\tilde{R}_{\mu\rho} =& R_{\mu\rho} - (n-2)\nabla_{\mu}\nabla_{\rho}\ln\Omega - g_{\mu\rho}g^{\alpha\beta}\nabla_{\alpha}\nabla_{\beta}\ln\Omega \\
&+ (n-2)\nabla_{\mu}\ln\Omega\nabla_{\rho}\ln\Omega - (n-2)g_{\mu\rho}g^{\alpha\beta}\nabla_{\alpha}\ln\Omega\nabla_{\beta}\ln\Omega
\end{aligned}
\tag{B.0.8}
$$

If we contract (B.0.8) with $\tilde{g}^{\mu\rho} = \Omega^{-2}g^{\mu\rho}$

$$
\tilde{R} = \Omega^{-2}\left[R - 2(n-1)g^{\alpha\beta}\nabla_{\alpha}\nabla_{\beta}\ln\Omega - (n-2)(n-1)g^{\alpha\beta}\nabla_{\alpha}\ln\Omega\nabla_{\beta}\ln\Omega\right]
\tag{B.0.9}
$$

in the case of 4 dimensional spacetime (B.0.8) and (B.0.9) become,

$$\begin{aligned}\tilde{R}_{\mu\rho} =& R_{\mu\rho} - 2\nabla_\mu\nabla_\rho \ln\Omega - g_{\mu\rho}g^{\alpha\beta}\nabla_\alpha\nabla_\beta \ln\Omega \\ &+ 2\nabla_\mu \ln\Omega\nabla_\rho \ln\Omega - 2g_{\mu\rho}g^{\alpha\beta}\nabla_\alpha \ln\Omega\nabla_\beta \ln\Omega,\end{aligned} \tag{B.0.10}$$

$$\tilde{R} = \Omega^{-2}\left[R - 4g^{\alpha\beta}\nabla_\alpha\nabla_\beta \ln\Omega - 6g^{\alpha\beta}\nabla_\alpha \ln\Omega\nabla_\beta \ln\Omega\right]. \tag{B.0.11}$$

These are the transformation laws of Ricci tensor and Ricci scalar by conformal transformation. To derive the potential of Starobinsky inflation, we use (B.0.11).

Starobinsky inflation

The starting point to derive the action of Starobinsky inflation is

$$S = \int d^4x\mathcal{L} = \frac{M_{pl}^2}{2}\int \sqrt{-g}d^4x\left(R + \frac{\alpha}{2M_{pl}^2}R^2\right). \tag{B.0.12}$$

We have to find a expression that is equivalent to this action and that has the kinetic term and potential of inflaton. To do so, we first use (B.0.12) with scalar fields φ and Lagrange multiplier χ,

$$S = \frac{M_{pl}^2}{2}\int \sqrt{-g}d^4x\left(\xi\varphi + \frac{\alpha}{2M_{pl}^2}(\xi\varphi)^2 + \chi(R - \xi\varphi)\right). \tag{B.0.13}$$

(B.0.13) is equivalent to $R = \xi\varphi$ (B.0.12). ξ is a parameter for matching the mass dimension.

(B.0.13) with φ to derive the relationship between φ and χ. φ is an auxiliary field without kinetic term, and so the equation of motion is not obtained, it gives a constraint equation.

$$1 + \frac{\alpha\xi}{M_{pl}^2}\varphi = \chi, \qquad \xi\varphi = \frac{M_{pl}^2}{\alpha}(\chi - 1) \tag{B.0.14}$$

Substitute the second expression of (B.0.14) into (B.0.13), and we can remove φ.

$$
\begin{aligned}
S &= \frac{M_{pl}^2}{2}\int\sqrt{-g}d^4x\left(\frac{M_{pl}^2}{\alpha}(\chi-1)+\frac{\alpha}{2M_{pl}^2}\left(\frac{M_{pl}^2}{\alpha}(\chi-1)\right)^2+\chi R-\chi\frac{M_{pl}^2}{\alpha}(\chi-1)\right)\\
&= \frac{M_{pl}^2}{2}\int\sqrt{-g}d^4x\left(\chi R+\frac{M_{pl}^2}{\alpha}(\chi-1)\left(1+\frac{1}{2}(\chi-1)-\chi\right)\right)\\
&= \frac{M_{pl}^2}{2}\int\sqrt{-g}d^4x\left(\chi R-\frac{M_{pl}^2}{2\alpha}(\chi-1)^2\right)
\end{aligned}
\tag{B.0.15}
$$

(B.0.15) there is a coupling between χ and R (called non-minimal coupling). Thus graviton's kinetic term is not canonically normalized. Therefore, using the conformal transformation described above, let us consider moving to a frame without non-minimal coupling.

We introduce a new scalar field ϕ to χ in (B.0.15),

$$
\chi = \exp\sqrt{\frac{2}{3}}\frac{\phi}{M_{pl}} \tag{B.0.16}
$$

In addition to the above (B.0.11), conformal factor Ω is set to

$$
\Omega^2 = \chi = \exp\sqrt{\frac{2}{3}}\frac{\phi}{M_{pl}}, \qquad \Omega = \exp\frac{1}{\sqrt{6}}\frac{\phi}{M_{pl}} \tag{B.0.17}
$$

Now we have $\ln\Omega = \frac{1}{\sqrt{6}}\frac{\phi}{M_{pl}}$, and so

$$
\begin{aligned}
\chi R = e^{\sqrt{\frac{2}{3}}\frac{\phi}{M_{pl}}}R &= \tilde{R}-4\tilde{g}^{\alpha\beta}\tilde{\nabla}_\alpha\tilde{\nabla}_\beta\left(\frac{1}{\sqrt{6}}\frac{\phi}{M_{pl}}\right)-6\tilde{g}^{\alpha\beta}\tilde{\nabla}_\alpha\left(\frac{1}{\sqrt{6}}\frac{\phi}{M_{pl}}\right)\tilde{\nabla}_\beta\left(\frac{1}{\sqrt{6}}\frac{\phi}{M_{pl}}\right)\\
&= \tilde{R}-\sqrt{\frac{2}{3M_{pl}^2}}\partial^\mu\partial_\mu\phi-\frac{1}{m_{pl}^2}\tilde{g}^{\alpha\beta}\tilde{\nabla}_\alpha\phi\tilde{\nabla}_\beta\phi
\end{aligned}
\tag{B.0.18}
$$

However, here the frame with the tilde is replaced with the frame without the tilde, and it is just redefinition. Since this second term is total derivative, it can be dropped in the action integral.

From (B.0.15) and (B.0.18)

$$
\begin{aligned}
S &= \frac{M_{pl}^2}{2}\int\sqrt{-g}d^4x\left(\chi R - \frac{M_{pl}^2}{2\alpha}(\chi-1)^2\right) \\
&= \frac{M_{pl}^2}{2}\int\sqrt{-\tilde{g}}d^4x\left(\tilde{R} - \frac{1}{M_{pl}^2}g^{\alpha\beta}\partial_\alpha\phi\partial_\beta\phi - \frac{M_{pl}^2}{2\alpha}(e^{\sqrt{\frac{2}{3}}\frac{\phi}{M_{pl}}}-1)^2\right), \\
S &= \int\sqrt{-\tilde{g}}d^4x\left(\frac{M_{pl}^2}{2}\tilde{R} - \frac{1}{2}\tilde{g}^{\alpha\beta}\partial_\alpha\phi\partial_\beta\phi - \frac{M_{pl}^4}{4\alpha}(e^{\sqrt{\frac{2}{3}}\frac{\phi}{M_{pl}}}-1)^2\right).
\end{aligned}
\tag{B.0.19}
$$

Note that the covariant derivative of the scalar field becomes the normal derivative. (B.0.19) is an explicit expression of the action of Starobinsky inflation that we have wanted to obtain.

Bibliography

[1] A.Starobinsky, Phys. Lett. B91: 99 102 (1980).

[2] K.Sato, Phys. Lett. B33: 66?70 (1981).

[3] A.Guth, Phys. Rev. D 23, 347 (1981).

[4] D.Kazanas, Astrophys. J. 241 (1980)

[5] R.Brout, F.Englert and E.Gunzig, Annals Phys. **115**, 78 (1978).

[6] A. D. Linde, "Particle physics and inflationary cosmology," Contemp. Concepts Phys. **5**, 1 (1990) [hep-th/0503203].

[7] D. Baumann, "TASI Lecture : Inflation," arXiv:0907.5424 [hep-th].

[8] Y. Akrami *et al.* [Planck Collaboration], "Planck 2018 results. X. Constraints on inflation," arXiv:1807.06211 [astro-ph.CO].

[9] D. Baumann and L. McAllister, "Inflation and String Theory," arXiv:1404.2601 [hep-th].

[10] D. H. Lyth, K. A. Malik and M. Sasaki, JCAP **0505**, 004 (2005) doi:10.1088/1475-7516/2005/05/004 [astro-ph/0411220].

[11] D. Wands, K. A. Malik, D. H. Lyth and A. R. Liddle, Phys. Rev. D **62**, 043527 (2000) doi:10.1103/PhysRevD.62.043527 [astro-ph/0003278].

[12] J. M. Maldacena, *Non-Gaussian features of primordial fluctuations in single field inflationary models*, *JHEP* **05** (2003) 013, [astro-ph/0210603].

[13] M. Sasaki and E. D. Stewart, *A General analytic formula for the spectral index of the density perturbations produced during inflation*, *Prog. Theor. Phys.* **95** (1996) 71–78, [astro-ph/9507001].

[14] M. Sasaki and T. Tanaka, *Superhorizon scale dynamics of multiscalar inflation*, *Prog. Theor. Phys.* **99** (1998) 763–782, [gr-qc/9801017].

[15] D. J. Mulryne, D. Seery and D. Wesley, JCAP **1001**, 024 (2010) [arXiv:0909.2256 [astro-ph.CO]].

[16] D. J. Mulryne, D. Seery and D. Wesley, JCAP **1104**, 030 (2011) [arXiv:1008.3159 [astro-ph.CO]].

[17] D. J. Mulryne, arXiv:1302.4636 [astro-ph.CO].

[18] M. Dias, J. Frazer, D. J. Mulryne and D. Seery, JCAP **1612**, no. 12, 033 (2016) [arXiv:1609.00379 [astro-ph.CO]].

[19] E.Kolb，M.Turner「The Early Universe」(Frontiers in Physics，1994)

[20] D.Lyth，A.Liddle「Cosmological Inflation and Large–Scale Structure」(Cmblidge University Press，2000)

[21] D.Lyth，A.Liddle「The Primordial Density Perturbation: Cosmology, Inflation and the Origin of Structure」(Cmblidge University Press，2009)

[22] S.Weinberg「Cosmology」(Oxford University Press，2008)

[23] V.Mukhanov「Physical Foundations of Cosmology」(Cambridge University Press，2005)

[24] N.Birrell，P.Davies「Quantum Fields in Curved Space」(Cambridge University Press，1982)

[25] D.Baumann，L.McAllister「Inflation and String Theory」(Cmblidge University Press，2015)

[26] D.Baumann;TASI Lectures on Inflation/arXiv:0907.5424

[27] J.Bardeen, Phys. Rev. D22, 1882 (1980).

[28] D.Lyth, Phys. Rev. Lett. 78, 1861 (1997), hep-ph/9606387

[29] A.Linde, "Chaotic Inflation," Phys.Lett. B129 (1983)

[30] K.Freese,, J.Frieman，A.Olinto, "Natural Inflation with Pseudo-Nambu-Goldstone Bosons," Phys.Rev.Lett. 65 (1990)

[31] T.Futamase and K.-i. Maeda, "Chaotic Inflationary Scenario in Models Having Nonminimal Coupling With Curvature," Phys.Rev. D39 (1989)

[32] R.Fakir and W. Unruh, "Improvement on Cosmological Chaotic Inflation Through Non-Minimal Coupling,"

[33] D.Kaiser, "Primordial Spectral Indices from Generalized Einstein Theories," Phys.Rev. D52 (1995)

[34] Planck Collaboration:Planck 2015 results. XX. Constraints on inflation (2015)

[35] C.Byrnes, Lecture notes on non-Gaussianity/arXiv:1411.7002

[36] S.Renaux-Petel, Primordial non-Gaussianities after Planck 2015: an introductory review/arXiv:1508.06740

[37] M.Sasaki, E. D. Stewart, Prog. Theor. Phys. 95, 71 (1996)/arXiv:9507001

[38] M.Sasaki, T. Tanaka, Prog. Theor. Phys. 99, 763 (1998)/arXiv:9801017

[39] F.Vernizzi, D.Wands, Non-gaussianities in two-field inflation JCAP 0605 (2006) 019

[40] D.Wands *et al*, A new approach to the evolution of cosmological perturbations on large scales/arXiv:0003278

[41] S.Renaux-Petel, Primordial non-Gaussianities after Planck 2015: an introductory review/arXiv:1508.0764

[42] D. I. Kaiser, E. A. Mazenc and E. I. Sfakianakis, Phys. Rev. D **87**, 064004 (2013) doi:10.1103/PhysRevD.87.064004 [arXiv:1210.7487 [astro-ph.CO]].

[43] D.Kaiser *et al*, Primordial Bispectrum from Multifield Inflation with Nonminimal Couplings/arXiv:1210.7487

[44] J.Maldacena:Non-Gaussian features of primordial fluctuations in single field inflationary models/arXiv:0210603

[45] R.Wald「General Relativity」(University of Chicago Press, 1984)

[46] Planck collaboration, P. A. R. Ade et al., *Planck 2015 results. XX. Constraints on inflation*, *Astron. Astrophys.* **594** (2016) A20, [1502.02114].

[47] SKA-Japan Consortium Cosmology Science Working Group collaboration, D. Yamauchi et al., *Cosmology with the Square Kilometre Array by SKA-Japan*, *PoS* **DSU2015** (2016) 004, [1603.01959].

[48] A. A. Starobinsky, *A New Type of Isotropic Cosmological Models Without Singularity*, *Phys. Lett.* **B91** (1980) 99–102.

[49] R. Kallosh and A. Linde, *Superconformal generalizations of the Starobinsky model*, *JCAP* **1306** (2013) 028, [1306.3214].

[50] C. van de Bruck and L. E. Paduraru, *Simplest extension of Starobinsky inflation*, *Phys. Rev.* **D92** (2015) 083513, [1505.01727].

[51] J. Ellis, M. A. G. Garcia, D. V. Nanopoulos and K. A. Olive, *A No-Scale Inflationary Model to Fit Them All*, *JCAP* **1408** (2014) 044, [1405.0271].

[52] J. Ellis, M. A. G. García, D. V. Nanopoulos and K. A. Olive, *Two-Field Analysis of No-Scale Supergravity Inflation*, *JCAP* **1501** (2015) 010, [1409.8197].

[53] D. H. Lyth and Y. Rodriguez, *The Inflationary prediction for primordial non-Gaussianity*, *Phys. Rev. Lett.* **95** (2005) 121302, [astro-ph/0504045].

[54] N. S. Sugiyama, E. Komatsu and T. Futamase, *δN formalism*, *Phys. Rev.* **D87** (2013) 023530, [1208.1073].

[55] A. De Felice and S. Tsujikawa, *f(R) theories*, *Living Rev. Rel.* **13** (2010) 3, [1002.4928].

[56] T. T. Nakamura and E. D. Stewart, *The Spectrum of cosmological perturbations produced by a multicomponent inflaton to second order in the slow roll approximation*, *Phys. Lett.* **B381** (1996) 413–419, [astro-ph/9604103].

[57] J.-O. Gong and T. Tanaka, *A covariant approach to general field space metric in multi-field inflation*, *JCAP* **1103** (2011) 015, [1101.4809].

[58] J. Elliston, D. Seery and R. Tavakol, *The inflationary bispectrum with curved field-space*, *JCAP* **1211** (2012) 060, [1208.6011].

[59] D. I. Kaiser, E. A. Mazenc and E. I. Sfakianakis, *Primordial Bispectrum from Multifield Inflation with Nonminimal Couplings*, *Phys. Rev.* **D87** (2013) 064004, [1210.7487].

[60] D. Seery and J. E. Lidsey, *Primordial non-Gaussianities from multiple-field inflation*, *JCAP* **0509** (2005) 011, [astro-ph/0506056].

[61] D. H. Lyth and I. Zaballa, *A Bound concerning primordial non-Gaussianity*, *JCAP* **0510** (2005) 005, [astro-ph/0507608].

[62] B. A. Bassett, S. Tsujikawa and D. Wands, *Inflation dynamics and reheating*, *Rev. Mod. Phys.* **78** (2006) 537–589, [astro-ph/0507632].

[63] A. Naruko and M. Sasaki, *Conservation of the nonlinear curvature perturbation in generic single-field inflation*, *Class. Quant. Grav.* **28** (2011) 072001, [1101.3180].

[64] X. Gao, *Conserved cosmological perturbation in Galileon models*, *JCAP* **1110** (2011) 021, [1106.0292].

[65] C. Gordon, D. Wands, B. A. Bassett and R. Maartens, *Adiabatic and entropy perturbations from inflation*, *Phys. Rev.* **D63** (2001) 023506, [astro-ph/0009131].

[66] D. Langlois and S. Renaux-Petel, *Perturbations in generalized multi-field inflation*, *JCAP* **0804** (2008) 017, [0801.1085].

[67] C. van de Bruck, P. Dunsby and L. E. Paduraru, *Reheating and preheating in the simplest extension of Starobinsky inflation*, 1606.04346.

[68] N. Deruelle and M. Sasaki, *Conformal equivalence in classical gravity: the example of 'Veiled' General Relativity*, *Springer Proc. Phys.* **137** (2011) 247–260, [1007.3563].

[69] G. Domènech and M. Sasaki, *Conformal Frame Dependence of Inflation*, *JCAP* **1504** (2015) 022, [1501.07699].

[70] N. Makino and M. Sasaki, *The Density perturbation in the chaotic inflation with nonminimal coupling*, *Prog. Theor. Phys.* **86** (1991) 103–118.

[71] T. Chiba and M. Yamaguchi, *Extended Slow-Roll Conditions and Primordial Fluctuations: Multiple Scalar Fields and Generalized Gravity*, *JCAP* **0901** (2009) 019, [0810.5387].

[72] J.-O. Gong, J.-c. Hwang, W.-I. Park, M. Sasaki and Y.-S. Song, *Conformal invariance of curvature perturbation*, *JCAP* **1109** (2011) 023, [1107.1840].

[73] J. White, M. Minamitsuji and M. Sasaki, *Curvature perturbation in multi-field inflation with non-minimal coupling*, *JCAP* **1207** (2012) 039, [1205.0656].

[74] J. White, M. Minamitsuji and M. Sasaki, *Non-linear curvature perturbation in multi-field inflation models with non-minimal coupling*, *JCAP* **1309** (2013) 015, [1306.6186].

[75] T. Chiba and M. Yamaguchi, *Conformal-Frame (In)dependence of Cosmological Observations in Scalar-Tensor Theory*, *JCAP* **1310** (2013) 040, [1308.1142].

[76] F. Vernizzi and D. Wands, *Non-gaussianities in two-field inflation*, *JCAP* **0605** (2006) 019, [astro-ph/0603799].

[77] K.-Y. Choi, L. M. H. Hall and C. van de Bruck, *Spectral Running and Non-Gaussianity from Slow-Roll Inflation in Generalised Two-Field Models*, *JCAP* **0702** (2007) 029, [astro-ph/0701247].

[78] M. Sasaki, *Multi-brid inflation and non-Gaussianity*, *Prog. Theor. Phys.* **120** (2008) 159–174, [0805.0974].

[79] J. Meyers and N. Sivanandam, *Non-Gaussianities in Multifield Inflation: Superhorizon Evolution, Adiabaticity, and the Fate of fnl*, *Phys. Rev.* **D83** (2011) 103517, [1011.4934].

[80] J. Elliston, D. J. Mulryne, D. Seery and R. Tavakol, *Evolution of fNL to the adiabatic limit*, *JCAP* **1111** (2011) 005, [1106.2153].

[81] T. Faulkner, M. Tegmark, E. F. Bunn and Y. Mao, *Constraining f(R) Gravity as a Scalar Tensor Theory*, *Phys. Rev.* **D76** (2007) 063505, [astro-ph/0612569].

[82] Y. Watanabe and E. Komatsu, *Reheating of the universe after inflation with f(phi)R gravity*, *Phys. Rev.* **D75** (2007) 061301, [gr-qc/0612120].

[83] S. Yokoyama, T. Suyama and T. Tanaka, *Primordial Non-Gaussianity in Multi-Scalar Inflation*, *Phys. Rev.* **D77** (2008) 083511, [0711.2920].

[84] Y. Watanabe, *δN versus covariant perturbative approach to non-Gaussianity outside the horizon in multifield inflation*, *Phys. Rev.* **D85** (2012) 103505, [1110.2462].

[85] X. Calmet and I. Kuntz, *Higgs Starobinsky Inflation*, *Eur. Phys. J.* **C76** (2016) 289, [1605.02236].

[86] T. d. P. Netto, A. M. Pelinson, I. L. Shapiro and A. A. Starobinsky, *From stable to unstable anomaly-induced inflation*, *Eur. Phys. J.* **C76** (2016) 544, [1509.08882].

[87] M. Grana, "Flux compactifications in string theory: A Comprehensive review," Phys. Rept. **423**, 91 (2006) doi:10.1016/j.physrep.2005.10.008 [hep-th/0509003].

[88] M. R. Douglas and S. Kachru, Rev. Mod. Phys. **79**, 733 (2007) doi:10.1103/RevModPhys.79.733 [hep-th/0610102].

[89] S. Kachru, R. Kallosh, A. D. Linde and S. P. Trivedi, Phys. Rev. D **68**, 046005 (2003) doi:10.1103/PhysRevD.68.046005 [hep-th/0301240].

[90] V. Balasubramanian, P. Berglund, J. P. Conlon and F. Quevedo, "Systematics of moduli stabilisation in Calabi-Yau flux compactifications," JHEP **0503**, 007 (2005) doi:10.1088/1126-6708/2005/03/007 [hep-th/0502058].

[91] J. P. Conlon, F. Quevedo and K. Suruliz, "Large-volume flux compactifications: Moduli spectrum and D3/D7 soft supersymmetry breaking," JHEP **0508**, 007 (2005) doi:10.1088/1126-6708/2005/08/007 [hep-th/0505076].

[92] J. P. Conlon and F. Quevedo, "Kahler moduli inflation," JHEP **0601**, 146 (2006) doi:10.1088/1126-6708/2006/01/146 [hep-th/0509012].

[93] M. Cicoli, C. P. Burgess and F. Quevedo, "Fibre Inflation: Observable Gravity Waves from IIB String Compactifications," JCAP **0903**, 013 (2009) doi:10.1088/1475-7516/2009/03/013 [arXiv:0808.0691 [hep-th]].

[94] J. Polchinski, "String theory. Vol. 2: Superstring theory and beyond,"

[95] K. Becker, M. Becker and J. H. Schwarz, "String theory and M-theory: A modern introduction,"